Post-print of: Molenda J., Kupecki J., Baron R., Belsznowski M., Brus G., Brylewski T., Bucko M., Chmielowiec J., Cwieka K., Gazda M., Gil A., Jasiński P., Jaworski Z., Karczewski J., Kawalec M., Kluczowski R., Krauz M., Krok F., Lukasik B., Małys M., Mazur A., Mielewczyk-Gryń A., Milewski J., Molin S., Mordalski G., Mosiałek M., Motyliński K., Naumovich E., Nowak P., Paściak G., Pianko-Oprych P., Pomykalska D., Rękas M., Sciazko A., Swierczek K., Szmyd J., Wachowski S., Wejrzanowski T., Wrobel W., Zagórski K., Zajac W., Zurawska A.: Status report on high temperature fuel cells in Poland – Recent advances and achievements. INTERNATIONAL JOURNAL OF HYDROGEN ENERGY. Vol. 42, iss. 7 (2017), p. 366-403. DOI: 10.1016/j.ijhydene.2016.12.087

# Status report on high temperature fuel cells in Poland e Recent advances and achievements

J. Molenda [a], J. Kupecki [b] R. Baron [c], M. Blesznowski [b], G. Brus [d], T. Brylewski [e], M. Bucko [e], J. Chmielowiec [f,q], K. Cwieka [c], M. Gazda [h], A. Gil [e], P. Jasinski [i], Z. Jaworski [j], J. Karczewski [h], M. Kawalec [k], R. Kluczowski [k], M. Krauz [k], F. Krok [l], B. Lukasik [m], M. Malys [l], A. Mazur [m], A. Mielewczyk-Gryn [h], J. Milewski [n], S. Molin [i,o], G. Mordarski [p], M. Mosialek [p], K. Motylinski [b], E.N. Naumovich [b], P. Nowak [p], G. Pasciak [f,g,q], P. Pianko-Oprych [j], D. Pomykalska [e], M. Rekas [e], A. Sciazko [d], K. Swierczek [a], J. Szmyd [d], S. Wachowski [h], T. Wejrzanowski [c], W. Wrobel [l], K. Zagorski [h], W. Zajac [a], A. Zurawska [b]

[a] AGH University of Science and Technology, Faculty of Energy and Fuels, Department of Hydrogen Energy, al. Mickiewicza 30, 30-059 Cracow, Poland

[b] Institute of Power Engineering, Thermal Processes Department, ul. Augustowka 36, 02-981 Warsaw, Poland

[c] Warsaw University of Technology, Faculty of Materials Science and Engineering, ul. Woloska 141, 02-507 Warsaw, Poland

[d] AGH University of Science and Technology, Faculty of Energy and Fuels, Department of Fundamental Research in Energy Engineering, al. Mickiewicza 30, 30-059 Cracow, Poland

[e] AGH University of Science and Technology, Faculty of Materials Science and Ceramics, al. Mickiewicza 30, 30-059 Cracow, Poland

[f] Electrotechnical Institute, Division of Electrotechnology and Materials Science, M. Sklodowskiej-Curie 55/61, 50-369 Wroclaw, Poland

[g] Centre for Advanced Materials and Smart Structures, Polish Academy of Sciences, Okolna 2, 50-950 Wroclaw, Poland

[h] Gdansk University of Technology, Faculty of Applied Physics and Mathematics, ul. Narutowicza 11/12, 80-233 Gdansk, Poland

[i] Gdansk University of Technology, Faculty of Electronics, Telecommunications and Informatics, ul. Narutowicza 11/12, 80-233 Gdansk, Poland

[j] West Pomeranian University of Technology, Faculty of Chemical Technology and Engineering, Institute of Chemical Engineering and Environmental Protection Processes, Al. Piastów 42, 71-065 Szczecin, Poland

[k] Institute of Power Engineering, Ceramic Department CEREL, ul. Techniczna 1, 36-040 Boguchwala, Poland

[l] Warsaw University of Technology, Faculty of Physics, Koszykowa 75, 00-662 Warszawa, Poland

[m] Institute of Aviation, Center of Space Technologies, Al. Krakowska 110/114, 02-256 Warsaw, Poland

[n] Warsaw University of Technology, Institute of Heat Engineering, ul. Nowowiejska 21/25, 00-665 Warsaw, Poland

[o] Department of Energy Conversion and Storage, Technical University of Denmark, Frederiksborgvej 399, 4000 Roskilde, Denmark

http://dx.doi.org/10.1016/j.ijhydene.2016.12.087

[p] Jerzy Haber Institute of Catalysis and Surface Chemistry, Polish Academy of Sciences, ul. Niezapominajek 8, 30-239 Cracow, Poland
[q] Institute of Low Temperature and Structure Research, Polish Academy of Sciences, P.O. Box 1410, 50-950 Wrocław 2, Poland

**a b s t r a c t**

The paper presents recent advances in Poland in the field of high temperature fuel cells. The achievements in the materials development, manufacturing of advanced cells, new fabrication techniques, modified electrodes and electrolytes and applications are pre-sented. The work of the Polish teams active in the field of solid oxide fuel cells (SOFC) and molten carbonate fuel cell (MCFC) is presented and discussed. The review is oriented to-wards presenting key achievements in the technology at the scale from microstructure up to a complete power system based on electrochemical fuel oxidation. National efforts are covering wide range of aspects both in the fundamental research and the applied research. The review present the areas of (i) novel materials for SOFC including $ZrO_2$-based elec-trolytes, $CeO_2$-based electrolytes, $Bi_2O_3$ based electrolytes and proton conducting electro-lytes, (ii) cathode materials including thermal shock resistant composite cathode material and silver-containing composites, (iii) anode materials, (iv) metallic interconnects for SOFC, (v) novel fabrication techniques, (vi) pilot scale SOFC, including electrolyte supported SOFC (ES-SOFC) and anode supported SOFC (AS-SOFC), (vii) metallic supported SOFC (MS-SOFC), (viii) direct carbon SOFC (DC-SOFC), (ix) selected application of SOFC, (x) advances in MCFC and their applications, (xi) advances in numerical methods for simulation and optimization of electrochemical systems.

Keywords: SOFC, MCFC, Experiments, Simulations, Fabrication techniques

## Introduction

High temperature fuel cells offer great promise for efficient power generation in various applications such as: residential systems, stationary commercial power generators, auxiliary power supply units, micro- and small-propulsion systems.

High temperature fuel cells comprise of the two technologies – molten carbonate fuel cells (MCFC) and solid oxide fuel cells (SOFC). The former currently enjoy a strong position, as is demonstrated by a 59 MW fuel cell park in Hwasung City in South Korea; the latter are still in the phase of subsidized commercialization. Attempts of commercialization of the SOFC were initiated in the 1990s with successful demonstration of the operating multi-kWt-class tubular stacks by Westinghouse (then Siemens–Westinghouse) [1,2]. However, tubular design cannot reach neither acceptable fabrication costs, nor substantial efficiency, while patented ECVD technology (for example Ref. [3] and related) cut-off potential competitors. Breakthrough in SOFC both performance and costs was made by fabrication of the anode-supported planar cells [4]. This design substantially shift technological requirements from unique to industrial-grade equipment and allows to employ technologies of mass production, like screen-printing and tape-casting, for fabrication of the cells. As well, gradual decrease of the thickness of a gas-tight electrolyte membrane resolves the problem of moderate ionic conductivity in stabilized zirconia electrolytes. Present best cells available on market offer sufficient performance at temperatures about 650 °C [5], mainstream solutions include cells with operating temperatures from 750 and higher [6]. Decrease of the operating temperature allows to use metal interconnects and housings, which, as well require special protecting coatings to cancel evaporation of the chromium compounds in cathodic gas flow and so-called cathodic contact materials [7–10]. Last ones are necessary to compensate imperfect plane-to-plane electric contact between cathode and interconnect [11]. Secondary positive effect of the lowering of the operation temperatures is more relaxed requirements to compatibility in thermal expansion. As result, ELCOGEN offers cells with (La,Sr)$CoO_3$ cathode, which demonstrated excellent conductivity, high mobility of the oxygen and electrochemical activity [12]. Further decrease of the operating temperature allows usage of the low-chromium steels [13], which will lead to reduction in fabrication costs and minimization of the problems of chromium poisoning of cathodes. In general, one can note that the key tendency in current SOFC developments is drop of production costs to the level sufficient for commercial production. Strategy of the attainment of this target is based on optimization of the materials and technology for fabrication of the anode-supported cells and on improvement of structural elements of the stacks, including elaboration of the cost-effective sealings and special coatings. As it is shown below, Polish studies in SOFC area are conforming to this tendency and targeted substantially on elaboration of the practical solutions for cost-effective fuel-cell based energy generators.

## Development of novel materials for SOFC technology

### *Requirements for electrolyte, cathode, anode and interconnect materials*

Research in the field of electroceramic materials and devices in Poland was launched back in the 1970s. Research into $ZrO_2$-based ceramic materials in Poland started at the Faculty of Materials Science and Ceramics, AGH University of Science and Technology in Krakow. While initial investigations were related to mechanical aspects of these materials, the area of study later extended to the transport properties of such ceramics. The rapid development witnessed in both the theoretical and applied approach to ion conducting and mixed ionic–electronic conducting materials was reflected by intense exploration of this field in leading research centers across Poland.

At the Department of Hydrogen Energy at AGH University of Science and Technology activities in this field are directed towards investigating the transport properties of non-stoichiometric transition metal and lanthanide oxides as candidate electrode materials and electrolytes for high temperature solid oxide fuel cells (SOFC). Design and modeling of useful properties of such materials demand basic knowledge of physicochemistry of nonstoichiometric oxides, structure of ionic and electronic defects, transport properties and mechanisms of charge transport.

In the international literature there are many works dedicated to solid electrolytes and electrode materials, but still there is a lack of basic investigations aimed at uncovering and understanding the fundamental relations between crystallographic structure, the nature of ionic and electronic defects related to nonstoichiometry in anionic and cationic sublattices, doping levels, electronic structure and transport properties, as well as catalytic activity. The Department of Hydrogen Energy with its unique facilities in Poland fills this gap. Its experience accumulated over the years is being harnessed to design and tailor functional properties of such materials on the basis of methods provided by defect chemistry, as used in nonstoichiometric systems.

Studies of this type involve a multidisciplinary approach and wide collaboration owing to the demanding requirements a solid electrolyte has to meet, including:

- high ionic conductivity (>$10^{-2}$ S $cm^{-1}$)
- transference number for an active ion close to 1
- chemical long term stability in both highly reducing and oxidizing atmospheres ($10^{-20}$ atm $\leq p_{O_2} \leq$ 1 atm)
- chemical and thermo-mechanical compatibility towards both electrode materials
- feasible fabrication of gas-tight thin ceramic membranes
- mechanical strength.

This is also true concerning electrode materials for high-temperature applications, for which the following points are of importance:

- high mixed ionic–electronic conductivity (>100 S $cm^{-1}$) with as high as possible ionic component, especially if applied in the intermediate temperature range
- high catalytic activity for the oxygen/fuel reactions for cathode and anode materials, respectively
- high temperature thermal and chemical stability in relation to other cell components in operating conditions
- stability against chromium poisoning in the case of usage of Cr-containing interconnects
- $CO_2$ tolerance
- in the case of anode material, tolerance for carbon deposition and sulfur poisoning when the cell is fueled by non-hydrogen fuel
- adequate thermomechanical properties, thermal expansion coefficient matched with that of the electrolyte and interconnect
- possibility of preparation of electrode layers with suitable porosity, adhesion and mechanical strength
- lowest possible cost of fabrication
- environmental friendliness.

### *$ZrO_2$-based electrolytes*

Materials based on zirconium dioxide are currently the most widely used solid electrolytes [14]. Introduction into $ZrO_2$ structure of cations with a valence of lower than four causes two effects that greatly affect its performance: stabilization of the high-temperature phase, tetragonal and/or cubic, and formation of oxygen vacancies responsible for the flow of electric charges [15]. The level of ionic conductivity of solids of this type is strongly associated with both the nature and amount of the dopant cations. Materials with a cubic structure achieve the highest conductivity if next conditions are met: a) composition of the solid solution correspond to the minimum amount of dopant sufficient to stabilize cubic lattice; b) differences between the ionic radii of Zr(IV) cation and the dopant ones are minimal [16]. This corresponds to the general criterion of weaknesses in bonds in solid electrolyte structures [17].

Dependence of conductivity on a type of dopant cation provides ample opportunities for modification of transport properties of zirconia; usage of two kinds of doping cations is one possible strategy for improving these properties [18]. The authors of the work studied the influence of the chemical composition on the electrical conductivity of solid solutions in the $La_2O_3$–$Y_2O_3$–$ZrO_2$, CaO–$Y_2O_3$–$ZrO_2$ and $MnO_x$–$Y_2O_3$–$ZrO_2$ [19–22].

For the $La_2O_3$–$Y_2O_3$–$ZrO_2$ ternary oxide system, the total molar concentration of dopants in zirconia was 16 mol%. It was found that for the solid solutions with the cubic structure an increase of lanthanum ions concentration led to rise of activation energy of conductivity. As result, La-doped solid electrolytes demonstrated higher conductivity at higher temperatures, while at lower ones ionic transport found to be hampered as compared to the YSZ [19].

Solid solutions in the CaO–$Y_2O_3$–$ZrO_2$ system were obtained so that the amounts of the two cations were changed in the whole range and levels of oxygen vacancies were 8, 10 or 12 mol%. For ceramics with 8 or 10 mol% oxygen vacancies stability of the cubic phase depends on total concentration of the dopants and their mutual proportions. In general, increase of calcium content leads to the formation of the tetragonal and monoclinic zirconia phase. Results of the Rietveld refinement of the respective X-ray diffraction patterns showed that the cubic zirconia structure leads to a local network distortion – oxygen ions instead of the Wyckoff position 8c occupy the low symmetry positions 48g. As the solid solutions are approaching a stabilization threshold of the cubic phase, the shift of oxygen ions and their amount at the positions 48g are increasing (Fig. 1). This means that in materials that are close to transformation of the cubic to tetragonal phase a specific "loosening" of the anion sub-lattice takes place and the effect is most pronounced in materials containing 8 mol% oxygen vacancies.

The structural changes described above strongly influenced the electrical properties of the investigated materials. An increased calcium concentration in the zirconia solid

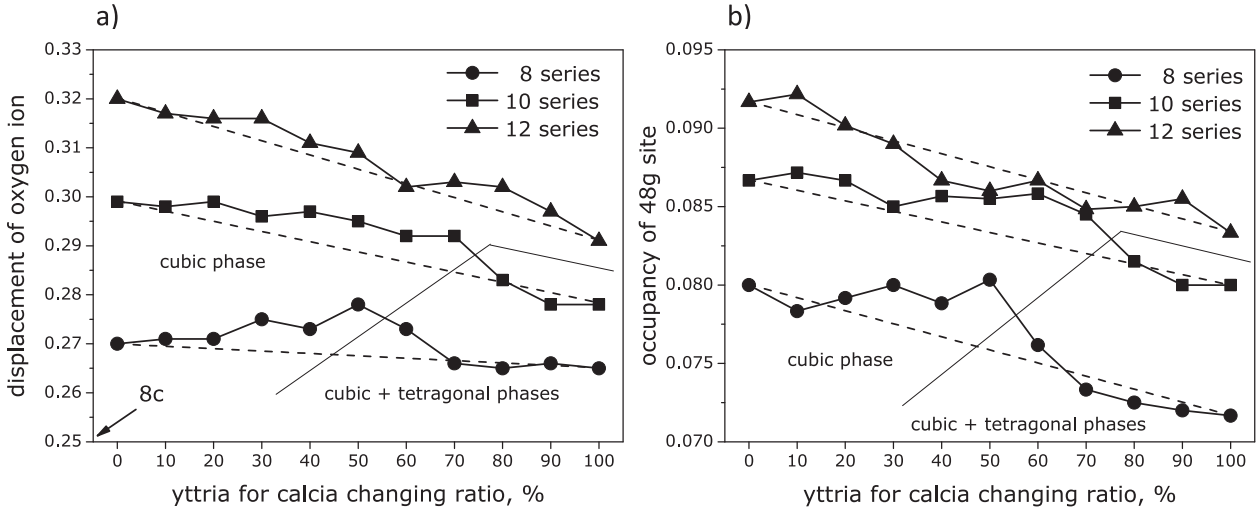


**Fig. 1 – Shift of oxygen ions from the position 8c to 48g (a) and occupancy of the position 48g by oxygen ions (b) in the structure of the solid solutions in CaO–$Y_2O_3$–$ZrO_2$ [21].**

solutions increases the activation energy of conductivity, although these changes do not occur linearly with the change of chemical composition, Fig. 2. In the series with 8% oxygen vacancies, a minimum of the activation energy is visible and it is approx. 15% lower than in the zirconia stabilized only with yttria.

Based on these results it can be concluded that the modification of conductivity of the $Me_2O_3$–$Y_2O_3$–$ZrO_2$ solid solutions is associated primarily with some diversity of dissociation energy of complex defects containing doping cations and oxygen vacancies. Substitution of a small amount of other cations for yttrium ones only causes changes in lattice parameters of the zirconia cubic phase. Changes of a different nature can be observed in the ternary MeO–$Y_2O_3$–$ZrO_2$ systems. An incorporation of calcium ions in place of yttrium ones causes several modifications, both microstructural and structural, that significantly affect the ionic conductivity of the materials. In the materials whose chemical composition causes the cubic phase is close to the transformation to the tetragonal one the observed structural changes may be defined in terms of "loosening" the anion sub-lattice of the cubic phase. In general, increase in the content of calcium oxide in the zirconia solid solution leads to an increase in the activation energy of ionic conductivity, but the materials near the cubic to tetragonal phase transformation show local reduction in the activation energy of conductivity and exhibit the best conductivity.

Interaction of the "classic" (La,Sr)$MnO_3$ (LSM) cathode and YSZ was a subject of the vast studies, targeted mainly on elimination of the negative side-effects of co-sintering [23–25]. However, doping of the YSZ with $MnO_x$ may lead to positive outcome [22]. In this case, increasing amounts of manganese oxide were introduced in the zirconia solid solution stabilized with 8 mol% $Y_2O_3$. A decrease in activation energy of conductivity and an increase in total conductivity were observed with an increase of manganese oxide content, Fig. 3. These effects can be attributed to electron conductivity, as confirmed by a decrease in oxygen transference numbers as the manganese content increased. This phenomenon can be used to form a thin layer, which is a mixed ionic–electronic conductor on the surface of the zirconia solid electrolyte, thus reducing the resistance of the electrode–electrolyte boundary.

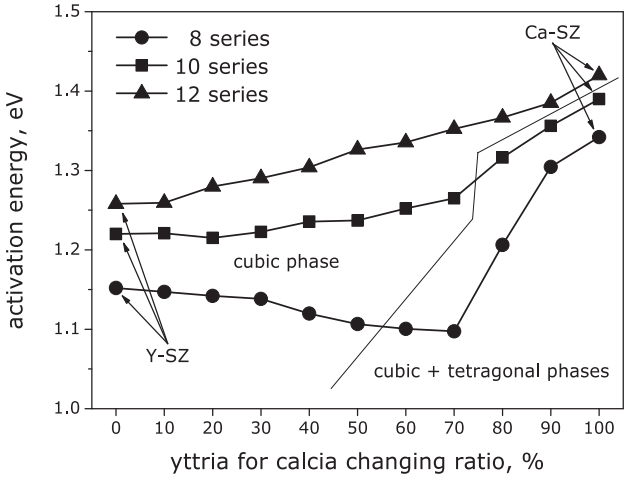


**Fig. 2 – Compositional changes of the activation energy of ionic conductivity of the zirconia solid solutions in the CaO–$Y_2O_3$–$ZrO_2$ system [21].**

### *$CeO_2$-based electrolytes*

Comprehensive studies related to the development of new materials, especially the oxide electrolytes for IT-SOFCs (IT – intermediate temperature) working in the 600–800 °C temperature range, performed in J. Molenda's group [26–29], yielded state of the art materials based on $Ce_{0.8}Sm_{0.2}O_{1.9}$ and $Ce_{0.8}Gd_{0.2}O_{1.9}$ (Fig. 4), with a high ionic conductivity, ca. $10^{-1}$ S $cm^{-1}$ at 800 °C.

One crucial advantage of the designed electrolyte, in relation to the $ZrO_2$-based one, is its very good chemical and thermal compatibility in relation to the new generation, perovskite-type cathode materials, based on Sr- or Ba-doped $LnMO_3$ (Ln – lanthanides; M – Mn, Fe, Co, Ni). Additionally, thermal expansion coefficients of these materials are well-matched in relation to high-chromium, ferritic steels used for interconnectors. Multidimensional efforts made to achieve the highest possible ionic ($O^{2-}$) conductivity and to improve resistance against reduction brought us to multiple ion doping and simultaneous directed grain-boundary decoration by transition-metal oxides for improved sinterability and ionic conductivity due to scavenging from siliceous impurities and control over space-charge effect.

### *$Bi_2O_3$ based electrolytes*

One of the main research areas in the Solid State Ionics Division (SSID) at the Faculty of Physics Warsaw University of Technology are oxide ion conductors for application as electrolytes in solid oxide fuel cells (SOFC). The research studies in this field are focused on the new electrolytic materials, which could be an alternative for commonly used yttria stabilized zirconia (YSZ). The new highly conducting, chemically and thermally stable oxide ion conductor would allow to design fuel cells operating in temperature range from 700 down to 500 °C, which is significantly lower than working temperatures (800 °C and higher) of conventional high temperature SOFC (HT-SOFC) based on YSZ.

The investigations carried out in the SSID are focused on bismuth oxide based compounds, which show at intermediate temperatures (400–700 °C) exceptional oxide ion conductivities, more than 10 times higher than YSZ used in SOFCs [30]. There is a concern about stability of these compounds at low oxygen partial pressures as well as thermal stability: significant conductivity decay of these compounds on annealing at intermediate temperatures. However, the comprehensive studies of the Wachsman group show that these drawbacks can be overcome, mainly by proper doping of $Bi_2O_3$ as well as by the use of bilayer design for electrolyte membrane, and as a result bismuth oxide based electrolytes can be incorporated into IT-SOFCs [31].

Crystal structure and electrical conductivity studies on the new oxide ion conductors based on $Bi_2O_3$, carried out in the SSID, are mainly focused on determination of defect structure and the mechanisms of ionic transport in these compounds. For this purpose various experimental techniques and data

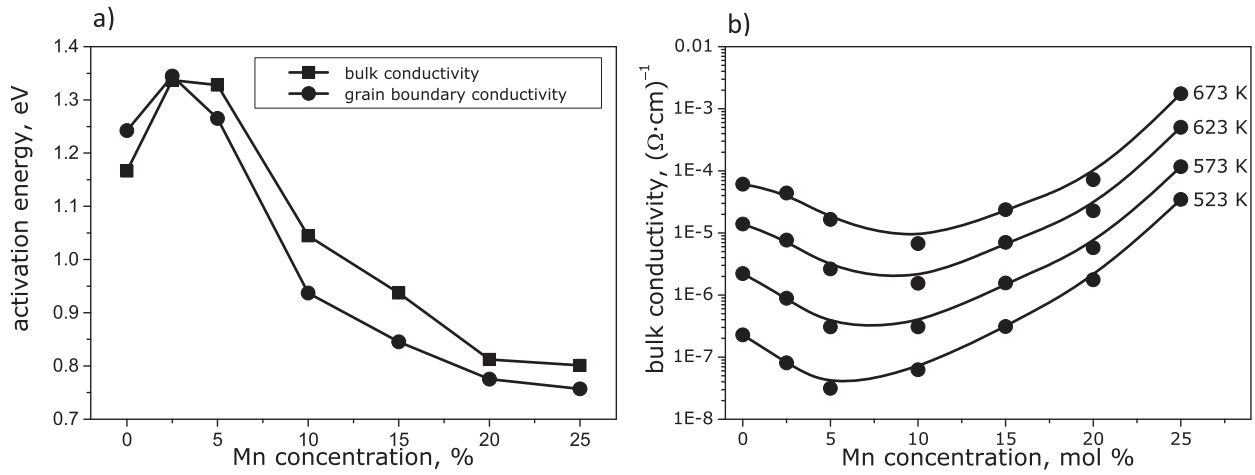


**Fig. 3 – Compositional changes of the activation energy of conductivity (a) and bulk conductivity (b) of the solid solutions in the $MnO_x$–$Y_2O_3$–$ZrO_2$ system [22].**

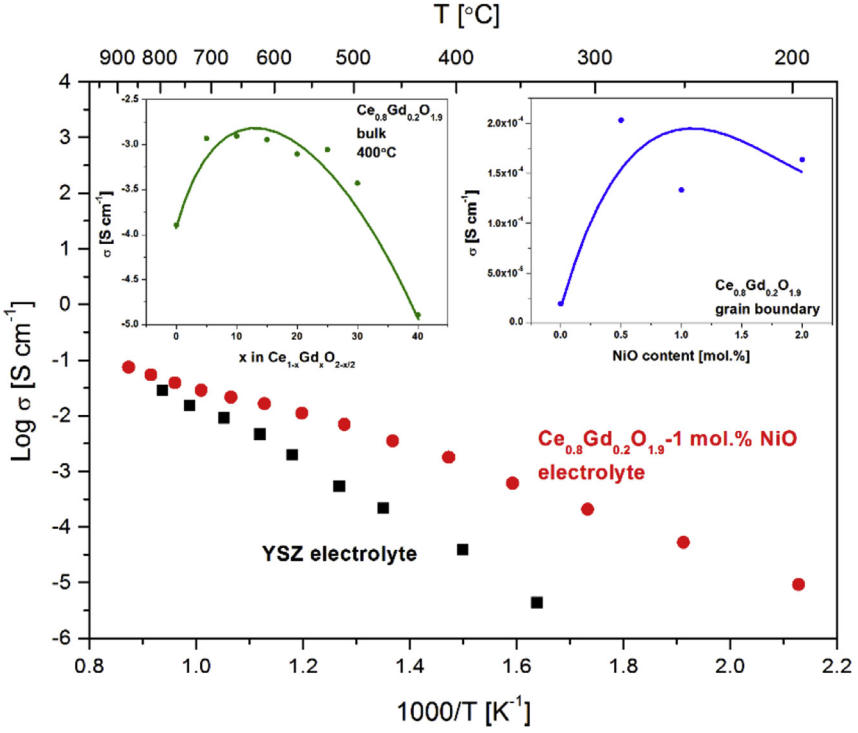


**Fig. 4 – Arrhenius plot of electrical conductivity of $Ce_{0.8}Gd_{0.2}O_{1.9}$ enriched with 1 wt.% NiO. Insets: isothermal evolution of electrical conductivity as a function of gadolinium and NiO content.**

analysis methods have been used, including a.c. impedance spectroscopy, transference numbers measurements (using modified EMF method, with external adjustable voltage source), X-ray and neutron powder diffraction, computer modeling. To characterize the short-range structure, i.e. co-ordination environments of the cations and the oxide ion vacancy ordering, the neutron *total scattering* and Reverse Monte Carlo (RMC) simulations have been used. Bismuth oxide based conductors are studied in close collaboration with Dr I. Abrahams from Queen Mary University of London.

The parent compound, $Bi_2O_3$, in the cubic fluorite δ-phase, which is only stable above *ca.* 730 °C, exhibits the highest oxide ion conductivity of any known solid [32]. Therefore, numerous studies have been carried out to stabilize this phase to room temperature by partial substitution of bismuth atoms. Isovalent ($Y^{3+}$, $Yb^{3+}$, $Er^{3+}$, $La^{3+}$), supervalent ($W^{6+}$, $Nb^{5+}$, $Ta^{5+}$, $Zr^{4+}$, $Ce^{4+}$) and subvalent ($Pb^{2+}$) dopant cations, in respect to $Bi^{3+}$, were tested in the SSID group. Also double substitution systems were investigated with the bismuth atoms partially substituted by the two of Nb, Y, Yb, Er, Zr or Ta cations. As a result, apart from the fluorite type structure, number of phases was obtained including BIMEVOX type phase. BIMEVOX-es are observed in the system $Bi_2O_3$–$V_2O_5$–MEO (MEO = metal oxide) and show exceptionally high conductivities at

intermediate temperatures. The BIMEVOX-es are obtained by partial substitution of V by other metal cations in the parent compound, $Bi_4V_2O_{11}$. BIMEVOX-es show layered structure consisting of alternating bismuth and vanadate layers. The SSID group found out, that the stabilization of BIMEVOX-type phase is governed by a combination of valence state of the metal dopant cation and its preferred coordination. Based on the proposed model of defect structure the theoretical solid solution limit of BIMEVOX phase was calculated for various metal dopant cations [33]. It was also shown, that the ionic transport is limited only to defect vanadate layer and the proposed transport mechanism is based on the ability of vanadium atoms to adopt various coordination environments (Fig. 5). However, thermal stability investigations show significant conductivity decay of BIMEVOXes during annealing at working temperatures of IT-SOFCs.

It was shown, that for certain dopant types and concentrations, the fluorite type phase can be stabilized to room temperature. In particular, in the double substituted systems of the general formula $Bi_3Nb_{1-x}ME_xO_y$ (ME = Er, Yb and Y) the $\delta$-$Bi_2O_3$ type phase was obtained in the wide range of substitution levels, x, and wide range of temperatures. Neutron diffraction studies reveal some superlattice peaks, which reflect some ordering phenomena observed in the oxide ion sublattice. However, character of the ordering is changing with the composition: from the long-range ordering at low substitution levels to short-range ordering for high substitution levels.

X-ray and neutron diffraction crystallographic data was analyzed using Rietveld method. The unit cell parameters, crystallographic sites and their occupancies were determined for different systems as a function of composition and temperature. Changes in the lattice parameters with increasing dopant concentration were explained on the basis of the difference in the ionic radii of bismuth and dopant cation. The increase of the lattice parameter as a function temperature as well as the change in thermal expansion coefficient at temperature near 500 °C was observed for all of the studied compounds. This change in the thermal expansion coefficient was associated with the redistribution of oxide ions over possible crystallographic sites, i.e. the increase of occupancy of 8*c* site at the expense of 32*f* site. In fact such a redistribution of oxide ions reflects the change of the vacancy ordering in the oxygen sublattice [34,35].

The defect structure model was described and the transport mechanism of the oxide ions in the studied system $Bi_3Nb_{1-x}ME_xO_{7-x}$ was proposed. The 32*f* site was found to play a key role in the transport mechanism, since the 32*f* site is located on the conduction pathway between two neighboring oxide ion cavities and the energy barrier for oxide ion jumps between 32*f* sites is smaller than between 8*c* sites (Fig. 6) [36]. Indeed, the activation energy, determined from the a.c. impedance spectroscopy studies, for the compounds with high 32*f* site occupancy is lower than in the systems with dominating 8c occupancy [36].

The Rietveld and RMC analysis of neutron diffraction data provides some information on the local environments of the cations, but sometimes it is difficult to draw definite conclusions, in particular when the scattering coefficients for cations are similar. To determine the influence of particular type of cations on oxide ion transport in the studied systems, the *ab-initio* simulations have been carried out. In the case of $Bi_3YO_6$, it was found that the average occupancy of oxide ion sites and the residence time in these sites are increasing with the number of dopant yttrium ions in the vicinity of these sites.

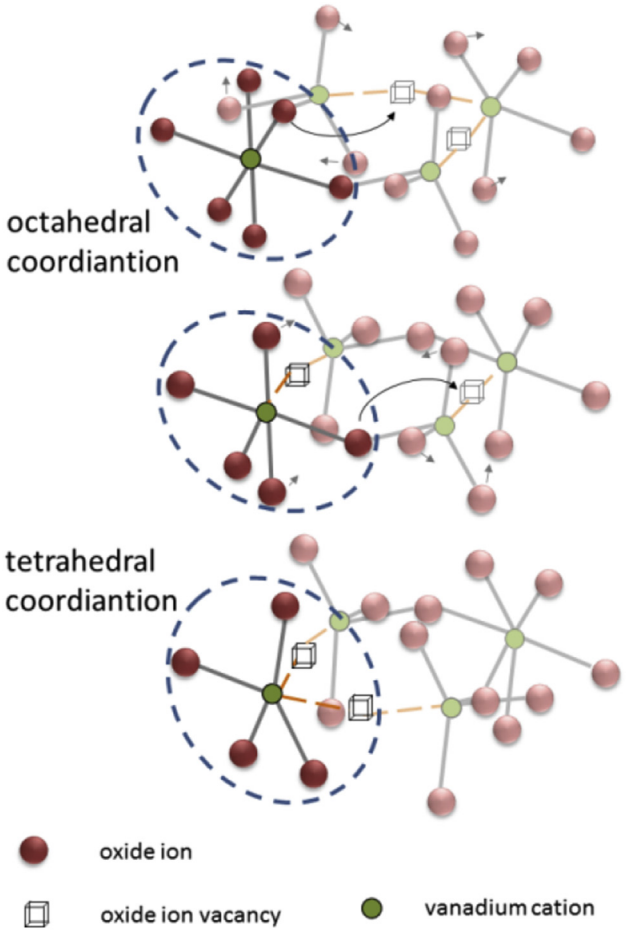


**Fig. 5 – Oxide ion transport mechanism in the BIMEVOXes.**

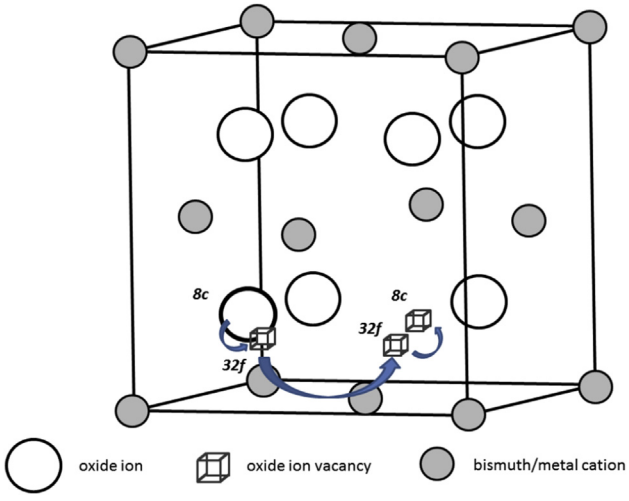


**Fig. 6 – Scheme of oxide ion movements in the bismuth oxide based cubic fluorite type compounds.**

This reflects trapping mechanism of oxide ions in the yttrium neighborhood [37]. In the case of $Bi_3NbO_7$ compound the opposite trend was observed, i.e. both the average occupancy of oxide ion sites and the residence time are decreasing with the number of niobium dopant ions in the vicinity of these sites. Moreover, most of the oxide ion jumps were found to be local, rotational motion around niobium ions rather than long-range movements contributing to oxide ion diffusion [38]. Since the *ab-initio* simulation shows high concentration of oxide ion vacancies in the niobium surroundings, this phenomenon has been defined as a trapping mechanism of oxide ion vacancies in the vicinity of niobium cations. Both phenomena, i.e. trapping of oxide ions in vicinity of yttrium ions in $Bi_3YO_6$ and trapping of oxide ion vacancies in vicinity of niobium ions in $Bi_3NbO_7$ would result in a significant decrease of electrical conductivity in these compounds, compared to undoped $Bi_2O_3$ as experimentally confirmed [37,38].

Oxide ion transference numbers measurements exhibit almost pure ionic conductivity of all studied bismuth oxide based systems at temperatures higher than approx. 500 °C, which is crucial for usage in the SOFCs [39,40]. Thermal stability studies show some conductivity decay during prolonged annealing at working temperatures of IT-SOFCs. However, doping of $Bi_3YO_6$ with tungsten causes significant stability increase: electrical conductivity of the compound with 10% $Y^{3+}$ substituted by $W^{6+}$ cations has retained 80% of initial value after annealing at 650 °C for 1000 h, whereas in the case of undoped compound the conductivity dropped to 10% of initial value. It means that the thermal instability can be significantly reduced by proper doping.

With a clear focus on superionic conductors (solid electrolytes) in 2000, the Laboratory of Unconventional Energy Sources of the Electrotechnical Institute in Wroclaw (IEL) was founded, which continues to research ceramic materials for use in SOFC (electrolytes, electrodes, construction materials and sealing) ever since. It allowed to extend the scope and to continue research related to SOFCs which was initiated in 1990s [41,42].

The last 10 years have seen increased interest in zirconium oxide, with substantial progress noted in two key directions. One is to adjust the capabilities of commonly used materials, such as $ZrO_2$, by doping it with, e.g., Sc and improving the manufacturing technology to allow commercial scale production of ceramic electrolytes in the form of very thin and flexible layers. The second route is to develop a range of new materials characterized by good ionic conductivity at temperatures as low as 600–800 °C (usually these materials are based on bismuth oxide or cerium).

The IEL focuses mainly on the latter path and so its research is directed at the development of new medium temperature electrolytic materials from the BIMEVOX family (BI – bismuth, ME – metal doping, V – vanadium, OX – oxygen). They are characterized by the presence of three crystal phases $\alpha$, $\beta$ and $\gamma$ (depending on the temperature) of which only one phase $\gamma$ has suitable ionic conductivity. However, materials based on bismuth are quickly reduced and degraded in the typical operating atmosphere of the fuel cell (due to hydrogen). Therefore, the main research objectives are to stabilize the $\gamma$ phase across a wide temperature range and improve the stability of the electrolyte in the target atmospheres. Research effort (PhD thesis [43], national and international projects [44–47]) analyzed the impact of synthesis and doping of the starting material $Bi_4V_2O_{11}$. The synthesis method used was either powdering of oxides and nitrides or the sol–gel method. The selection of optimal synthesis parameters, such as compacting process ("dry" or with a lubricant), pressure, pressing time, temperature and time of calcination as well as sintering, was based on the analysis of own material research using tools like XRD-DRON2, ASAP, SEM with EDS TGA/DSC1, dilatometer, Instron, Solartron SI1260 SI, stand for testing the effect of a reducing atmosphere. Similarly, when modifying electrolytic materials via doping, the effects of composition and crystalline structure, changes in the microstructure, thermal properties and electrical properties were analyzed. In the case of materials from the BIMEVOX family, other dopant metals were used (e.g. Cu, Cr, Zn, Fe, Co, Ti, Sb), each substituting vanadium in Aurivillius structure [44] and La, Pr substituting Bi [45].

Following on from discovering the impact of various percentage levels of particular dopants on the stability of the BIMEVOX material in the reduction atmospheres, a base material was developed with elevated bismuth levels – BIBIMEVOX (change from 66.7 to 68.5 mol% $Bi_2O_3$) doped with lanthanum BIBILAVOX.4 in an amount of 4% by weight $La_2O_3$ [46]. Such doping increased the material's resilience to the reducing atmosphere ($H_2$).

Additionally, other electrolytic materials were researched, e.g. materials based on lanthanum silicate, bismuth oxide – phase $\delta$ as well as gadolinium doped ceria (GDC) and zirconium oxide stabilized with yttrium and scandium.

Measurement capabilities available in IEL (some presented in Fig. 7) provide information on the synthesis and doping impact on the grain size, distribution of individual elements and their agglomeration (SEM + EDS), chemical composition and stability of the material in reducing atmospheres (DRON-2 XRD and the setup for electrical measurements at pre-set gases). An important parameter in ceramic electrolytes is its thermal expansion and compatibility with other elements such as electrodes, sealing and structural materials – dilatometry and differential thermal analysis enable the phase transitions in the material to be determined. However, the most important feature of electrolytes is the ionic conductivity – for this the institute has access to Agilent E4991A impedance analyzer and Solartron SI1260 with a potentiostat SI1296 and Norecs measurement setup that makes it possible to take measurements in two given atmospheres (operating condition of the cell).

### *Proton conducting electrolytes*

Parallel to efforts related to conventional fuel cells, there are studies towards the development of functional proton-conducting ceramic electrolytes ongoing at the Department of Hydrogen Energy at AGH [48–50]. Studies are focused on the most promising compositions among $(Ba,Sr)(Ce,Zr)O_3$ perovskite oxides doped with rare earth metals (Fig. 8).

Similarly to oxide-ion-conducting material, the research is devoted to understanding the relations between chemical composition, crystal structure, proton content and its mobility, as well as the fabrication of high performance ceramic

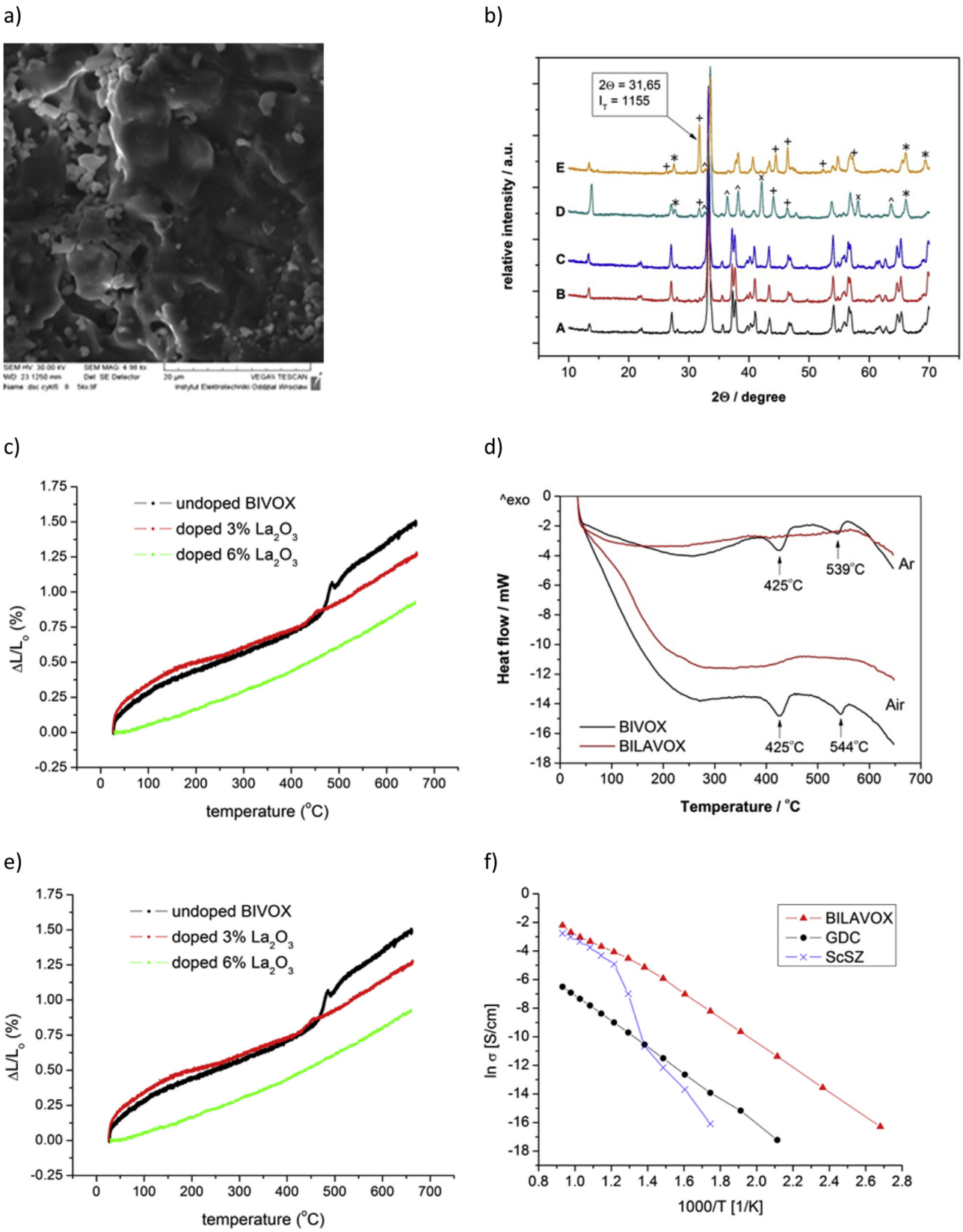


**Fig. 7 – A spectrum of selected measurement results for materials developed with various techniques: (a) SEM microscopy, (b) X-ray crystallography, (c) Dilatometer, (d) thermogravimetry, (e) and (f) impedance spectroscopy.**

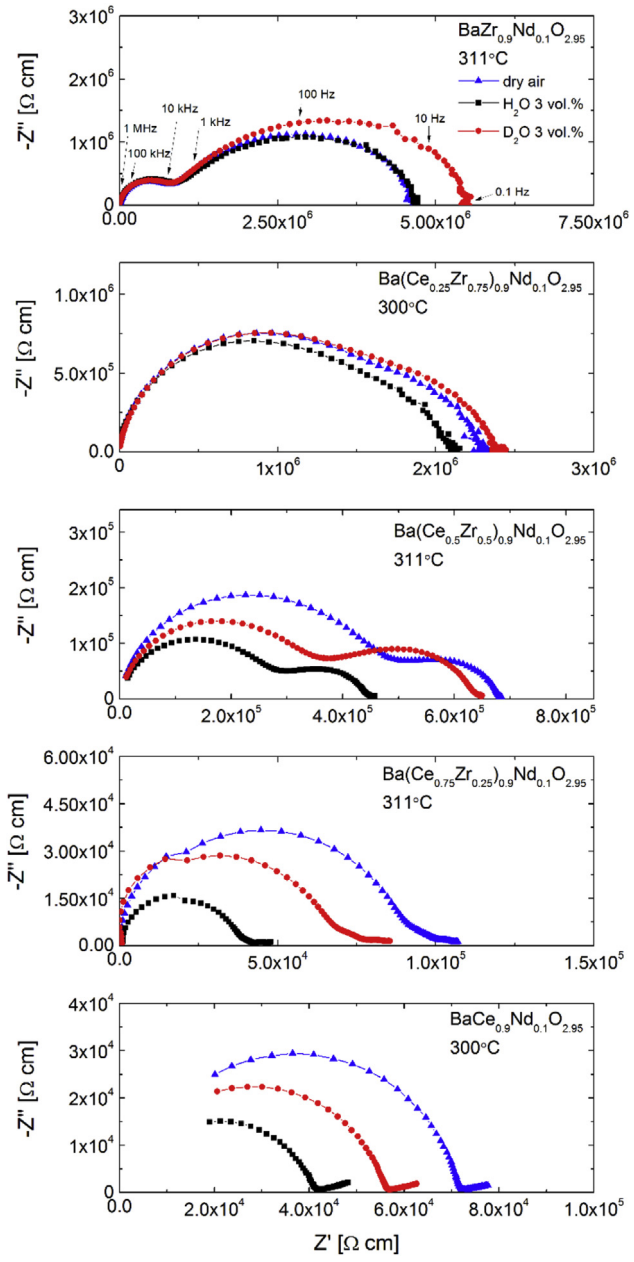


**Fig. 8 – Impedance spectra of $Ba(Ce_{1-x}Zr_x)_{0.9}Nd_{0.1}O_{2.95}$ in dry and humid ($H_2O$ or $D_2O$) air. Reprinted from Ref. [50], Copyright (2012), with permission from Elsevier.**

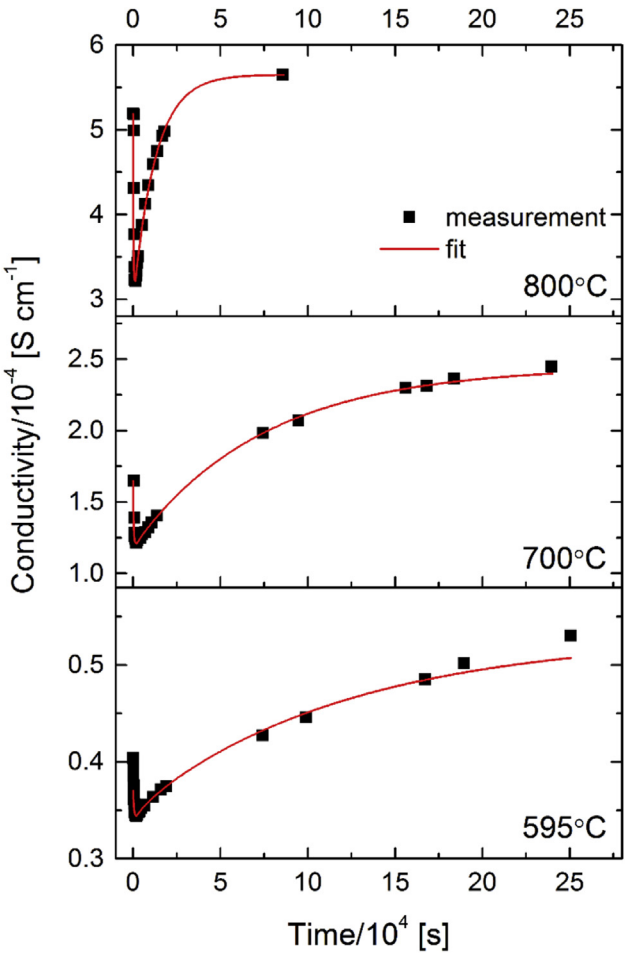


**Fig. 9 – Electrical conductivity relaxation upon hydration of $SrZr_{0.95}Gd_{0.05}O_{2.975}$. Reprinted from Ref. [49], Copyright (2013), with permission from Springer.**

membranes, using standard ceramic techniques, and the thin film Pulsed Laser Deposition method. Evaluation of constructed prototypes of fuel cells with (Ba,Sr)(Ce,Zr)$O_3$ electrolytes pointed to a strong need to develop new electrodes, since the currently used materials, especially on the cathode side, are inefficient and limit the overall performance of the cell.

Further research on proton conducting oxides rely on complementary application of kinetic methods: mass relaxation technique and electrical conductivity relaxation technique, which allow for a simultaneous determination of chemical diffusion coefficient $D$ of mobile ions (protons and oxygen ions) and surface exchange reaction coefficient $K$ (Fig. 9).

This, together with precise measurements of structural properties, oxygen nonstoichiometry and electrical conductivity, as well as microstructural and spectroscopic studies, provides a complete description of the physicochemical properties of the materials and determines transference numbers across wide temperature and oxygen partial pressure ranges.

Since 2008 the Department of Solid State Physics at Gdansk University of Technology (GUT) has carried out research on proton conducting fuel cells, focusing on compounds in a group of lanthanum niobates.

Since that time extended research into the physical and chemical properties of these materials has been done in collaboration with multiple worldwide research groups. Rare-earth based compounds have been used as materials for solid oxide fuel cells for more than three decades. Oxygen ion conductors including yttria stabilized zirconia (YSZ) and gadolinium doped ceria (CGO) as well as proton conductors like barium cerate and lanthanum niobate can be given as major examples. The difference in status between the families of oxide and proton conducting rare-earth materials is that only in the case of the first group were suitable electrolytes for SOFCs found and successfully utilized in operating cells. As

regards proton conducting ceramics, the properties of known materials are insufficient to exploit them in working devices [51].

The main problem with rare-earth based proton conducting materials is the compromise between chemical stability and conductivity level. For instance, the conductivity of Y-doped $BaCeO_3$ is $4 \times 10^{-2}$ S/cm in the temperature range of 600–800 °C [52]. However, it is not stable in atmospheres that contain $CO_2$. Conversely, Haugsrud and Norby reported chemically stable Ca doped orthoniobate with conductivity of $1 \times 10^{-2}$ S/cm at 950 °C [53]. Therefore, these two examples highlight the competing problems of insufficient stability and low conductivity. Mather et al. in their work modeled possible substitutions both on the La and Nb site and postulated that the ionic radius of the doping element can influence the possible electrical properties of the compound [54]. Also for the La site, Mg, Fe and Ba can be considered while for the Nb site – germanium, lead and tin. The theoretical conclusions were experimentally proved in the case of doping on the La site by calcium, strontium, and barium [55].

Apart from the transport properties of the lanthanum niobate group, an interesting area of research is the high temperature transformations of the crystal structure. It is a good field of study also because the symmetry of the crystal structure and its packing density influences proton mobility. $LaNbO_4$ at room temperature belongs to the monoclinic Fergusonite structural group and at temperatures above 500 °C transforms to the tetragonal Scheelite structure. Fergusonite and Scheelite unit cells are presented in Fig. 10.

The first research concerning lanthanum niobate focused on the introduction of cation acceptor dopants into lanthanum sublattice, with special interest put on the magnesium doping [57]. The stoichiometry chosen for investigation was $La_{0.98}Mg_{0.02}NbO_4$. A new synthesis method for such compounds was optimized – molten salt synthesis. The molten salt synthesis method harnesses energy produced during the melting of the salt, which becomes a liquid environment for powder synthesis. The stoichiometric amounts of substrate powders are mixed (at fixed ratios) with salt (e.g. NaCl, KCl and other) and then heat treated in an alumina crucible at temperatures above the salt's melting temperature.

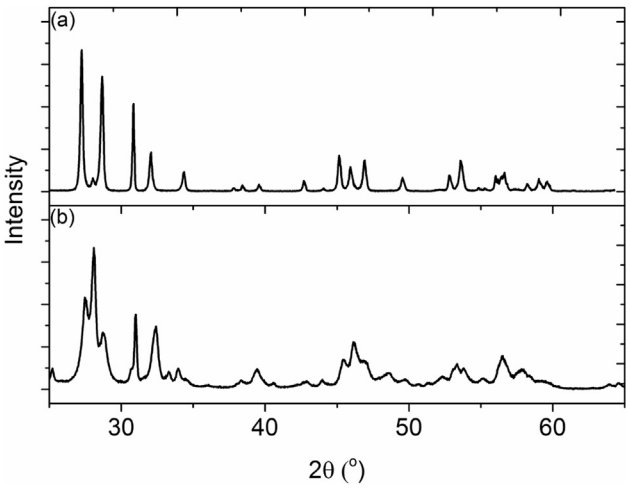


**Fig. 11 – XRD patterns of Fergusonite with preferred orientation of crystallites [60] (a) and a material containing a high amount of tetragonal Scheelite phase (b).**

After cooling down to room temperature, the salt is removed from the powder by repeatedly washing with deionized water. The resulting powder is then dried in air. In this method usage of different salts, calcination time, temperature and heating/cooling ratio can strongly influence the powder microstructure, resulting in smaller or bigger grains [58,59]. This method also made it possible to produce samples with preferred orientation of crystallites [60] and samples containing a high amount of tetragonal Scheelite phase. Fig. 11 presents examples of the XRD patterns of these materials.

The introduction of Mg to lanthanum sublattice influenced the electrical properties of the material. It was also shown that the conductivity of magnesium doped lanthanum orthoniobate synthesized by the molten salt route reaches values of ~1 mS/cm at 720 °C in wet hydrogen, which should be considered as being relatively high compared to other dopants [60].

Another important part of the research focused on microstructural properties, especially at high temperatures [60,61].

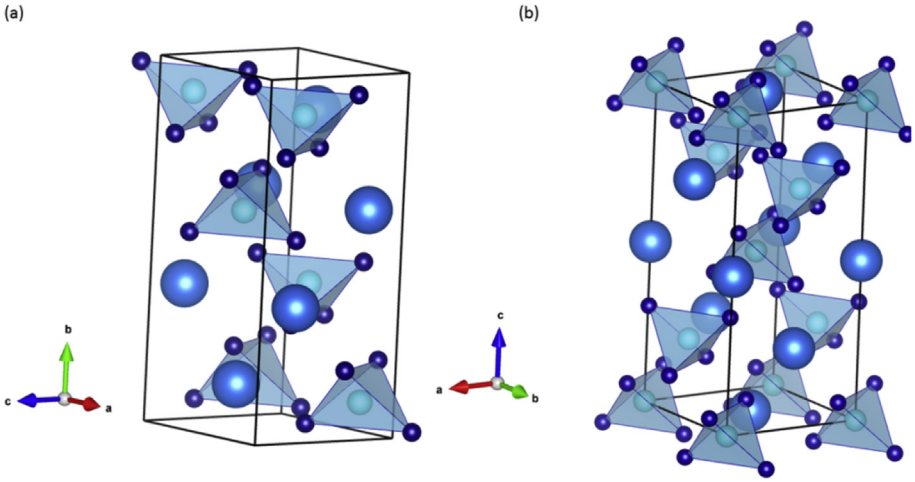


**Fig. 10 – Fergusonite (a) and Scheelite (b) unit cells of lanthanum orthoniobate [56].**

The influence of magnesium substitution on spontaneous strain was analyzed and this way the lack of change of the nature of the phase transition was proved [62]. An attempt was made to utilize ion doped calcium titanate as a material for operation in lanthanum niobate based fuel cells, with the conclusion being reached that there is a strong reaction between the two materials [63].

Since 2012 research at Gdansk University of Technology on lanthanum niobates has been focused on niobium site isovalent doping. The influence of niobium site doping on phase transition was analyzed. Special interest was devoted to the antimony substituted lanthanum niobate, which is a new material in this group. The thermal expansion coefficient of the antimony substituted samples above the transition temperature is in the range 8.1–9.1 $\times$ $10^{-6}$ 1/K, whereas below the transition temperature the TEC value is between 14 and 17.3 $\times$ $10^{-6}$ 1/K. For sample with 30 mol% doping, a stable tetragonal structure was achieved at room temperature, which is strongly beneficial in the sense of future technical application due to the lack of TEC change [64]. Further research on these materials in cooperation with the University of California, Davis has shown the influence of antimony doping on the stability of the material. It has been shown that antimony substitution does not influence the value of enthalpy of formation from oxides for samples with dopant content 0–25 mol% (with monoclinic structure at RT), but for sample with 30 mol% the enthalpy of formation appeared to be less exothermic – less stable in RT [65]. Moreover, in this work it was also showed that the antimony substitution did not influence the nature of phase transition. Calculations of Landau order parameter and strain tensor dependency proved the structural phase transition for antimony doped samples was of the second order. Further research to be published in coming months is focused on heat capacity measurements of antimony substituted samples, their electrical conductivity, oxygen diffusion and the chemical state of dopants.

This leads one to the conclusion that chemical substitutions as well as microstructural modifications of lanthanum orthoniobate allow for its phase transition temperature to be lowered and proton conductivity to be increased. While proton conductivity of lanthanum niobates is not very high, this group of materials is still very interesting for both conventional and single layer solid oxide fuel cells.

## Cathode materials

It is known that the catalytic activity of cathode material is very important in terms of the electrochemical effectiveness of working fuel cells. Investigations indicate that the kinetics of cathodic reaction (oxygen reduction) and the polarization process at the electrolyte/cathode materials interface are the limiting parameters of electrochemical effectiveness. While the microscopic mechanism of the process has not yet been entirely explained, it has been established that the rate of oxygen adsorption on the cathode material depends on the concentration of oxygen vacancies and quasi-free electrons in the cathode material. A deviation from stoichiometry towards the oxygen deficiency introduces defect centers, the ionization of which leads to a change in the concentration of charge carriers. Therefore, the oxygen nonstoichiometry and the presence of dopants shift the position of the Fermi level, which, according to the electronic theory of catalysis is a vital factor for catalytic activity of the cathode material. The magnitude of the oxygen nonstoichiometry is related to the synthesis conditions (i.e. temperature, the oxygen partial pressure) and the type and concentration of the dopant.

Research in the Department of Hydrogen Energy AGH on novel cathode materials includes work on Sr- or Ba-doped $LnMO_3$ (Ln – lanthanides; M – Mn, Fe, Co, Ni) with mixed ionic–electronic conductivity, which are used in IT-SOFCs (Figs. 12 and 13) [66–72].

As can be seen in Fig. 12, oxygen vacancy defect (catalytic centers for oxygen reduction) starts to form effectively from 800 °C.

Among the developed novel oxides, very promising properties were found for the $GdBaCo_{1.7}Fe_{0.3}O_{5.5-\delta}$, candidate cathode material, which should enable the material to operate at 600 °C or below in IT-SOFC [73]. This oxide shows a very high mixed ionic–electronic conductivity across a wide

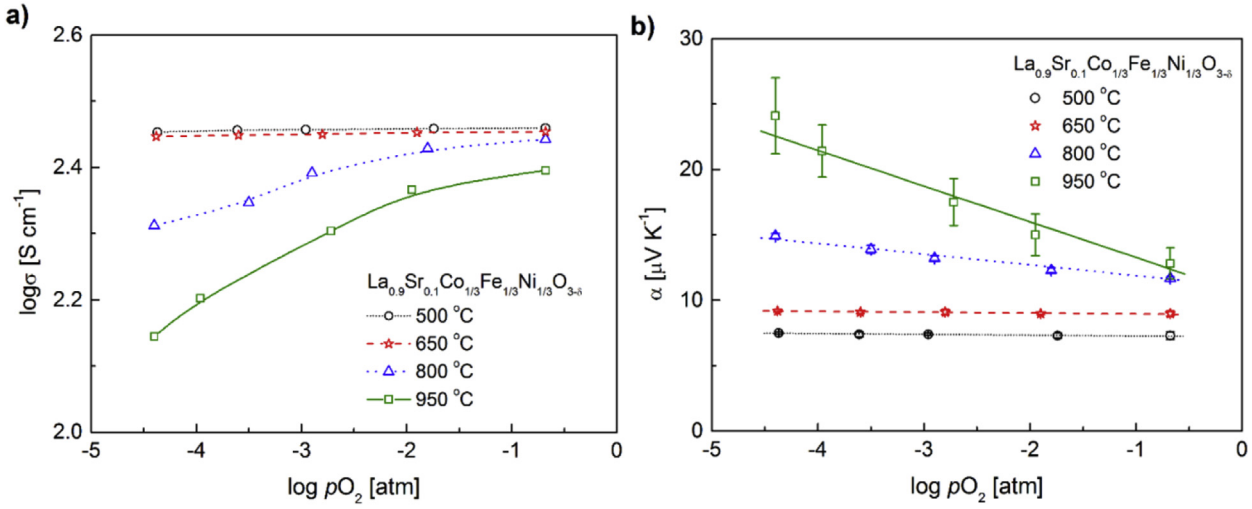


**Fig. 12 – (a) Equilibrium dependences of the electrical conductivity and (b) the thermoelectric power of $La_{0.9}Sr_{0.1}Co_{1/3}Fe_{1/3}Ni_{1/3}O_{3-\delta}$ as a function of the oxygen partial pressure. Reprinted from Ref. [67], Copyright (2007), with permission from Elsevier.**

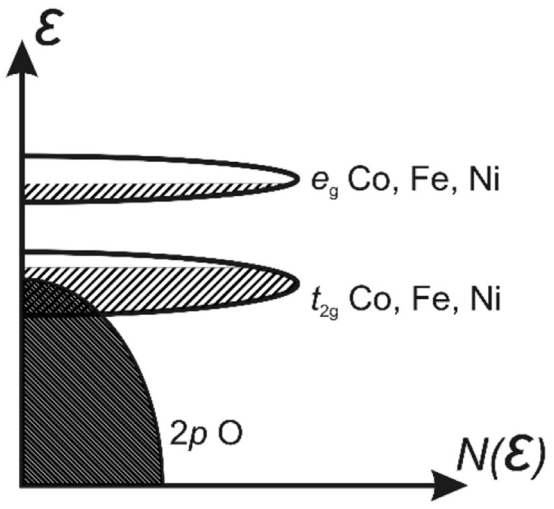


**Fig. 13 – Schematic representation of the electronic structure of the $La_{1-x}Sr_xCo_{1-y-z}Fe_yNi_zO_{3-\delta}$ perovskites. Reprinted from Ref. [67], Copyright (2007), with permission from Elsevier.**

temperature range and exhibits extremely low enthalpy of formation of the oxygen vacancies (~0.2 eV) – catalytic centers for oxygen reduction, which is crucial for fuel cell efficiency.

Taking into account issues related to microstructure of the electrodes, as well as chemical and thermal compatibility of all materials in the working cell, the following cell with intermediate, composite layer was proposed, constructed and tested: $H_2$|Ni-8YSZ|CGO(1%NiO)|CGO-GBCF|GBCF|$O_2$ (CGO = $Ce_{0.8}Gd_{0.2}O_{1.9}$, GBCF = $GdBaCo_{1.7}Fe_{0.3}O_{5.5-\delta}$) (Fig. 14).

### *Thermal shock resistant composite cathode material*

Composites consisted of a component showing good electronic conductivity and high catalytic activity in ORR and a component showing good ionic conductivity are frequently used as cathode materials. Such structures enable the 2D reaction zone to expand to the 3D reaction zone, leading to increased catalytic activity. However, the elements of fuel cells are exposed to thermal shocks during intentional or accidental shutdown events. If the thermal expansion coefficients of the components of the composite differ from each other, the change in temperature may cause cracking and lead to disruption of the current paths. That, in turn, may eliminate parts of the electrode material from participation in the reaction and the cause decreased conductivity. That problem can be avoided if the ionic conducting composite component also shows some electronic conductivity, and the electronic conducting component shows some ionic conductivity in the case of $Sm_{0.5}Sr_{0.5}CoO_{3-\delta}$–$La_{0.6}Sr_{0.4}FeO_{3-\delta}$ composite [74]. In that case crashing does not cause disruption to either ionic or electronic conduction paths.

### *Toward more efficient cathode materials: silver-containing composites*

Fortunately, silver migration seems not to occur in the case of composites that consist of a ceramic material and silver

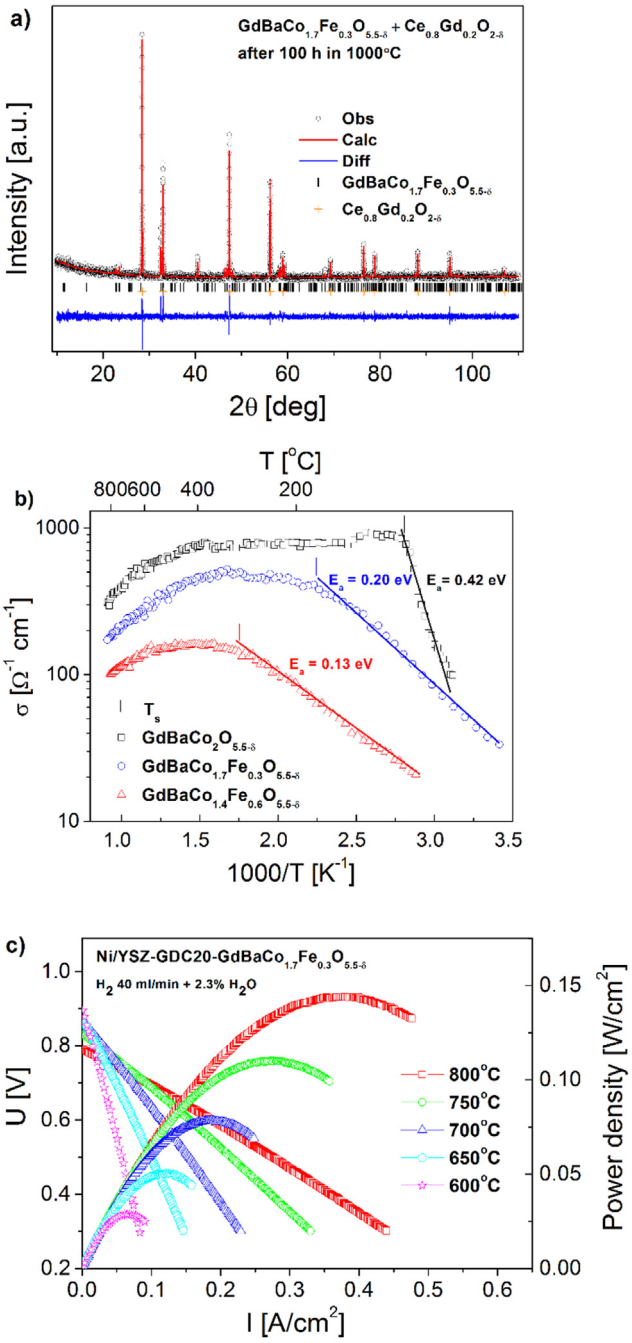


**Fig. 14 – (a) Chemical stability studies, (b) electrical conductivity and (c) electrochemical performance of the developed $GdBaCo_{1.7}Fe_{0.3}O_{5.5-\delta}$ in IT-SOFC. Figures b and c reprinted from Ref. [73], Copyright (2011), with permission from World Scientific Publishing Co Pte Ltd.**

particles. Several combinations of cathodes of this type were tested at ICSC (Institute of Catalysis and Surface Chemistry, Krakow). In all cases cathode performance improved when silver was added to the ceramic material [75,76]. Even in the case of a catalytically active material like BSCF ($Ba_{0.5}Sr_{0.5}Co_{0.8}Fe_{0.2}O_3$) the addition of silver led the fuel cell with the cathode made of Ag–BSCF composite to show higher power density than the cell with the cathode made of pure BSCF [75]. Moreover it was observed [76] that the half-cells with a silver

current collector showed lower ASR (area-specific resistance) than the half-cells with gold current collector, which is also suggestive of the catalytic effect of silver in ORR. An interesting solution was applied in the case of Ag–$La_{0:8}Sr_{0:2}MnO_{3-\sigma}$ composite. The ceramic matrix was prepared by mixing ceramic submicron particles with organic polymer beads and sintering. The ceramic matrix obtained was then saturated with $AgNO_3$ solution, dried and sintered again giving a composite with hierarchical pore structure, well dispersed silver nanoparticles and high catalytic activity in ORR.

## Anode materials

Beside the developments related to cathode materials, the research oriented at the development of novel anodic materials is done at AGH. This addresses the fuel flexibility of solid oxide fuels cells and provides a solution that assures effective work of SOFC fed by non-hydrogen fuels [77–79]. Instead of hydrogen, the use of non-hydrogen or carbon-containing fuels would considerably reduce the fuel cost and increase the feasibility of SOFC commercialization, especially for near-term adoption. One of the main challenges with SOFCs running directly on carbon containing fuels is carbon deposition on the anode, which results in a significant, and sometimes detrimental decrease in performance. Furthermore, carbon containing fuels contain sulfur (usually in the form of $H_2S$), which can dramatically degrade performance even at ppm levels. Prevention of carbon deposition and sulfur poisoning on the anode are considered key technical challenges. The works conducted led to the development of Mo/W-containing anode materials from $Sr_{2-x}Ba_xM_{2-y}(Mo,W)_yO_{6-\delta}$ (M = Mg, Mn, Fe, Co, Ni) group, suitable for application in IT-SOFCs and which can be fueled by carbon containing fuels.

## Interconnects – steel materials for SOFC

A substantial part of the work related to improving SOFC stacks relates to improvements in physicochemical properties of metallic interconnects.

The interconnect, also known as a bipolar plate, is used to connect individual fuel cells in series to form a stack; the net voltage of the stack is the sum of the voltages of individual cells. This element also provides mechanical support to the entire structure, and the channels located on both sides allow gaseous reagents to be transported to the anode and the cathode. Interconnects applied in intermediate temperature solid oxide fuel cells (IT-SOFCs) are manufactured from chromium-rich ferritic stainless steels (FSS) [80–83]. These steels have a thermal expansion coefficient similar to those of the ceramic elements of the cells, i.e., the anode, the cathode, and the electrolyte. They are also much cheaper than other metallic or ceramic interconnect materials. A major drawback of all metallic interconnects is their susceptibility to corrosion in media such as reaction gases. A protective $Cr_2O_3$ forms on the surface of ferritic stainless steels, and its thickness gradually increases with operation time [82–86]. Unfortunately, $Cr_2O_3$ reacts with oxygen and water vapor, forming volatile chromium oxides and oxyhydroxides, which may then react with the anode and cathode materials, affecting their catalytic properties. Cathodic material is especially vulnerable to this type of degradation. The drop in the power output of a fuel cell resulting from changes in the phase composition of the cathode material in known in the literature as cathode poisoning [87–89].

It is impossible to completely inhibit high-temperature corrosion of metal alloys, since the diffusion of reagents in the corrosion product layer, induced by the gradient of the chemical potential of the oxidant, cannot be prevented. However, the chemical and phase composition of the alloy can be selected in such a way as to allow the oxide product layer to maintain good contact with the metallic phase and to grow very slowly throughout the entire operation of the cell. If these conditions are met, then it is possible for the area-specific resistance (ASR) of the interconnect not to exceed the allowed maximum level (0.1 $\Omega\,cm^2$), even during long term operation. The increase in the internal resistance of a fuel cell causes its power output to decrease. Examples of ferritic stainless steels manufactured exclusively for application in interconnects include: Crofer 22 APU (Thyssen Krupp VDM GmnH), ZMG 232 (Hitachi Metals America, LLC), and SUS 430 (JX Nippon Mining&Metals).

There are limited possibilities of modifying the properties of ferritic stainless steels in metallurgic process. One of the barriers is the low solubility of metals that belong to the group of 'active elements' (Y, Ce, La, …) in ferrite (α-Fe phase); these metals decrease the growth rate of the $Cr_2O_3$ scale and improve its adhesion to the metallic phase. Further improvements in the oxidation resistance of ferritic steels can be achieved by applying selected surface-engineering methods, e.g., implantation of active element ions or deposition of nanoparticles of active element oxides on the surface of the steels [8,90,91]. Another approach utilizes protective-conducting coatings composed of oxide semiconductors with a structure of a perovskite [92–95] or spinel [85,96,97], or compounds such as M–Cr–Al–Y–O (where: M = Ti, Co and/or Mn) [98]. Such coatings serve more than one role; they are beneficial with regard to the oxidation resistance of the steel, and they inhibit the oxidation of chromium oxide to its volatile compounds.

Research on metallic interconnect materials at the Faculty of Materials Science and Ceramics, AGH University of Science and Technology has been ongoing since the mid-1990s. The subject was also investigated in cooperation with two globally renowned research centers: the Tokyo Institute of Technology in Japan and Forschungszentrum Jülich in Germany. Studies concerning the application of protective-conducting coating have focused on the modification of selected physicochemical properties of commercially available ferritic stainless steels to be applied in IT-SOFC interconnects. Among other things, it was demonstrated that metal/ceramics layered systems composed of a metallic substrate consisting of a ferritic stainless steel with a chromium content of up to 25 wt.% and a ceramic component comprising the protective-conducting coating, an intermediate reaction layer and a $Cr_2O_3$ layer, exhibit a lower area-specific resistance than the $Cr_2O_3$ scale formed on unmodified steel. The investigated substrate materials included the following steels: SUS 430 (ca. 16 wt.% of

Cr), DIN 50049 (ca. 25 wt.% of Cr), and AL453 (ca. 22 wt.% of Cr). The layered metal/ceramics systems were studied with the following types of protective-conducting coatings:

a) $(La,Sr)CoO_3$,
b) $(La,Ca)CrO_3$,
c) $(La,Sr)CrO_3$,
d) $Mn_{1.5}Cr_{1.5}O_4$,
e) X–Mn–Co–O (where: X = Cu, Y, Sm, Yb, Nd).

These studies made a significant contribution to scientific knowledge on metallic interconnect materials, as proven by the high citation index of papers from this period ([20] – 232 citations according to the Web of Knowledge, November 2015). Using transmission electron microscopy (TEM) and selected area diffraction (SAD), it was also demonstrated that a continuous $SrCrO_4$ reaction layer forms on DIN 50049 ferritic steel during oxidation in air at 1073 K due to the diffusion of strontium from the $(La,Sr)CoO_3$ layer to $Cr_2O_3$. Since the electrical conductivity of $SrCrO_4$ is higher than that of $Cr_2O_3$, the electrical resistance of this system is extremely low (5 mΩ $cm^2$) [99]. It should also be added that the oxide layer was deposited on the ferritic steel using the very cheap and simple screen printing technique.

In order to design interconnect materials for solid oxide fuel cells fueled by light hydrocarbons originating from natural sources of energy (natural gas, coal gas, biogas, etc.), layered systems such as $(La,Sr)CrO_3$/Fe–25Cr and $(La,Ca)CrO_3$/Fe–25Cr were examined. It was demonstrated that interconnect materials with deposited oxide layers with a perovskite structure is characterized not only by low area-specific resistance, but also by high chemical stability in the Ar–$CH_4$–$H_2O$ medium [100,101].

The transpiration method was used to investigate the kinetics of the oxidation of chromium oxide to its volatile compounds. It was demonstrated that an $Mn_{1.5}Co_{1.5}O_4$ layer with a thickness of ca. 30 μm deposited on the surface of AL453 steel causes the vaporization rate of chromium at 1073 K, in an atmosphere consisting of air enriched with water vapor, to decrease by 20 times. Moreover, this layer effectively decreases the area-specific resistance. Research conducted using electrochemical impedance spectroscopy for a cylindrical interconnect cathode system, in a steel/coating/conducting layer/cathode/conducting layer/coating/steel configuration, showed that area-specific resistance had decreased by an order of magnitude compared to the system without the oxide layer [102]. The cylindrical system also exhibited an area-specific resistance of ca. 0.025 Ω $cm^2$, which was nearly constant in time. This value was thus four times lower than the maximum value allowed for interconnects to be applied in IT-SOFCs. A disadvantage of the $Mn_{1.5}Co_{1.5}O_4$ spinel is its insufficient chemical stability, as the ferritic steel components and the components of the layer react with one another. In addition, in order to prepare a dense $Mn_{1.5}Co_{1.5}O_4$ layer on the surface of the steel via screen printing, complex thermal treatment is required, involving not only air, but also an Ar–$H_2$–$H_2O$ mixture. Consequently, new spinel coating materials were designed with the formula $X_{0.1}Mn_{1.45}Co_{1.45}O_4$, where X denotes a rare earth metal (Y, Sm, Yb or Nd). Studies of oxidation kinetics in air at 1073 K showed that the parabolic oxidation rate constant observed for steel coated with $Yb_{0.1}Mn_{1.45}Co_{1.45}O_4$ ($1.8 \times 10^{-14}$ $g^2/cm^4$ s) was lower by an order of magnitude than that in the case of uncoated steel ($1.7 \times 10^{-13}$ $g^2/cm^4$ s). This proves that the steel/ceramics layered system exhibits higher resistance to high-temperature corrosion than steel alone. The area-specific resistance of this system at 1073 K was 0.0174 Ω $cm^2$, and it was lower by more than one order of magnitude than the ASR of the material without the coating (0.2755 Ω $cm^2$).

The oxidation resistance of alloys forming the protective $Cr_2O_3$ scale can be significantly improved by implanting ions of active elements underneath their surface. It should be noted, however, that ion implantation is used mostly for the purpose of obtaining new insight. There is little interest in the practical application of this method due to high operating costs and limitations concerning the size and shape of the modified elements. Studies of oxidation kinetics performed in air and the Ar/$H_2$/$H_2O$ and Ar/$CH_4$/$H_2O$ gas mixtures at 1073 K demonstrated that the implantation of active element ions at a dose of $2 \times 10^{16}$ Y/$cm^2$ may reduce the corrosion rate of steel such as the commercially available DIN 50049 ferritic steel by as much as one order of magnitude [103]. The ASR values measured for scales formed on modified steel were over four times lower than the maximum value allowed for interconnects.

Materials for SOFC interconnects were investigated as part of the long-term scientific collaboration between AGH UST and the Forschungszentrum Jülich focused on corrosion studies. These materials included the oxide dispersion strengthened (ODS) Cr–5Fe–1%$Y_2O_3$ alloy, which was oxidized in an $H_2$/$H_2O$ gas mixture at 1273 K. It was observed that this material, which featured $Y_2O_3$ particles with a size of up to 1 μm, gained mass at a rate that was five times higher than that for an alloy with $Y_2O_3$ particles no larger than several dozen nanometers. After 100 h of oxidation, the mass gains were 2.5 and 0.5 mg/$cm^2$, respectively. It was also shown that the implantation of yttrium ions at a dose of $10^{16}$ Y/$cm^2$ underneath the surface of both alloys caused them to exhibit the same mass gain of ca. 0.2 mg/$cm^2$ after 100 h of oxidation.

Nickel does not undergo corrosion in the anode gas environment, since the dissociation pressure of NiO is higher than that of $O_2$ in the $H_2$/$H_2O$ gas mixture. It precisely for this reason that selected support elements of the fuel cell, such as meshes, are manufactured from nickel. Designing a multilayer interconnect with nickel on the cathode size proved to be a rather complex issue [104]. Studies conducted for Ni/FeCrAl sandwich systems in Ar/4% vol. $H_2$/3% vol. $H_2O$ at 1073 K showed that a significant increase in the area-specific resistance was observed with time. This increase was due to the internal oxidation of silicon and magnesium, which diffused along grain boundaries in the FeCrAl alloy to the surface of nickel. Numerous precipitates of these oxides, located near grain boundaries, formed an insulating layer that inhibited the flow of electric current.

## Novel fabrication techniques

Development trend of solid oxide fuel cells concentrate on lowering the operation temperature from around 800 °C to a

range of 750 °C–700 °C. Lowering the temperature causes electrode polarization resistances to increase, thus novel materials or preparation methods must be sought to counteract these losses. Application of nanocrystalline ceramics and functional thin films can have a beneficial effect on fuel cell performance.

The team from Gdansk University of Technology was from the beginning centered on novel fabrication technologies for ceramic layers. This included spin coating of polymeric precursors and "net-shape" technology [105] and was followed by the development of spray pyrolysis as deposition methods. This is used to produce unique nanocrystalline ceramic films at relatively low temperatures.

Spray pyrolysis deposition method, employing metallo-organic precursors, enables the production of nanocrystalline, thin and homogeneous layers without requiring high temperature processing. The morphology and structure (porosity) of the films can be controlled by tailoring deposition parameters (temperature, time, nozzle distance). The group's experience shown that it is possible to produce up to 500 nm thick layer of electrolyte in a single deposition step [106]. Thicker layers can be prepared by a multi-step deposition procedure. Any materials for which appropriate precursors are available can be in principle deposited (YSZ, CGO, LNF, LSM, etc.). Typically, the deposition occurs on a heated substrate (Fig. 15), with the surface temperature not exceeding 400 °C. After the deposition films require heat treatment to remove residual organics, but this takes place at a maximum of 900 °C.

In Fig. 15, a fracture cross-section of an anode supported cell is presented. On a sintered NiO–YSZ anode support, a thin electrolyte layer was deposited by spray pyrolysis. Its thickness is on average less than 1 μm and it covers the surface uniformly. Maximum processing temperature after the substrate sintering did not exceed 900 °C, whereas normally electrolyte sintering requires temperatures >1250 °C. Spray pyrolysis shows great potential in the production of very thin electrolytes for fuel cells.

On the back of previous studies new methods were proposed by the GUT team for lowering the cathode polarization by introducing a thin and dense cathode interfacial functional layer. It is generally accepted that the cathode overpotential is the dominating one regarding the functioning of the solid oxide fuel cell. Activity is oriented at improving the contact between the electrolyte and the cathode, which should decrease the resistance of the interface.

Thin perovskite cathode interfacial layers were fabricated using spin coating of metallo-organic precursors. Fracture cross-section of an electrolyte–cathode interface with an interface layer deposited in-between is shown in Fig. 16. By careful investigations of the effects of thickness, the microstructure and the composition of the layers, it is possible to decrease the resistance of the interface at the same temperature by at least 20% [107]. This is directly related to increasing fuel cell performance (Fig. 16). Still, many different interfacial layer material combinations can be studied with a view to enhancing these effects even more and thus leading to lowering the operating temperature while retaining the power output.

Work oriented on new materials for SOFC includes oxide-based materials [108], cathode materials [109] and studies related to catalytic activity of electrodes towards fuel cells operating on biogas [110].

## Pilot scale SOFC

Since 2004 the Ceramic Department (CEREL) at the Institute of Power Engineering has worked consistently to improve methods of producing solid oxide fuel cells, and has developed new competitive techniques for scaling up production. Steady progress was made during this period leading to pilot-scale preparation of ESC (electrolyte supported cell) and ASC (anode supported cell) types of SOFC [111]. ESC (Fig. 17a) gains its main mechanical strength from 100 to 200 μm thick electrolyte, with 30 μm thick anode and cathode layers. In the ASC configuration (Fig. 17b), mechanical strength is derived from 500 to 1000 μm thick anode. As the mechanical function of the electrolyte is no longer needed in these configurations, very thin 5 μm electrolyte layers can be used, resulting in reduced

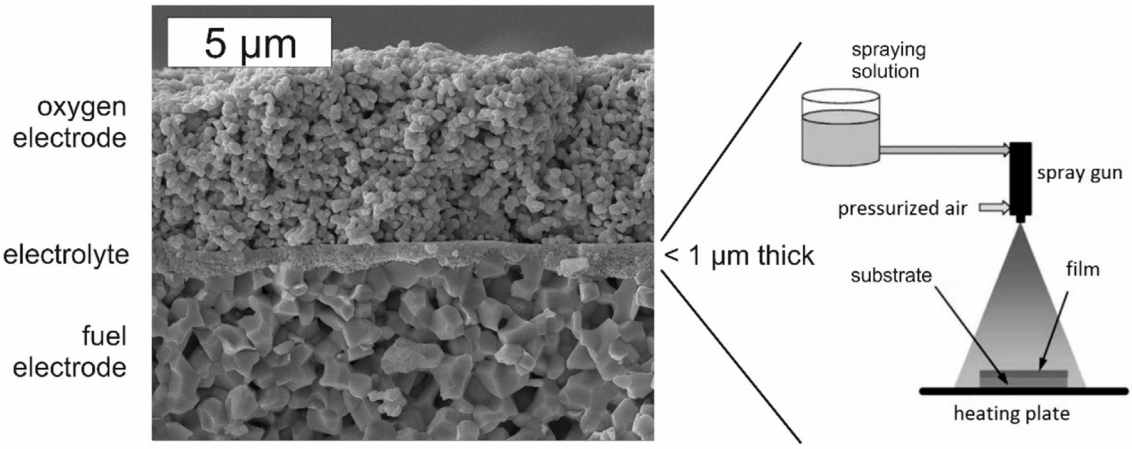


**Fig. 15 – Anode supported fuel cell with 1 μm nanostructural YSZ electrolyte fabricated by spray pyrolysis method and a schematic of spray pyrolysis apparatus.**

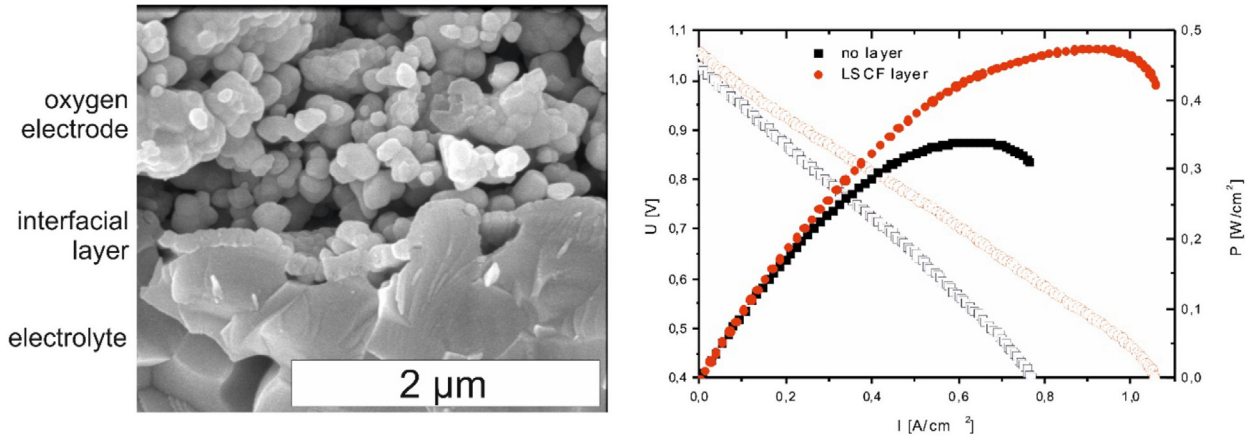


**Fig. 16 – SEM fracture cross-section image of the cathode–electrolyte interface with 150 nm cathode functional layer and its influence on fuel cell performance.**

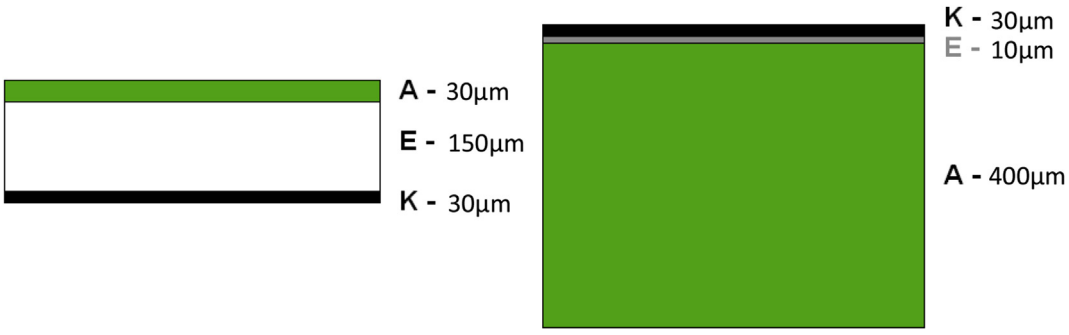


**Fig. 17 – Construction and relative thickness of two types of cells: ES-SOFC (left) and AS-SOFC (right).**

ohmic resistance and significantly increased power of the full cell. Cathode thickness is 30 μm.

### *Electrolyte supported solid oxide fuel cells (ES-SOFC)*

Electrolyte supported solid oxide fuel cells are manufactured in IEn OC CEREL using two technologies. Electrolyte is made by tape casting, whereas anode and cathode layers are applied by screen printing.

Full 100 mm × 100 mm ES-SOFCs are shown in Fig. 18. The electrolyte is made from 3 mol% $Y_2O_3$ partially stabilized $ZrO_2$ (3YSZ), the anode is made from a mixture of nickel oxide (NiO) and electrolyte material, and the cathode is made from perovskite material (LSM) and electrolyte material (3YSZ).

Manufactured cells were tested. The results of electrical measurements are shown in Fig. 19a and the electrical test rig, designed and manufactured in IEn OC CEREL, in Fig. 19b. For comparison, a commercially available ECN fuel cell was tested.

### *Anode supported solid oxide fuel cells (AS-SOFC)*

In IEn OC CEREL anode supports for AS-SOFC are produced by two different methods: traditional method of tape casting and more novel high-pressure injection molding. AS-SOFC configuration is shown in Fig. 20.

Currently, all of AS-SOFC supports at CEREL are made by high-pressure injection molding (Fig. 21).

Other necessary layers are produced using a screen printer or ink-jet printer.

The CEREL team produces complete fuel cells of various sizes and shapes (Fig. 22a):

- rectangular 50 × 50, 100 × 100 $mm^2$ made by high-pressure injection molding
- circular with variable diameters up to ø100 mm made by high-pressure injection molding and laser cutting

The microstructure of the produced cell is shown at Fig. 22b.

AS-SOFCs made by the above methods were electrically tested (Fig. 23).

Maximum power density obtained was 1.25 W/$cm^2$ at 800 °C [112].

The expected fields of activity include the development of modern low temperature deposition technologies which will pave the way for future research in solid oxide fuel cells.

## Metal supported solid oxide fuel cell (MS-SOFC)

The issue of the mechanical stability of fuel cells requires new solutions to ensure high durability. Recent studies in Poland focused on the development of metallic supports for high temperature fuel cells. Beside the interest in the

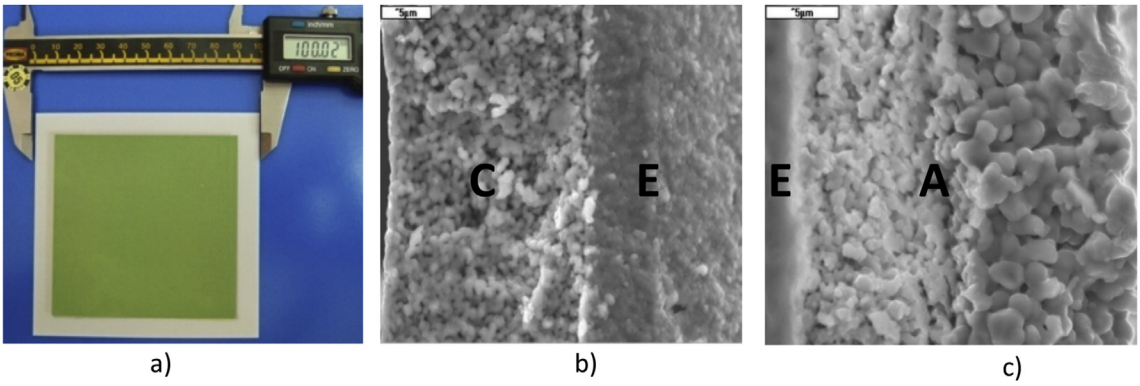


**Fig. 18 – ES-SOFC a) anode view b) cathode and electrolyte c) electrolyte and anode microstructure.**

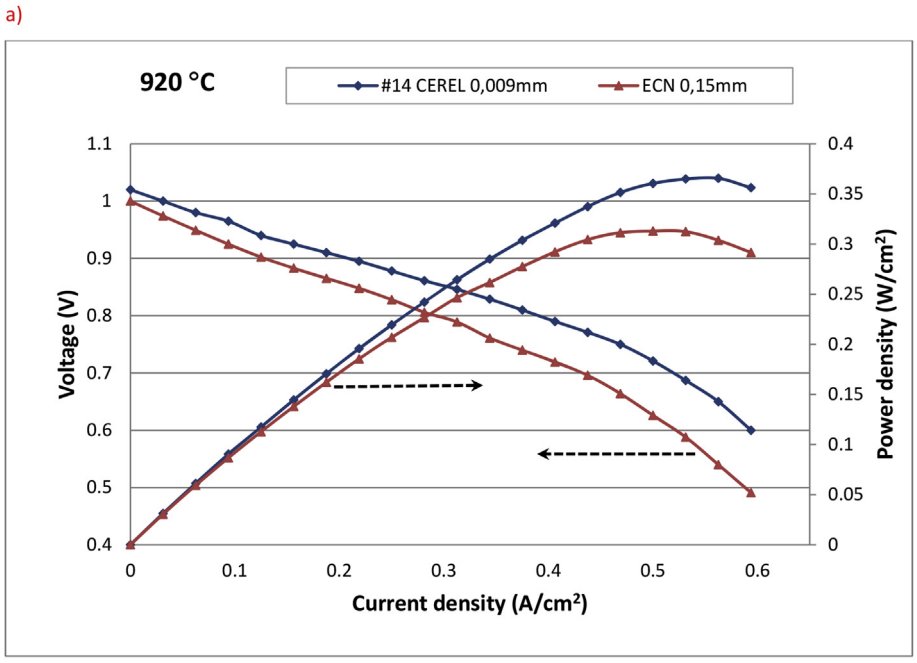


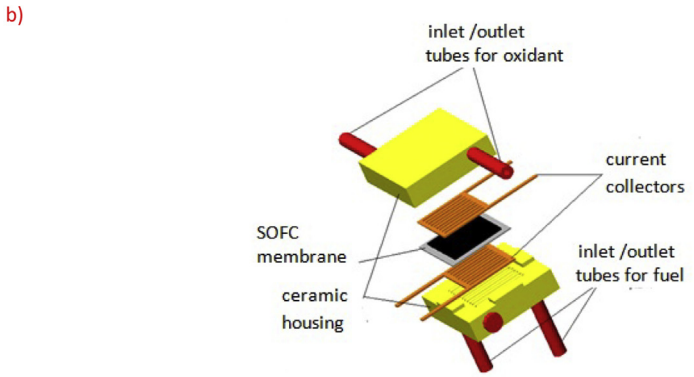


**Fig. 19 – Electrical measurement of ES-SOFC. a) Voltage–current density characteristics [112], b) electrical test rig [113].**

fabrication of such supports, a substantial part of the research was oriented at resolving key problems related to high temperature corrosion of metallic alloys used in the support and interconnects [115]. Porous metal supported cells are regarded as next generation solid oxide fuel cells [116]. However, their widespread introduction is hindered by rapid corrosion of porous supports due to the enhanced surface to volume ratio and limited chromium reservoir [117]. An example of a Hastelloy X alloy oxidized for 100 h at 800 °C in air is presented in Fig. 24.

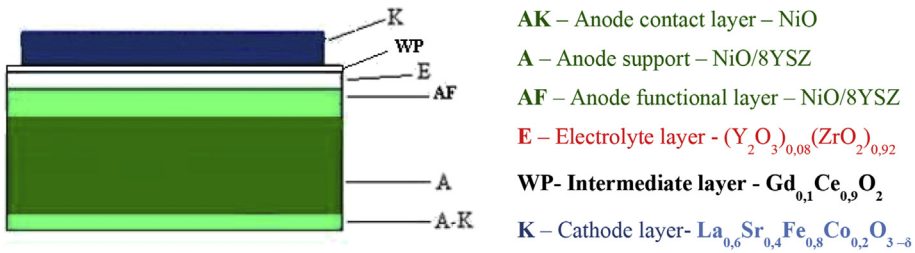


**Fig. 20 – Diagram of AS-SOFC made in IEn OC CEREL.**

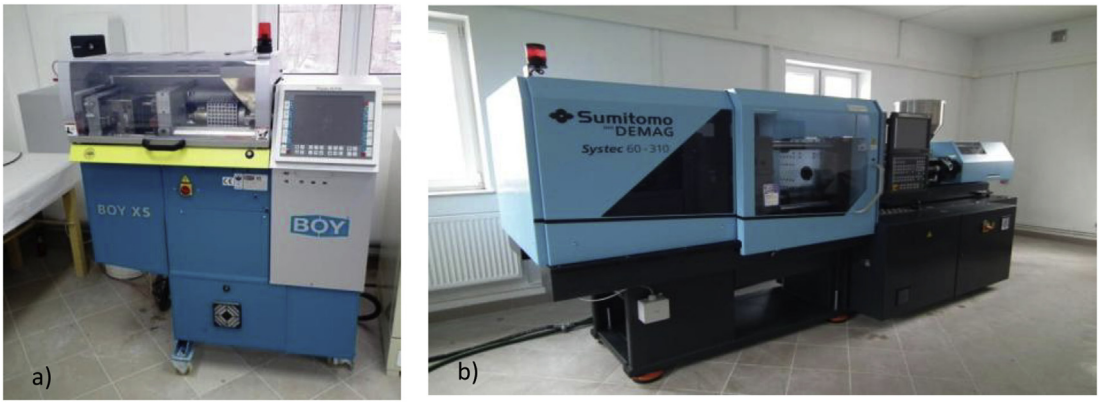


**Fig. 21 – High-pressure injection molding devices for production of anode supports a) Boy's BOY XS, b) Sumitomo-DEMAG's Systec 60-310.**

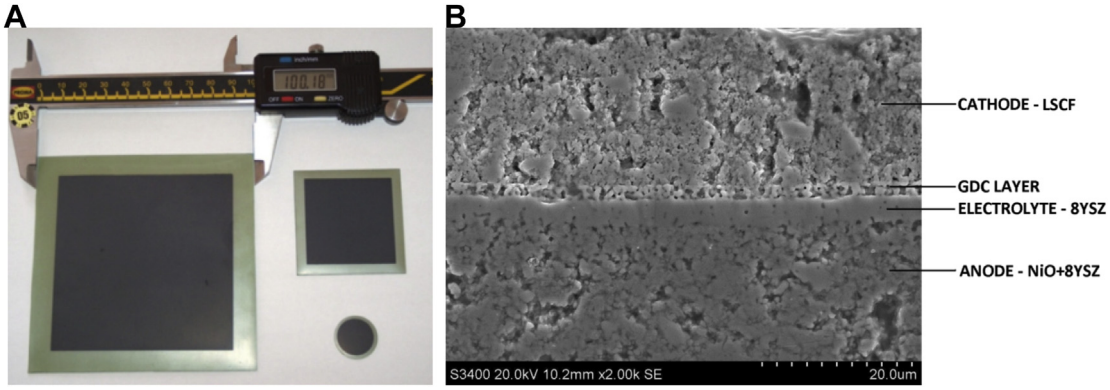


**Fig. 22 – a) Examples of AS-SOFC made at IEN OC CEREL b) Cross section of AS-SOFC.**

The sample shows the formation of large amounts of $Cr_2O_3$ oxide, already filling to a large extent available pore space and thus lowering the porosity and gas permeability of the support. Several different alloy materials in the porous state have been studied [118–120] for their high temperature corrosion and successful protective coatings for porous materials have been proposed by the GUT team.

Corrosion of fuel cell interconnects is an important degradation phenomenon when considering the lifetime of the fuel cell stacks. Corrosion on the hydrogen side and especially applications of protective coatings on the hydrogen side of the interconnect is a relatively new field of research. The group is evaluating thin $CeO_2$ coatings deposited by spray pyrolysis on Crofer 22 APU steel as possible protective coatings as shown in Fig. 24 [121]. Compared to the uncoated interconnect, ceria slows down oxide growth and offers a longer lifetime for the interconnect.

## Direct carbon fuel cells (DCFC)

Direct carbon fuel cell (DCFC), directly fueled with carbonaceous fuels, is a technology for high efficiency conversion of carbon fuel chemical energy into electrical energy, through electrochemical reactions, without combustion. The development of that fuel cell technology of due to high energy conversion efficiency can help to reduce emissions of pollutants such as $NO_x$, $SO_2$ and fly ashes.

Hard coal is the main raw material for energy production in Poland. Increasingly stringent EU regulations concerning $CO_2$

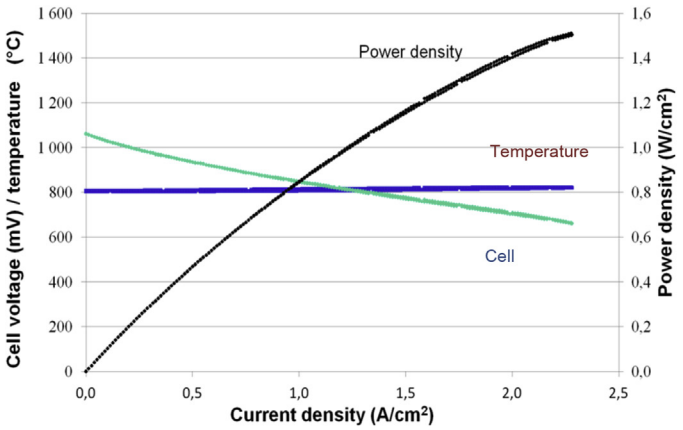


| Temperature [°C] | OCV [mV] | ASR [Ωcm$^2$] | Max power density [W/cm$^2$] | Hydrogen flow [ml/min] | Oxidant flow [ml/min] |
|---|---|---|---|---|---|
| 650 | 1062 | 0.80 | 0.25 | 400 | 498 $O_2$ + 1843 $N_2$ |
| 750 | 1048 | 0.20 | 0.77 | 400 | 498 $O_2$ + 1843 $N_2$ |
| 800 | 1061 | 0.25 | 1.50 | 1000 | 420 $O_2$ + 1580 $N_2$ |
| 850 | 1026 | 0,15 | 1,37 | 400 | 498 $O_2$ + 1843 $N_2$ |

**Fig. 23 – Results of electrical testing of AS-SOFC [114].**

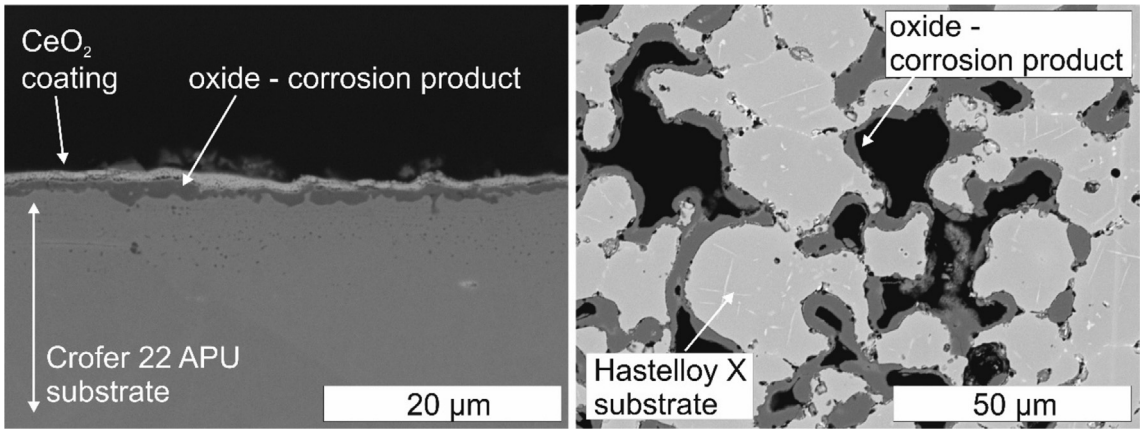


**Fig. 24 – Polished cross-sections images of dense Crofer 22 APU steel coated with $CeO_2$ protective layer and oxidized at 800 °C for 1000 h in humidified hydrogen and porous Hastelloy-X alloy oxidized at 800 °C for 100 h in air.**

emissions and the environment are driving intense research into clean coal technology. The solution of choice is direct carbon fuel cell (DCFC) technology [122]. Investigations into the construction of DCFCs have been undertaken since 2010 by a consortium composed of the Institute of Power Engineering (IPE), AGH University of Science and Technology, ICSC and several industrial partners, with promising preliminary results. The consortium aims to demonstrate coal-fueled fuel cell technology on a scale enabling technical evaluation. On the basis of preliminary evaluations, solid oxide fuel cell (SOFC) technology has been selected by the consortium for further development. In the consortium, AGH has been working on boosting DC-SOFC performance through developing SOFC materials, catalytic additives to specific layers and fuels as well as carbon modification techniques [123–126]. ICSC has concentrated on direct carbon molten carbonate fuel cell technology development [127].

IEN has focused on scaling up the direct carbon solid oxide fuel cell (DC-SOFC) technology to the semi-industrial and industrial level. To date, successful operation of 16 cm$^2$ active

area cells fueled by biomass charcoals [125], catalyzed activated carbon [128], lignite and $CO/CO_2$ gaseous mixture [129,130] has been reported. The anode processes, including gas exchange mechanisms, have been studied at IEN (Fig. 25) [130] and stable operation of DC-SOFC at up to 100% fuel utilization in a batch-mode has been achieved (Fig. 26) [128].

## Selected developed solutions for SOFC and their applications

Solid oxide fuel cells offer a great advantage in stationary applications. In order to benefit from the high achievable efficiency, single cells are put together to form a stack. Full-scale stacks can be employed directly as an electric power generator or optionally can be embedded in a co-generative power unit.

The Institute of Power Engineering (IEn) has been working on its original solid oxide fuel cells (SOFC) stack since 2007, developing three generations of the prototype stacks. The first prototype SOFC stack was designed, assembled and tested in the scientific network POLSTOS – Poland Fuel Cell Technology and was named a 1st generation stack. It was dedicated to planar SOFC of dimensions 50 × 50 mm and operating temperature range from 750 to 800 °C. The inlet and outlet pipes were located in the middle of the system. The air and fuel flows were directed to the intermediate chamber and then to the manifolds. The biggest drawback of this design was the high risk of leakage in the internal gasket.

The 2nd generation SOFC stack was assembled in 2010, the result of further development. Design work was supported by CFD modeling [131] in order to secure proper flow distribution under electric load conditions and under high utilization conditions. Additionally, several modifications of the internal gasket and manifolds were implemented, but the same planar SOFC and operating temperature range were applied. Fuel cell stack technology was further developed under the Strategic National Programme (2010–2015) "Development of integrated technology of fuels and energy production from biomass, agricultural and other wastes".

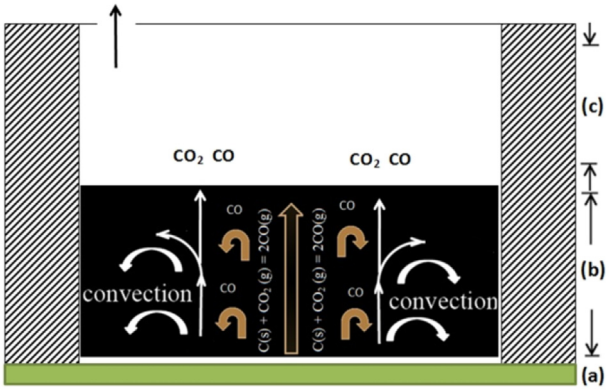


**Fig. 25 – Convection mechanism induced by the reverse Boudouard reaction: (a) lower pressure in interface anode/carbon bed, (b) higher pressure in carbon bed, (c) lower pressure above carbon bed. Reprinted from Ref. [130], Copyright (2015), with permission from Elsevier.**

The 3rd generation SOFC stack, developed in 2014, differs significantly from the previous ones. It was designed to operate at a lower temperature range of 600–700 °C and to apply commercially available full size AS-SOFCs of dimensions 110 × 110 mm. Lowering the operating temperature translated into lower production costs of the stack compared to high-temperature technology, especially in terms of the fabrication of interconnects and seals. Modular construction of the stack with a low number of elements is more suitable for mass production. The power of the 3rd generation stack can be easily increased through increasing the number of single repeating units. The stack housing includes its own pressurized system and has targeted operation at high power density. In this design the crossflow of processing gases was abandoned in favor of a counter-flow or co-flow working mode, due to the uneven temperature distribution on the electrode surface. This innovative solution for the gas flow system makes the stack more thermally efficient than other reported works, which is one of its best advantages. Another advantage is the minimal thickness of the interconnects (<1 mm), so the height of single repeating unit (SRU) of the stack is about 1.5 mm which results in lowering thermal capacity and increasing volumetric power density of the whole system.

The concept of the 3rd generation SOFC stack (Fig. 27) is the subject of an international patent application. Presently IEn owns European Patent [132] which concerns short SOFC stacks (internal fuel and air manifolds) and full size SOFC stacks (open air size). The Institute of Power Engineering possesses laboratories and a long list of existing equipment, machinery with application to SOFCs: single cell test setup, SOFC short stack (up to 300 W) test stand and 700 W–2500 W SOFC stacks test sites.

Parallel to the development of the stack design at IEn, some supporting research activities were conducted concerning the materials of interconnect and seals, the most crucial elements of the stack beside the SOFC.

The first two generations of the IEN stacks were based on Haynes® 230® alloy – a key structural material. However, electric resistance of the scale for this steel was found to be too high and unstable. The stack of 3rd generation was developed using Crofer® 22APU. This is a steel alloyed with ~22% of chromium and some minor quantities of REE targeting high stability to oxidation and low resistance of scale, designed especially for SOFC application. However, for such types of steels a typical phenomenon "chromium evaporation" is observed, which leads to chemical transfer of volatile $Cr^{VI}$ compounds to the cathode and thus poisoning of the electrode. To prevent this process special protective ceramic layers, known as "chromium barriers", must be applied on the cathode side of the interconnect. Analysis of the published data pointed to $(Mn,Co)_3O_4$ spinels as the most appropriate material for the protective layer. During 2014–2015 low-cost technology was elaborated to form a protection layer from $Mn_{1.5}Co_{1.5}O_4$ on corrugated plate from Crofer® 22APU.

The interconnects for the 3rd generation stack were fabricated by the cold stamping method, which gave a strong positive effect on production costs, but also emphasized the problem of the contact between the interconnect and the cathode. Relatively low precision of the stamping coupled

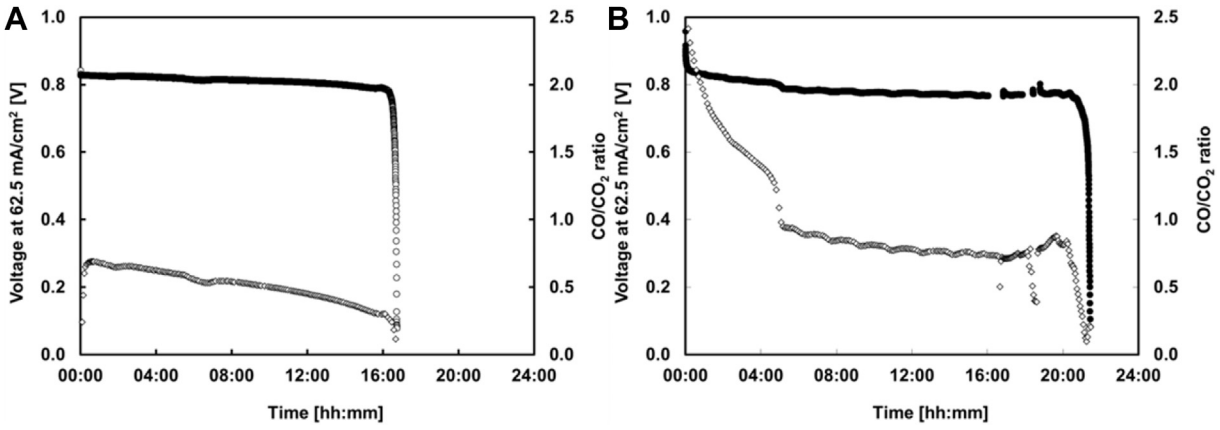


**Fig. 26 – Evolution of DC-SOFC voltage and $CO/CO_2$ ratio in exhaust stream for at constant current load (62.5 mA/cm$^2$) (a) Case A – anode impregnated with $Fe_2O_3$, fuel not impregnated and (b) Case F – standard anode with carbon impregnated with $Fe_2O_3$; temperature 1123 K; anode gas inlet: none; cathode gas: air. Reprinted from Ref. [128], Copyright (2015), with permission from Elsevier.**

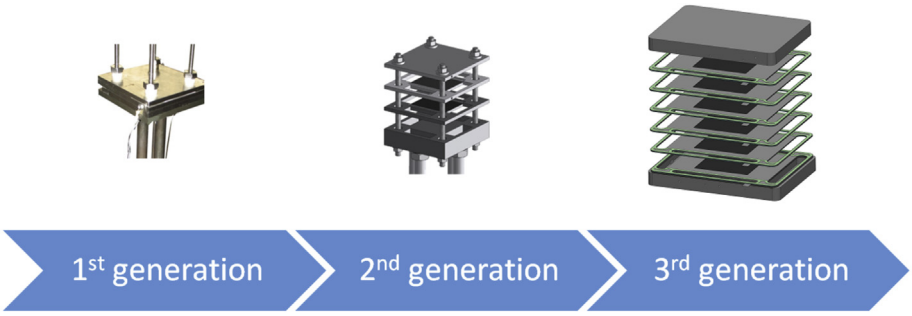


**Fig. 27 – Development of SOFC stack technology at the Institute of Power Engineering.**

with imperfect flatness of the cells raised a requirement for a special layer of "contact helper" – oxide material of high conductivity which should be applied on the tops of the interconnect ribs to ensure good electric contact between the interconnect and the cathode. This problem had no obvious solution for the 3rd generation stack, because in addition to good conductivity, the contact helper should demonstrate sinterability in conditions of the SOFC assembly and operation, which means short term heating up to 750 °C and operation below 700 °C. A set of commercially available materials was tested in a specially designed setup (Fig. 29). The setup enables simultaneous measurement of two samples using the pseudo-4-probe technique at temperatures up to 900 °C in continuous totally automated mode. Small Crofer® 22APU (active surface 0.785 cm$^2$) coupons covered with a protective layer and contact helper were treated at conditions which reproduce SOFC assembly and operation, including temperature profiles and applied forces. As a result, a $(La_{0,60}Sr_{0,40})_{995}Co_{0,20}Fe_{0,80}O_{3-d}$ solid solution was selected for production, but the search for novel, more "sinterable" oxides is still ongoing. Area specific resistance of the samples with this contact helper was found to be in the range 4–3 mΩ cm$^2$ *vs.* polished Pt in a temperature range 650–680 °C.

Lowering the operating temperature of the stack to 650–700 °C simplified the fabrication of seals, which are usually a crucial challenge for stack design. The function of seals is to prevent the air and fuel from mixing and to separate the processes running on the cathode and anode sides of SOFCs, enabling stable work of the stack. There are few commercially available materials that meet the precise requirements (such as stability at high temperature, chemical resistance, adequate thermal expansion coefficient) and one of the most popular is a specially designed glass. The design of the 3rd generation stack gave the seals another function too – mechanical support between the single repeating units which determines the correct distance between the following interconnects. For to this reason a composite material was manufactured, consisting of glass and mica layers, and successfully applied in the assembled stacks, as can be seen in the photos of the stack after thermal treatment (Fig. 28). The seals were fabricated from a supplied glass powder, by means of tape casting, lamination and laser cutting, which all was done at the laboratories of IEn. The manufactured seals were also tested in a specially designed setup for measuring gas permeability in defined temperature and pressure ranges, equivalent for SOFC stack operating conditions.

The Institute of Power Engineering was responsible for the development of the first-of-a-kind micro-combined heat and power unit. To achieve that goal the National Center for Research and Development funded the National Strategic Programme particularly dedicated to this initiative. This initiative was oriented on resolving key issues at the level of

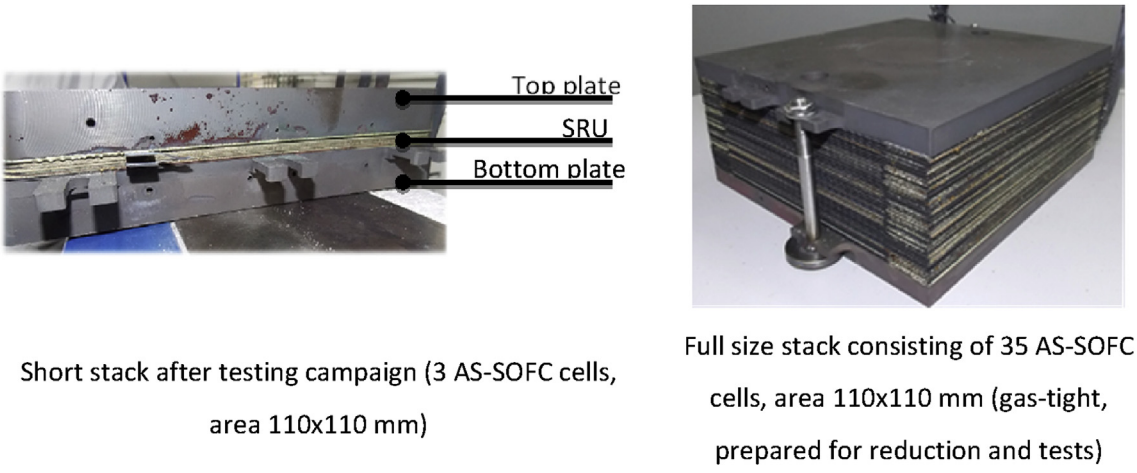


**Fig. 28 – Photos of SOFC stacks developed and assembled at the Institute of Power Engineering.**

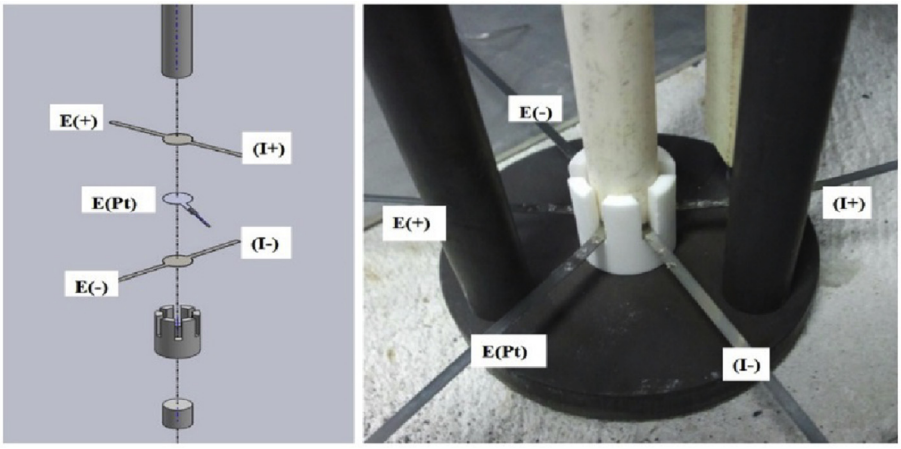


**Fig. 29 – Sample holder for measurements of the area specific resistance of the ceramic layers on steel at elevated temperature [133].**

single cell, short stacks, full-scale stacks, system design and operation. As an effect, the Institute of Power Engineering completed the task related to defining the conceptual design of the first Polish micro-combined heat and power unit with solid oxide fuel cells.

Originally, several alternatives were under consideration, including different fuel processing systems, optional fuels [134], and different methods for achieving high electrical efficiency by elevating the overall fuel utilization [135].

The modeling activities were followed by design and construction of the unit. It was customized to operate on pretreated biogas. Adaptation of the fuel processing system, which is based on a steam reformer, makes it possible to utilize other gaseous and liquid fuels, including natural gas. The electric and thermal output of the system, up to 2 kW and about 2 kW, respectively, corresponds to the typical requirements of a detached dwelling or a small commercial site. The functionality of the system was increased by engaging two separate start-up modules which are used for preheating the system from the cold state to nominal working conditions. The first module is based on a set of electric heaters, while the second module relies on an additional start-up burner.

The system is shown in Fig. 30, in which the two identical SOFC stack connected in-series can be seen. This type of connection offers several benefits and allows high overall fuel utilization without involving an advanced recirculation machine, such as a high temperature blower [136].

Basic specification of the unit is summarized in Table 1.

The fuel flexibility of the system is currently under investigation. Further work is oriented at adaptation of the fuel processor to operate with a wide range of fuels, including liquid and gaseous.

The Electrotechnical Institute, Wroclaw has for many years been working on electrolytic and electrode materials for use in SOFC [137,138] as well as concrete projects and individual research cases using the developed materials (Fig. 31A and B). Due to the special nature of superionic conductors (electrolytes), the IEL is also carrying out an application analysis of their potential use in electrochemical devices: oxygen sensor and pump (Fig. 31C) as well as a high temperature SOEC electrolytic cell (Fig. 31D).

Latest research conducted in the Unconventional Sources of Energy Laboratory focuses on application of $CO_2$ in a SOEC electrolytic cell to produce synthetic gas substrates.

**Fig. 30 – Micro-combined heat and power unit with SOFC, design and constructed in the Institute of Power Engineering.**

**Table 1 – Specification of the micro-combined heat and power systems designed and constructed in the Institute of Power Engineering.**

| Item | Value |
|---|---|
| Nominal electric power, kW | 2.0 |
| Thermal power, kW | Up to 2.0 |
| Electric efficiency, % | in range 32–44 |
| Overall efficiency, % | >80 |
| Dimensions (H × L × D), mm | 1875 × 1370 × 1479 |
| Weight, kg | ca. 700 |
| Fuel type | Biogas (cleaned), hydrogen/nitrogen mixture |
| Hot water storage tank capacity, l | 140 |
| Water temperature, °C | 30–70 |
| Power supply during start-up (electric heaters), V | 1 × 400 |
| Power supply during start-up (electric heaters), A | 18.5 |
| Type of thermal insulation | Micro-porous, mineral wool |
| Gas connections, mm | hydrogen: 6<br>nitrogen: 6<br>methane: 6<br>carbon dioxide: 6<br>air: 12 |
| Water connection, inch | ¾ |
| Sensors | 49 N-type thermocouples<br>13 precise pressure transducers<br>Set of mass-flow regulators |

Beside the ability to efficiently generate electricity in stationary application, recent advances in SOFC technology proved the applicability of the cells in the aviation industry. In the Institute of Aviation Warsaw a few thousand flights of medium range aircraft were analyzed in terms of emissions. Through this study, it was demonstrated that, at present, quantitative emissions during a typical three-hour flight are as follows: $NO_x$: 115 kg, CO: 38 kg, $CO_2$: 30,000 kg [139]. The aviation development strategy presented by both the Advisory Council for Aviation Research and Innovation in Europe (ACARE) and by the National Aeronautics and Space Administration (NASA) assumes, within the next four decades, a drastic reduction in mission energy consumption, reduction in carbon oxides and nitrogen oxides ($NO_x$) emissions, as well as a significant reduction in noise generated by aircraft. The key assumptions of the Vision for European Aeronautics in 2020 of the ACARE are an 80% reduction in $NO_x$ and a 50% reduction in $CO_2$ [140]. According to the Strategic Research and Innovation Agenda (SRIA) the $CO_2$ emission reduction can be achieved by improving propulsion and power systems, airframe, air traffic and aircraft operations [141]. Regarding the propulsion and power systems of aircraft, current development of the aviation sector is moving towards the More Electric Aircraft (MEA) concept concerning reduced fuel use and emissions on the ground and in flight operations [142]. The idea of MEA architecture is not only to replace onboard subsystems like pneumatic and hydraulic installations by full-electric ones, but mainly by introducing electric systems as a source of propulsive force [143]. For general aviation, the use of fully electric systems powered by rechargeable batteries is being considered. However, to drive larger aircrafts hybrid and turbo-electric systems are being taken into account. These systems would involve non-Brayton power generation or/and storage sources that would provide additional propulsive energy to a conventional Brayton cycle powered turbofan engine. Currently, aircraft power generation is typically carried out by engine-driven generators, reducing the power available for the flight, ram air turbines (RATs) and auxiliary power units (APUs) with low efficiency and generating a lot of heat, noise and $CO_2$ emissions [143]. Considering powering aircraft and subsystems as a key area for improvement, the MEA idea offers new opportunities that can take advantage of advances in electrical power generation technology including advances in fuel cells. That can result in supplementing power distribution systems and subsystems on board commercial aircraft, ram air turbine (RAT) and auxiliary power units (APU) by fuel cell technology, which currently has limited use in aviation [142].

Current research and development in fuel cell application in aviation focuses on two types of fuel cells: polymer electrolyte membrane (PEM) and solid oxide fuel cells (SOFC). For the purpose of this study only solid oxide fuel cells (SOFC) will be considered, due to the high operating temperature and flexibility in terms of using different types of fuel. Implementing SOFC as an additional energy source for aircraft can deliver potential advantages, like efficient energy conversion by reducing electrical power transmission losses, reduction in aircraft engine size or fuel burn, leading to increase in fuel efficiency and consequently lower $CO_2$ emission.

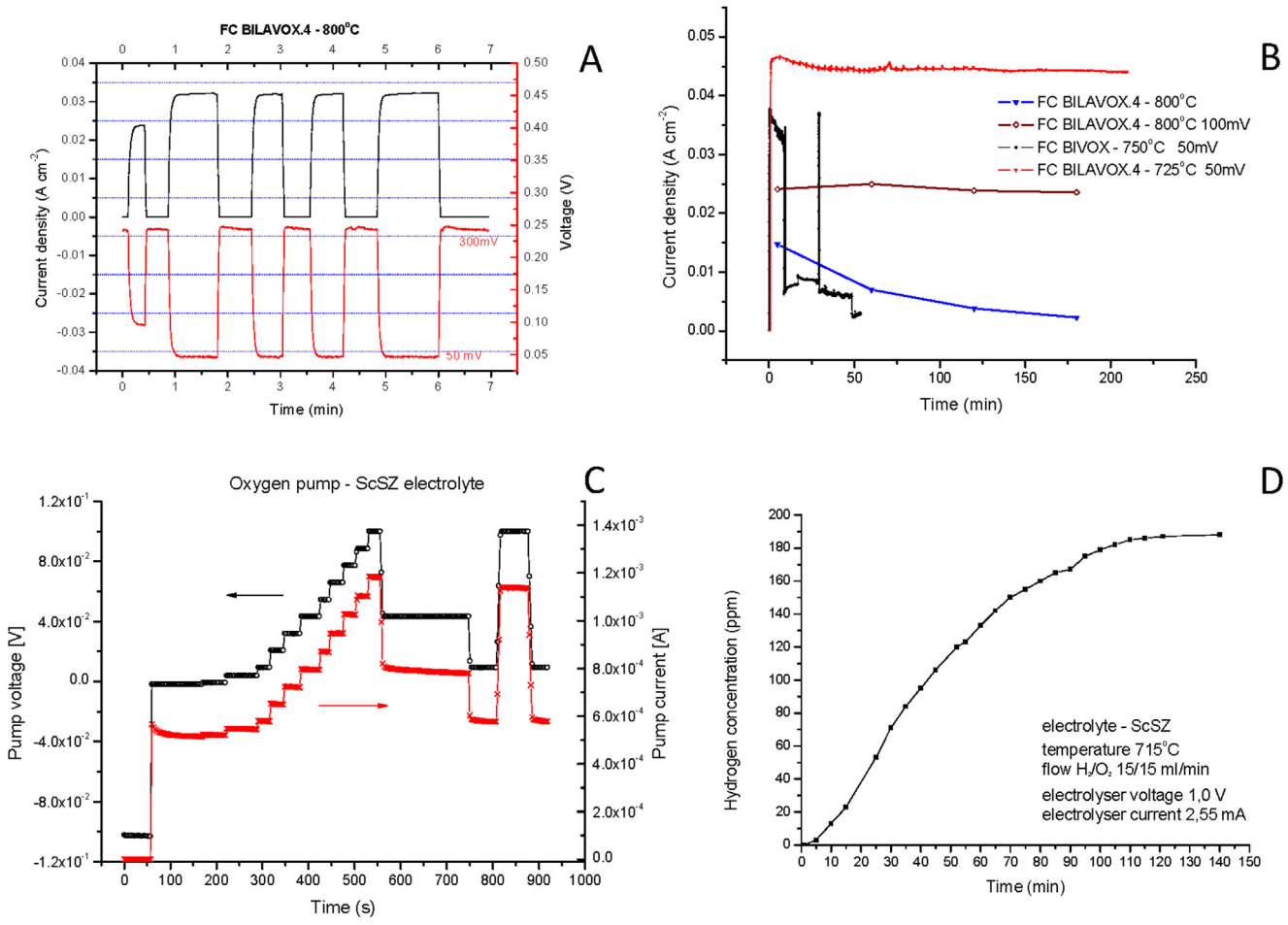


**Fig. 31 – Selected research results of particular electrochemical devices (A and B – SOFC cell, C – oxygen pump, D – SOEC cell).**

In response to the above strategies the Institute of Aviation, Warsaw is running a project to analyze the possibility of using full-electric, hybrid and turbo-electric technologies for future aircraft propulsion systems. The main goal of this project is to develop a tool in the Numerical Propulsion System Simulation (NPSS) environment capable of modeling different electric, hybrid and turbo-electric system architectures. The main advantage of the numerical modeling over experimental measuring is the efficient and cost-effective investigation of the overall system performance and efficiency [144]. NPSS is an object-oriented, engineering design and simulation environment developed to model air-breathing systems. It enables development, configuration, modeling and integration of various user-defined system elements and functions including thermodynamic and rocket propulsion cycles models. Object-oriented modeling is performed by employing software libraries in respect of different elements, which define the behavior of various engine components. Components such as inlet, compressor, burner, turbine, nozzle, motor, shaft etc. can be assembled by a user-defined method to model the required propulsion system. NPSS environment does not provide libraries of elements such as: batteries, fuel cells, generators, electric motors, power busses etc. However, NPSS provides a possibility to model, develop and add new libraries of created elements to the software. User defined functions are implemented using the C++ programming language.

Considering fuel cells as a promising alternative power source for use in aviation in military and commercial aircraft systems and subsystems, the model will be developed to evaluate the performance of the system, including the submodel of the fuel cell. According to the assumptions and requirements of the described project, the model will be implemented on the basis of solid oxide fuel cell (SOFC) technology. That particular fuel cell is optimal in this system configuration due to its very high overall efficiency and generation of high quality exhaust heat that is used to increase system efficiency and provides effective energy conversion [144,145]. The integrated fuel cell – engine assembly model is presented in the figure below (Fig. 32).

Modeling of the SOFC stack will be performed at the system level using the zero-dimensional approach and steady-state conditions. That methodology enables analysis of the entire system with all components using input–output parameters. The SOFC stack model will be developed using fundamental equations of electrochemical, heat generation and the mass

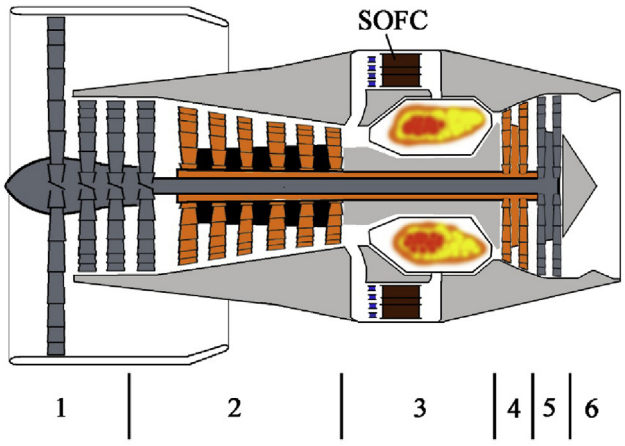


**Fig. 32 – Architecture of the turbofan engine with SOFC; 1. Fan with booster; 2. High pressure compressor; 1. Combustion chamber; 4. High pressure turbine; 5. Low pressure turbine; 6. Nozzle [Based on Ref. [146]].**

and volume continuity equation [135,147,148]. The exemplary system design of the conducted project is shown in the figure below (Fig. 33).

The new element will evaluate the fuel cell parameters based on the cell temperature, pressure and the current density resulting from application requirements. The fuel cell stack current results from current density and active area. In the design of a fuel cell stack, the polarization curve, representing the relation between cell potential and current density, will be defined. The general form of Nernst's equation is used to analyze the electrochemical parameters and to estimate the maximum (reversible open circuit) voltage of the SOFC. The maximum voltage of the fuel cell is usually determined by the type of fuel used and depends on the electrochemical reaction with oxygen occurring on the electrode surfaces. In order to estimate the actual operating voltage of the SOFC, the three overpotentials (voltage losses): activation, ohmic and concentration need to be subtracted from the ideal voltage of the cell. Knowing the operating voltage, the fuel cell stack will be designed based on the required power output, which will be determined by the active area and number of cells [150,151].

The developed SOFC model will be implemented in the complete propulsion system that will be used in order to evaluate the performance of different architectures of the propulsion systems with SOFCs and will help to set the designed targets.

## Numerical multi-level fuel cell studies

Several issues related to fuel processing were addressed at AGH University of Science and Technology. The development of efficient and safe steam reforming systems for SOFC application was based on combined numerical and experimental approaches with a view to developing a durable and efficient SOFC system.

Research into fuel processing dedicated for use in SOFC started in 2006 and involved a broad spectrum of topics, including experimentation on methane steam reforming kinetics [152,153] and theoretical deliberation on phenomena occurring in reforming systems. Thermodynamic analysis of the chemical reactions involved has been proposed to determine optimal working conditions [154] and the novel approach of orthogonal least squares method was applied to increase the security of kinetic modeling [155,156]. It was proved that the uncertainty of the reaction rate expression can be reduced by increasing the number of constraint equations and including supplementary data in the problem description (Fig. 34a). Simultaneously, a numerical model of the SOFC internal indirect reformer was developed and optimized (Fig. 34b). The model was based on the introduced kinetics of chemical reactions and the heat and mass transfer equation derived for gas flows in porous media [157–159].

To address issues related to applications of fuel cells, the team at the Faculty of Energy and Fuels of AGH University of Science and Technology focused on developing a control strategy for SOFC. To make SOFCs efficient power sources in a commercial distributed system, they need to work in load-following condition, which resulted from variable consumption of electrical power over time. SOFCs are required to achieve a fast dynamic response. Thus, load-following capability is essential for grid independent power generation systems. In a conventional load-following SOFC system, the flow of hydrogen is set at a constant level and power output is

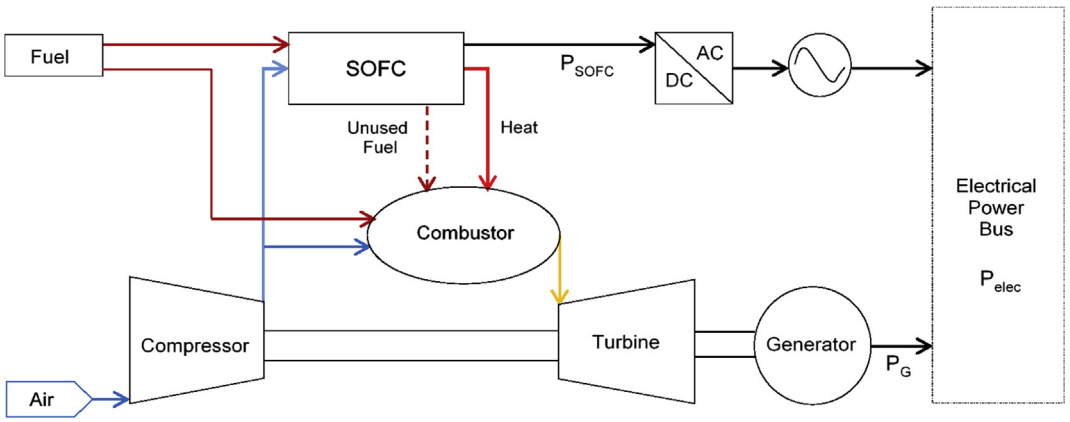


**Fig. 33 – System architecture [based on Ref. [149]].**

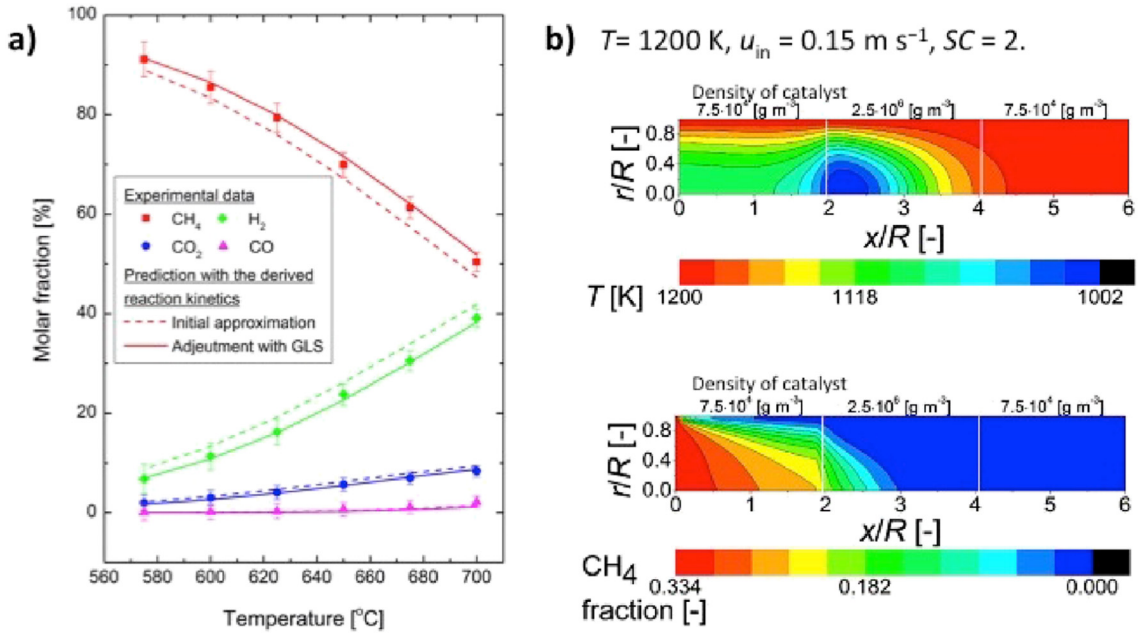


**Fig. 34 – a) Modeling of reforming methane/steam reaction rate [156]. Copyright (2015), with permission from Elsevier; b) Optimization of methane reformer – distribution of the molar fraction of methane [157]. Copyright (2016), with permission from Springer.**

controlled by the fuel utilization factor. This strategy is inefficient, especially for systems working at partial-load and this is one of the major reasons for investigating the transient behavior of the SOFC system. The group studied an alternative control strategy called Current-Based Fuel Control (CBFC). In this strategy fuel flow is adjusted to meet power demand, and the fuel utilization factor is kept at a constant level to moderate overconsumption of fuel. The investigation conducted by the group experimentally confirmed the adequacy of fuel flow rate adjustment together with the manipulation of an electric current [160,161] (Fig. 35). This was the first paper in the open literature measuring a transient characteristic for building an appropriate control strategy on this scale of SOFC stack (300 W). The fast changing conditions during dynamic

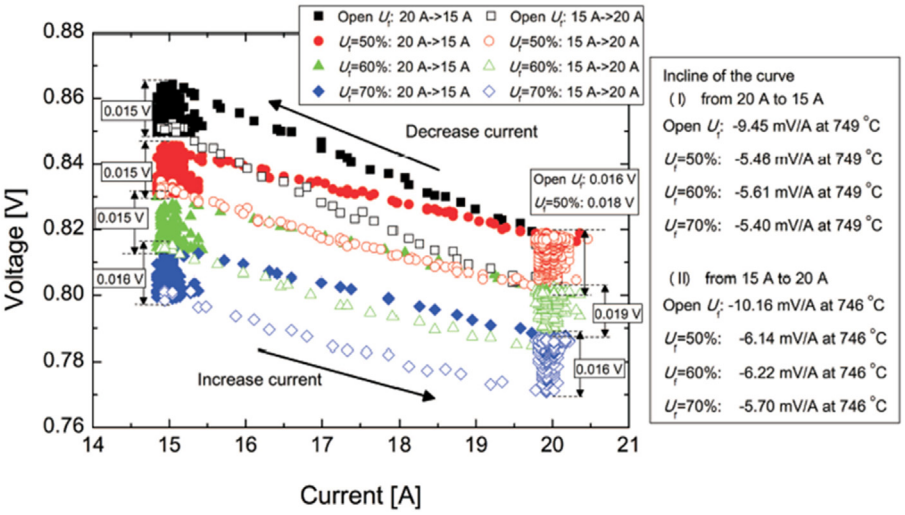


**Fig. 35 – The current–voltage characteristic curves for developing a SOFC control strategy (current changes from 20 to 15 A and from 15 to 20 A while the fuel utilization factor is kept at 50, 60 and 70%) [160]. Copyright (2014), with permission from De Gruyter.**

analysis might be harmful for the SOFC stack. Therefore, the experimental researches were preceded by careful numerical analysis to build up confidence for a high risk stack level experiment [162,163].

As the SOFC slowly approaches commercialization, guaranteeing long-term and safe operation is becoming a key issue. Hence, detailed knowledge about degradation mechanisms is needed. These include transport phenomena at the microscopic level and anode microstructure morphology change during long-term operation. Researches focused on these topics were carried out in cooperation with Kyoto University under a common project: *Thermal Interaction between Stack and Reformer in Small Scale SOFC* (2013–2015) [164–167]. The project received financial support from the Polish Academy of Science (PAN) and the Japanese Society for the Promotion of Science (JSPS). In this research a cell stack with standard power output of 100 W was tested over a period of 3700 h. After an aging test, post-experiment analysis of the anode microstructure was conducted using a combination of a focused ion beam and scanning electron microscopy. The data obtained was reconstructed into three-dimensional images, based on which the microstructure parameters were quantified (Fig. 36a). By comparing the microstructure parameters after long-term operation with the initial condition, local evolution of the microstructure was discussed. The discussion focused on Triple Phase Boundary as a potential reaction side and one of the most important microstructure parameters. The results obtained indicate strong microstructure morphology change after long-term operation and revealed a non-homogeneous tendency of behavior (Fig. 36b). Those unique results shone an additional spotlight on the complex problem of electrode microstructure evolution during long-term operation. The application nature of the findings will help the future development of a more durable stack by optimizing transport phenomena at the micro and macro levels. This is a subject of a new PAN-JSPS research grant entitled: *Mechanism behind degradation in SOFC – from nano to macro-scale* (2016–2017).

The Process Modeling Group which was established in 1996 at the Institute of Chemical Engineering and Environmental Protection Processes of the West Pomeranian University of Technology, Szczecin (ZUT) uses the Computational Fluid Dynamics (CFD) and Finite Element Method (FEM) numerical methods together with a Process Simulation (PS) tool to investigate the performance and design at the cell, stack and system level modeling of solid oxide fuel cells. Since 2010 the Process Modeling Group has conducted its own dedicated research into the CFD and FEM modeling of fuel cells and stacks with different modeling tools: CFD codes – ANSYS Fluent with the Fuel Cell module or COMSOL Multiphysics with the Batteries and Fuel Cell module as well as FEM code – ANSYS Mechanical at the single and stack level, and the Aspen One Engineering process simulator.

Practical industrial applications of the CFD technique to the microtubular SOFC (mSOFC) at the single cell level were characterized in Ref. [168] as exemplified in Fig. 37A. Thermal and electrical fuel cell performance was also predicted for a new design of an anode supported planar SOFC with complex bipolar plates. The estimated pSOFC performance, i.e., voltage and power curves as well as the fuel utilization values were close to the experimental ones. In addition, the temperature distributions for the pSOFC were characterized by high nonuniformity. Maintaining the operating temperature below the maximum avoided high thermal stresses in the SOFC stack, which might cause microstructural instability and subcritical cracking. Examples of a joint analysis by the CFD and Computational Structural Mechanics FEM carried out to analyze thermal stresses in a mSOFC stack can be found in papers [169–171]. A full numerical model was based on the coupling of mass, momentum and energy balance equations plus electrochemical reactions and electrochemical potential equations (thermo-fluid model) with the total strain and stress-strain relationship for materials (thermo-mechanical model). Based on temperature distribution from the thermo-fluid model (Fig. 38A), stress distributions including the von Mises stress in ceramic material were derived in the thermo-

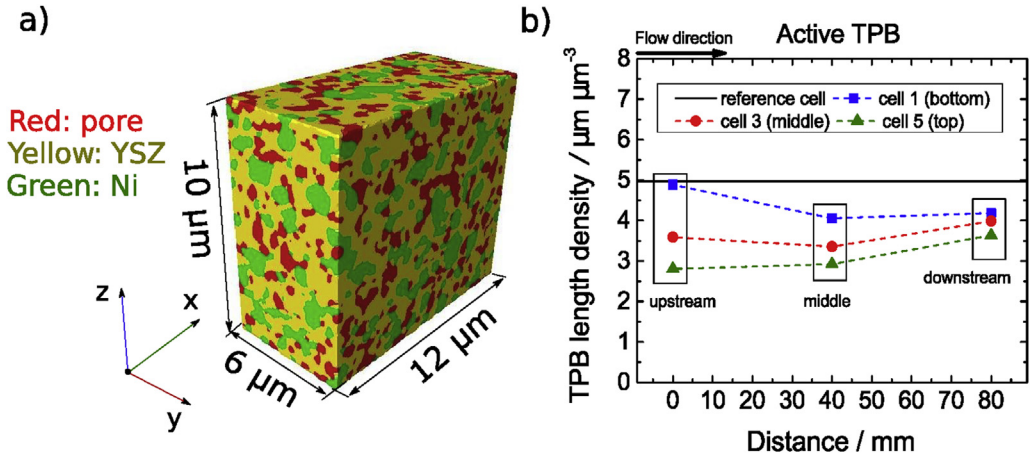


**Fig. 36 – a) 3D reconstruction of anode microstructure morphology [166], Copyright (2015), with permission from Elsevier; b) Quantitative evaluation of Triple Phase Boundary length density before and after aging experiment [167], Copyright (2015), with permission from Wiley.**

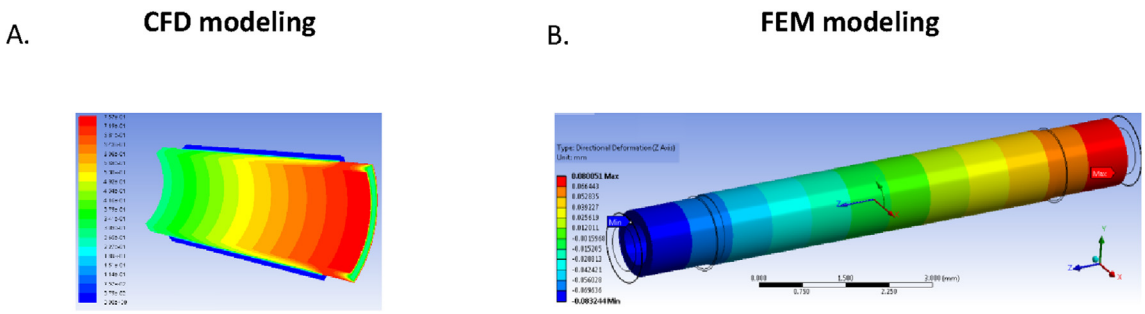


**Fig. 37 – A. Hydrogen molar fraction inside the fuel channel of the microtubular SOFC [mole/mole]. B. Axial displacement of the single microtubular SOFC under thermal stresses [mm].**

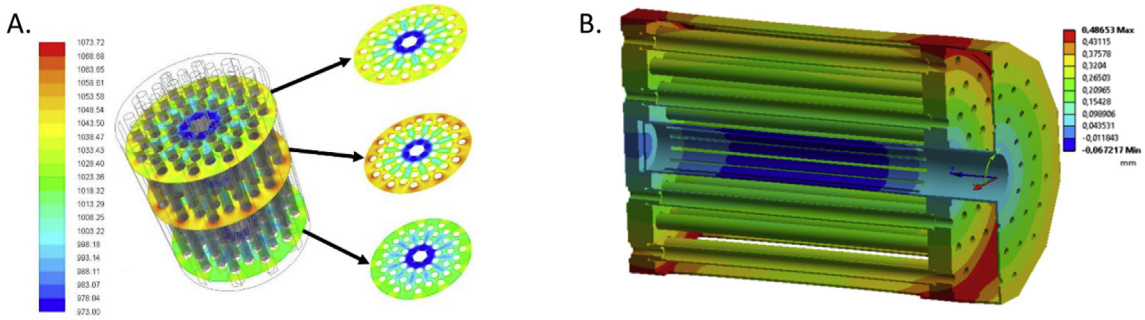


**Fig. 38 – A. Temperature distribution of the fuel cell tubes at inlet air velocity of 2 m/s for the cylindrical mSOFC stack [K]. B. Radial displacement of the assembly with supporting structure under thermal stresses [mm] for hexagonal mSOFC stack.**

mechanical model (Fig. 37B for a single cell, Fig. 38B for a stack). The residual and total axial stresses distributions were analyzed in selected sections of the SOFC stack, which were considered as particularly susceptible to damage. Parts at highest risk of damage within the SOFC stack were recognized [169–171]. The FEM predictions helped assess the effects of the geometry of flow channels, interconnectors, manifolds as well as designs of the inlet and outlet manifolds.

Knowledge of the physical and chemical processes taking place in microtubular and planar SOFCs at the cell and stack level achieved by the CFD modeling enables fully predictive control at the system level. The basic aspects of cell, stack and system modeling of the SOFC technology were characterized in Ref. [172]. Guidelines were also proposed for the integration of two types of software: CFD ANSYS Fluent with additional Fuel Cell module at the cell and stack levels with a process simulator tool – Aspen Plus at the system level modeling. The process simulator tool provided clear insight into various aspects of the system operation. The Balance of Plant (BoP) calculations provided greater understanding of the operating conditions and cost reduction of development and production of fuel cell systems.

The Institute of Power Engineering team together with partnering institutions is developing advanced numerical models which can be applied in power systems. Multi-level modeling addresses key processes related to mass and energy transfer, chemical and electrochemical reactions in systems based on solid oxide fuel cell. Over the years several stationary [173–175] and dynamic models were developed and aided in system-level studies oriented at optimizing the working conditions of system components [176–178].

Additionally, several completed studies, including work done within the framework of the EU project ONSITE were oriented on parametric evaluation of selected factors on system performance [179–181].

## Molten carbonate fuel cells

Activities in the field of MCFC are carried out in two departments at the Warsaw University of Technology. The Institute of Heat Engineering (IHE) of the Faculty of Power and Aeronautical Engineering investigates applications of molten carbonate fuel cell in the power industry with special attention drawn to use of MCFC as a $CO_2$ reducer of coal fired power plant flue gases. IHE has validated several single cell (16–120 $cm^2$) laboratory scale units for natural gas, biogas and hydrogen. Since 2013 IHE has had 1 kW MCFC stacks as well as a mobile container for *in situ* investigations.

IHE is also active in MCFC simulation, adopting new approaches to modeling cell voltage, called reduced order modeling. Electrochemical, thermal, electrical and flow parameters are collected in a 0-D mathematical model, which rivals the classic approach. MCFC voltage is described by a few factors which have physical explanations: maximum voltage; fuel utilization factor; maximum current density; area specific

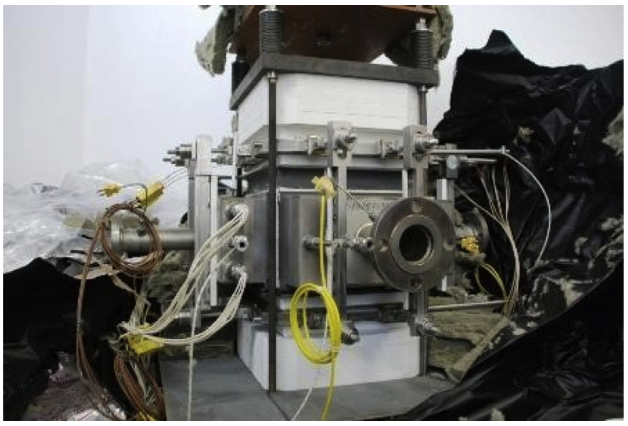

**Fig. 39 – 1 kW MCFC stack, Warsaw University of Technology.**

internal ionic resistance; and area specific internal electric resistance [182–185]. Thus, investigation of a specific component of the fuel cell (e.g., new electrolyte material, new catalyst layer, new fuel, etc.) is related to the factor listed, not for the whole current density–voltage curve as is currently practiced.

Preliminary studies in 2010 and 2011 related to research on 1 kW stacks (see Fig. 39) fed with a hydrogen/methane blend with external reforming. The MCFC stacks were bought from Ansaldo Fuel Cells company, where they were demonstrated successfully. A 1 kW external-reforming MCFC system was tested in order to evaluate the feasibility of MCFCs for co-generation applications. The test station can be seen in Fig. 40.

R&D has been concentrated on the promotion of internal reforming technologies. With support from NCBR, a concept of using MCFC for $CO_2$ separation is under development.

**Fig. 40 – MCFC single cell test facility, Warsaw University of Technology.**

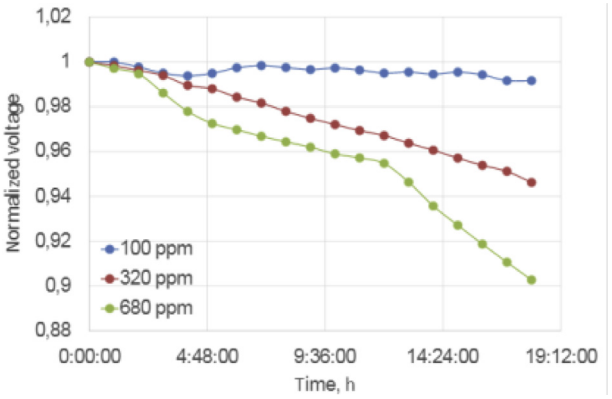


**Fig. 41 – The influence of $SO_2$ contamination at the MCFC cathode inlet.**

Key issues like $SO_x$ and dust contamination are under deep investigation. Stability of cell performance with a certain amount of $SO_2$ at the cathode inlet was confirmed with a 20 $cm^2$ single cell, as shown in Fig. 41. It is observed that the increase in sulfur dioxide concentration in gases results in an increase in the rate of voltage drop over time. The presence of a sulfur dioxide concentration not higher than 100 ppm results in a slight voltage drop over time. After 48 h of operation the voltage drop does not exceed 2% of nominal voltage, whereas an $SO_2$ concentration higher than 680 ppm results in a significant voltage drop.

For the experimental studies, a custom-made fuel cell manifold was designed by the team at the Warsaw University of Technology (see Fig. 42).

Steady progress has been made in the demonstration of molten carbonate fuel cells in the size range of 20–120 $cm^2$ at IHE during the past five years. The performance levels of these cells compare with the values (0.125 $W/cm^2$) reported by others. These investigations are indicative of our capabilities in testing MCFC for various purposes (CCS, sulfur poisoning) which will form the basis for future development and demonstration of a 1 kW MCFC stack.

The Faculty of Materials Science and Engineering (FMSE) is engaged in the design and manufacturing of materials for

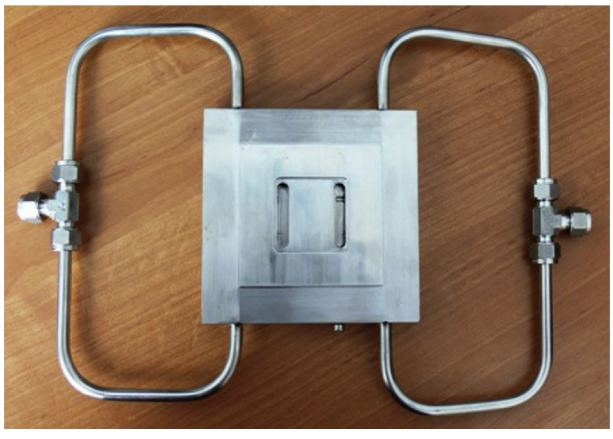

**Fig. 42 – Fuel cell manifold by Warsaw University of Technology, Poland.**

MCFC. The main thrust of the research is devoted to materials for electrodes and electrolyte matrix. These materials will be used in the assembly of single cells and, in future, multiple stacks in prototypes of powerful fuel cell stations. The area of FMSE WUT research on MCFC materials design is related to the components of electrodes and electrolytes.

Although the abovementioned materials have an open-cell porous structure, they all play another role in the MCFC device and demand different chemical composition and microstructure.

High operating temperatures mean that expensive catalysts like platinum can be replaced with much cheaper nickel based ones. Nickel powder with suitable size distribution is the base material in the FMSE manufacturing process. In order to investigate the influence on catalytic and mechanical properties or thermal stability, nickel based materials with additions are produced. Presently at the Faculty both theoretical and experimental research is being carried out to optimize the chemical composition of electrodes. The material of the matrix is based on lithium aluminum oxides, characterized in high thermal, chemical and electrical resistance. Unfortunately, they exhibit crack susceptibility.

Microstructure optimization is important in the design of materials for MCFC, in particular suitable porosity level, pore size distribution and pore shape. Anode material is characterized by smaller pores than cathode material (see Fig. 43). This is related to *in situ* oxidation of cathode material during the start-up process. Oxidation leads to a reduction of pore size compared to the initial size. Experimental and theoretical [186,187] research regarding the influence of porosity on the properties of materials was recently carried out at the Faculty.

The base material for matrix fabrication is lithium aluminate, which is mixed with polymer binders, solvents and dispersant to create the slurry for the tape casting process.

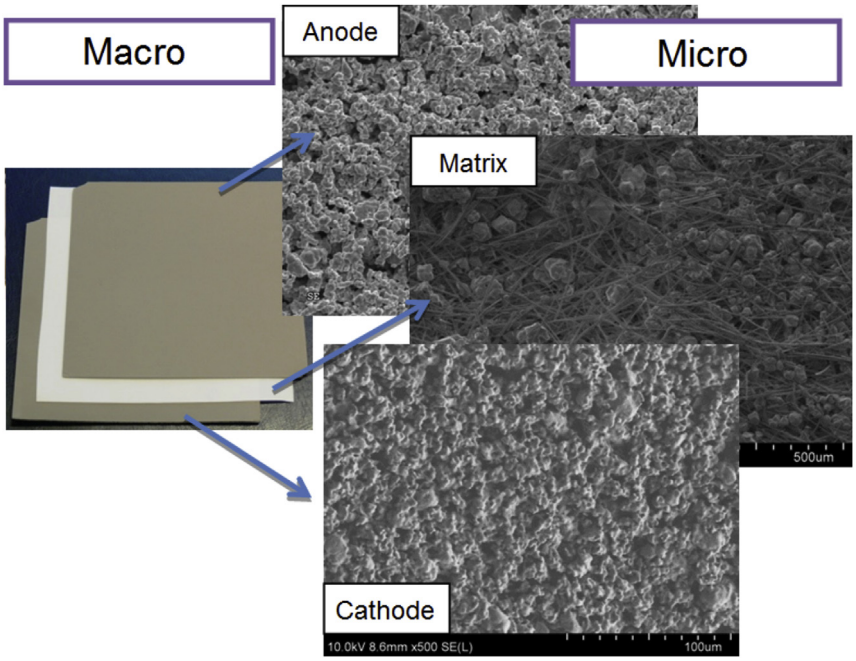


**Fig. 43 – Materials of key MCFC components in macro- and microscale.**

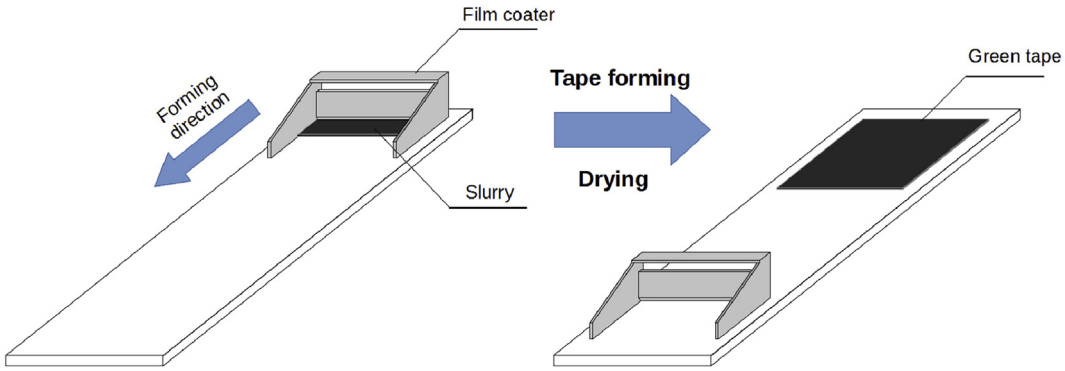


**Fig. 44 – A schematic of the tape casting process for forming green tapes.**

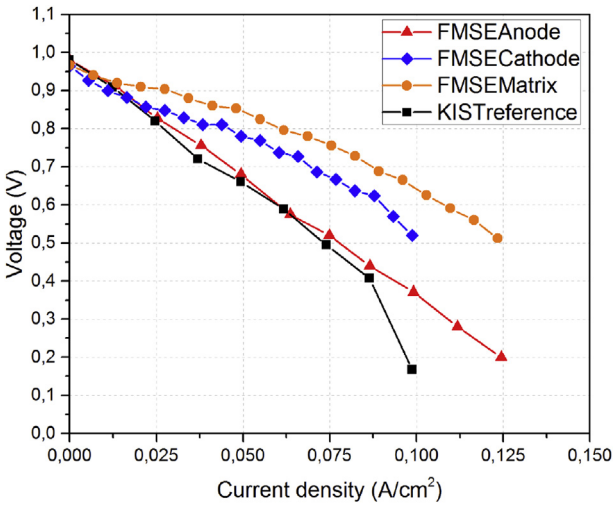


**Fig. 45 – Characteristics of a MCFC cell made by FMSE with modified anode, cathode and electrolyte matrix vs. characteristics of the reference cell from KIST.**

Due to the electrolyte upholding ability pore size in the matrix has to be precisely controlled by means of capillary forces. Current work on the matrix is focused on improving its properties and cutting the cost of fabrication. All of the abovementioned materials are manufactured in the tape casting process (see Fig. 44). This is a relatively simple technique that produces satisfactory results with the use of basic devices, which can be inexpensive. The slurry composition as well as the drying and firing parameters are key factors determining the structure and properties of the fabricated materials. Slurries used in FMSE WUT research are based on organic and inorganic solvents. Both economic and technological aspects are taken into account when selecting slurry ingredients.

Materials fabricated to date were tested in a device that provides adequate MCFC operating conditions. The results obtained exhibit satisfactory characteristics of the tested materials. In each case the results are better than those obtained for reference industrial components Fig. 45.

Presently, Warsaw University of Technology has a research project underway within the framework of the Applied Research Programme (Contract No PBS3/B4/14/2015). The main goal of the project is development and optimization of structural and material design for MCFC application. The aim is to obtain results that work toward making molten carbonate fuel cells fit for commercial use in industry. The Faculty of Materials Science and Engineering has an international cooperation in research and development of materials for MCFC with leading scientific centers: Hanbat National University (South Korea) and University of Perugia (Italy).

## Conclusions

Contributed review allows to appraise achievements of the Polish scientists in development of new materials, microstructural design and optimization of various components of the cells, as well as research on high temperature fuel cell-based systems. While demonstrated level of studies is strong enough, it is evident that further progress, especially in terms of up-scaling and commercialization of the research needs substantial investments, which should be supported by national funding agencies, as well as by the industry. In this aspect, it is clear that a very strong scientific potential of various groups of Polish scientists is not yet fully utilized. It should be emphasized that promising results obtained by Polish scientific teams working on novel materials and fabrication techniques can be integrated, addressing various fundamental problems related to a design of the high temperature cells, and that such basic research should be continued and appropriately funded. Similarity like in the case of other, competing technologies, financing by the industry sector for further progress in SOFCs and MCFCs is sought. With more interest and support from the governmental agencies and Polish companies from the energy sector, which should be focused on programs and grants enabling transition from the laboratory scale to the commercial product, a major progress can be achieved.

Before the commercial product emerges, the objectives related to cost reduction need to be achieved. The installation costs of fuel cell are related mainly to the used material. Fortunately, high temperature fuel cells do not require expensive catalyst (e.g. platinum). On the other hand the elevated temperature requires special and dedicated thermal management and heat balancing of the fuel cell and the stack. The material costs of MCFC manufactured by Warsaw University of Technology are estimated at $1000/kW, for laboratory size. The calculation is based on the 0.3 A/cm$^2$ current density and cell voltage equal to 0.55 V. These are relatively small values in comparison against SOFC technology, where current densities can be as large as 2–3 A/cm$^2$, thus the further progress is expected. It should be noted, that the materials which are used in MCFC technology are not very expensive (stainless steel, nickel powder). The crucial dimensions are also easy manageable (electrolyte thickness is about 1 mm, not in range of microns). Thus, there are good perspectives for decreasing the installation costs of MCFCs.

One of the projects which is ongoing at the Warsaw University of Technology (acronym Matrix) is oriented into new innovative solutions for the matrix materials. Once the project is successfully completed, the significant cost reduction is expected. If the material costs cannot be reduced any more, the increase in power density will be a sound alternative for decreasing the specific costs (per kW). By reaching the current densities similar to SOFC, the installation costs will be lowered by order of magnitude, without change amounts of used materials. One of the options here is the "Diamond" project oriented into a using cryogenic separation of the anode off gases to save at least 30% of fuel delivered to the cell—the solution can be applied for both technologies SOFC and MCFC.

In the field of solid oxide fuel cells several new initiatives oriented at lowering the cost of production of cells were started. They include the ongoing NewSOFC (*New designs materials and manufacturing technologies of advanced solid oxide fuel cells*) – the project of the Institute of Power Engineering related to fabrication of cells with corrugated anodes produced using high pressure injection molding. The project is expected to be

completed with (i) increasing the efficiency of fuel cells by from 5 to 20%-p., (ii) the development of new technologies and structural changes which lead to lowering the manufacturing costs of individual cells by about 40% in comparison to commercially available SOFC offered by foreign companies, (iii) decrease of the cell manufacturing costs by about half at the mass production, (iv) new technology for SOFC production with no waste material which is a great environmental advantage and leads to additional savings.

Polish programmes follow the annual and multi annual working plans (AWP and MAWP, respectively) of the Fuel Cell and Hydrogen Joint Undertaking which are related to specific cost, lifetime, availability and efficiency. These are organized in seven categories, including CAPES (in EUR/kW), durability (years of operation), availability (% of the plant), electrical efficiency (%, LHV-based), thermal efficiency (%, LHV-based) levelized cost of electricity or LCOE (EUR Ct/kWh) and emissions (mg/kWh). The seven key performance indicators apply to residential systems (0,3–0,5 kW), commercial (5–400 kW), industrial (0,3–10 MW) and grid supporting units (1–30 MW). Further detailed information is available in the FCH-JU Multi-annual working plan 2014–2020 [188].

Polish groups working on high temperature fuel cells are a part of the global technological pursuit. The current global community has identified the areas which require competitive solutions which can be brought to reality only by strong cooperation and exchange of information. The national teams established a strong position as members of international teams but it has to be noticed that several breakthrough solutions were developed in Poland. The selected advanced and achievement reported and discussed in the article are either a part of international activities or belong to frontier research oriented innovation in the materials, constructions and functionality.

Particular solutions developed by Polish research groups for the high temperature fuel cells concern various aspects of such systems. Development of MEA's, crucial for the technology, has been conducted widely, in the field of increasing the ionic conductivity of electrolyte materials as well as improvements of electrodes.

Especially polish power generation sector would benefit from rapid growth of SOFC electricity generation regardless of the applied fuels. Currently, in Poland, an average MWh of electricity produced generates 825 kg of $CO_2$ [189]. This is a result of the Polish energy mix, consisting in almost 83% of coal and lignite power plants [190]. Introducing to the market an electrical energy source of lower $CO_2$ emission per MWh than average polish coal/lignite power plant will result in lowering overall emissions of the country. The installed capacity in fuel cells across Europe reached ca. 40 MW in 2012 [191]. The estimation of $CO_2$ emission from generation of 1 MWh of electricity in a fuel cell plant, assuming 60% LHV electrical efficiency and natural gas as fuel, is ca. 380 kg. Installation of 1 MW fuel cell plant assuming availability equal 90% will generate annually 7884 MWh of electricity and allow mitigation of ca. 3500 tonnes of $CO_2$ emission per year.

While currently SOFC and MCFC technology in Poland exists only at the scale of single kilowatts (stacks developed in the Institute of Power Engineering, and later at the Warsaw University of Technology), with proper support, demonstration of MW-scale high temperature fuel cell-based systems seems feasible within 36–60-month timeframe. If Polish governmental agencies (mainly NCBR) continue their commitment to programs concerning renewable energy alongside with the increased usage of distributed energy system, it should encourage further development of high temperature fuel cell technologies that can scalable to the MW-class. In order to achieve so, the high temperature fuel cell technology has to be viewed as the alternative and promising way for modernizing energy sector. Concerning this, Polish Hydrogen and Fuel Cell Association is fully committed to encourage and support various educational, scientific, as well as industrial activities and projects.

## Acknowledgements

The authors would like to thank numerous funding bodies and cooperating agencies. Among them the following support should be noted:

At GUT, this work is partly supported by a project funded by National Science Center Poland based on decision DEC-2012/05/B/ST7/02153.

At IEL the research was partly supported by Wroclaw Research Center EIT+ within the project "The Application of Nanotechnology in Advanced Materials" – NanoMat (POIG.01.01.02-02-002/08) financed by the European Regional Development Fund (Innovative Economy Operational Programme, 1.1.2).

The IEN acknowledges several national and European projects including SOFCOM, ONSITE, UNIQUE, National Strategic Programme – Task 4, Consortium for Direct Carbon Fuel Cells and Statutory Grants from the Polish Ministry of Science and Higher Education (COP/17/STAT/2011, COP/21/STAT/2012, COP/23/STAT/2013, CPC/11/STAT/16 and CPC/36/STAT/2016).

The Warsaw University of Technology acknowledges the co-financing from the National Center of Research and Development within the framework of Contract PBS3/B4/14/2015 – Applied Research Programme – High efficiency molten carbonate fuel cells.

The ZUT acknowledges SUAV, SAPIENS and SAFARI project. The work was also financed from Polish research funds awarded for projects Nos. 2284/7.PR/11/2012/2; 2750/7.PR/2013/2 and 3043/7.PR/2014/2 of international cooperation within SUAV, SAPIENS and SAFARI in the period 2011–2016, respectively.

## REFERENCES

[1] Dollard WJ. Solid oxide fuel cell developments at Westinghouse. J Power Sources 1992;37(1–2):133–9.
[2] Raymond GA. Status of tubular SOFC field unit demonstrations. J Power Sources 2000;86(1–2):134–9.
[3] Isenberg AO, Zymboly GE. Apparatus and method for depositing coating onto porous substrate. United States patent 06/684,438 (US4609562 A). 1986 Sep 2/1986 Dec 20.
[4] Singhal SC. Solid oxide fuel cells for stationary, mobile, and military applications. Solid State Ionics 2002;152–153:405–10.

[5] Elcogen: Technical data. http://www.elcogen.com/en/sofc-single-cells/technical-data [Accessed 7 November 2016].
[6] SOFCMAN Energy Technology: SOFC. http://www.sofc.com.cn/siglecell.html [Accessed 7 November 2016].
[7] Huang K, Hou PY, Goodenough JB. Characterization of iron-based alloy interconnects for reduced temperature solid oxide fuel cells. Solid State Ionics 2000;129:237–50.
[8] Fontana S, Amendola R, Chevalier S, Piccardo P, Caboche G, Viviani M, et al. Metallic interconnects for SOFC: characterisation of corrosion resistance and conductivity evaluation at operating temperature of differently coated alloys. J Power Sources 2007;171:652–62.
[9] Brylewski T, Maruyama T, Nanko M, Przybylski K. TG measurements of the oxidation kinetics of Fe-Cr alloy with regard to its application as a separator in SOFC. J Therm Anal Calorim 1999;55(2):681–90.
[10] Shaigan N, Qu W, Ivey DG, Chen W. A review of recent progress in coatings, surface modifications and alloy. J Power Sources 2010;195:1529–42.
[11] Tucker MC, Cheng L, DeJonghe KC. Selection of cathode contact materials for solid oxide fuel cells. J Power Sources 2011;196:8313–22.
[12] Kilner JA, Burriel M. Materials for intermediate-temperature solid-oxide fuel cells. Annu Rev Mater Res 2014;44:365–93.
[13] Niewolak L, Wessel E, Singheiser L, Quadakkers WJ. Potential suitability of ferritic and austenitic steels as interconnect materials for solid oxide fuel cells operating at 600°C. J Power Sources 2010;195:7600–8.
[14] Yamamoto O, Arachi Y, Sakai H, Takeda Y, Imanishi N, Mizutani Y, et al. Zirconia based oxide ion conductors for solid oxide fuel cells. Ionics 1998;4:403–8.
[15] Badwal SPS. Zirconia-based solid electrolytes: microstructure, stability and ionic conductivity. Solid State Ionics 1992;52:23–32.
[16] Kharton VV, Marques FMB, Atkinson A. Transport properties of solid oxide electrolyte ceramics: a brief review. Solid State Ionics 2004;174:135–49.
[17] Kilner DA. Fast anion transport in solids. Solid State Ionics 1983;8:201–7.
[18] Hui SR, Roller J, Yick S, Zhang X, Deces-Petit C, Xie Y, et al. A brief review of the ionic conductivity enhancement for selected oxide electrolytes. J Power Sources 2007;172:493–502.
[19] Bucko M. Przewodnictwo jonowe w dwutlenku cyrkonu stabilizowanym tlenkami itru i lantanu. Ceramika/Ceramics 2003;80:523–8.
[20] Bucko M. Ionic conductivity of $CaO$-$Y_2O_3$-$ZrO_2$ materials with constant oxygen vacancy concentration. J Eur Ceram Soc 2004;24:1305–8.
[21] Bucko M. Some structural aspects of ionic conductivity of yttria and calcia stabilised zirconia. Mat Sci Pol 2006;24:39–44.
[22] Pomykalska D, Bucko M, Rekas M. Electrical conductivity of $MnO_x$-$Y_2O_3$-$ZrO_2$ solid solutions. Solid State Ionics 2010;181:48–52.
[23] Chen M, Hallstedt B, Gauckler LJ. Thermodynamic modeling of phase equilibria in the Mn–Y–Zr–O system. Solid State Ionics 2005;176:1457–64.
[24] Backhaus-Ricoult M. Interface chemistry in LSM–YSZ composite SOFC cathodes. Solid State Ionics 2006;177(19–25):2195–200.
[25] Liu YL, Hagen A, Barfod R, Chen M, Wang HJ, Poulsen FW, et al. Microstructural studies on degradation of interface between LSM–YSZ cathode and YSZ electrolyte in SOFCs. Solid State Ionics 2009;180(23–25):1298–304.
[26] Zajac W, Molenda J. Properties of doped ceria solid electrolytes in reducing atmospheres. Solid State Ionics 2011;192:163–7.
[27] Zajac W, Suescun L, Swierczek K, Molenda J. Structural and electrical properties of grain boundaries in $Ce_{0.85}Gd_{0.15}O_{1.925}$ solid electrolyte modified by addition of transition metal ions. J Power Sources 2009;194:2–9.
[28] Zajac W, Molenda J. Electrical conductivity of doubly doped ceria. Solid State Ionics 2008;179:154–8.
[29] Zajac W, Swierczek K, Molenda J. Thermochemical compatibility between selected $(La,Sr)(Co,Fe,Ni)O_3$ cathodes and rare earth doped ceria electrolytes. J Power Sources 2007;173:675–80.
[30] Shuk P, Wiemhofer HD, Guth U, Gopel W, Greenblatt M. Oxide ion conducting solid electrolytes based on $Bi_2O_3$. Solid State Ionics 1996;89:179–96.
[31] Wachsman ED, Lee KT. Lowering the temperature of solid oxide fuel cells. Science 2011;334:935–9.
[32] Harwig HA, Gerards AG. J Solid State Chem 1978;26:265–74.
[33] Abrahams I, Krok F. Defect chemistry of the BIMEVOXes. J Mater Chem 2002;12:3351–62.
[34] Leszczynska M, Liu X, Wrobel W, Malys M, Krynski M, Norberg ST, et al. Thermal variation of structure and electrical conductivity in $Bi_4YbO_{7.5}$. Chem Mater 2013;25:326–36.
[35] Leszczynska M, Borowska-Centkowska A, Malys M, Dygas JR, Krok F, Wrobel W, et al. The double rare-earth substituted bismuth oxide system $Bi_3Y_{1-x}Yb_xO_6$. Solid State Ionics 2015;269:37–43.
[36] Leszczynska M, Holdynski M, Krok F, Abrahams I, Liu X, Wrobel W. Structural and electrical properties of $Bi_3Nb_{1-x}Er_xO_{7-x}$. Solid State Ionics 2010;181:796–811.
[37] Krynski M, Wrobel W, Mohn CE, Dygas JR, Malys M, Krok F, et al. Trapping of oxide ions in δ-$Bi_3YO_6$. Solid State Ionics 2014;264:49–53.
[38] Krynski M, Wrobel W, Dygas JR, Malys M, Krok F, Abrahams I. An ab initio study of oxide ion dynamics in type-II $Bi_3NbO_7$. J Mater Chem A 2015;3:21882–90.
[39] Malys M, Dygas JR, Holdynski M, Borowska-Centkowska A, Wrobel W, Marzantowicz M. Ionic and electronic conductivity in a $Bi_2O_3$-based material. Solid State Ionics 2012;225:493–7.
[40] Malys M, Holdynski M, Krok F, Wrobel W, Dygas JR, Pirovano C, et al. Investigation of transport numbers in yttrium doped bismuth niobates. J Power Sources 2009;194:16–9.
[41] Pasciak G, Mielcarek W. Thick film $NO_2$ sensor-microsystem. Technol J 1996;3(1):28–30.
[42] Pasciak G, Prociów K, Mielcarek W, Górnicka B, Mazurek B. Solid electrolytes for gas sensors and fuel cells applications. J Eur Ceram Soc 2001;21:1867–70.
[43] Chmielowiec J. Opracowanie niskotemperaturowych, tlenkowych przewodników superjonowych do zastosowania w ogniwach paliwowych typu IT-SOFC [Doctoral dissertation]. 2008. Wroclaw.
[44] Pasciak G, Chmielowiec J, Bujlo B. New ceramic superionic materials for IT-SOFC applications. Mat Sci 2005;23:209–19.
[45] Pasciak G, Chmielowiec J. Conductivity of La- and Pr-doped $Bi_4V_2O_{11}$. Mat Sci Forum 2006;514:392.
[46] Chmielowiec J, Pasciak G, Bujlo P. Ionic conductivity and thermodynamic stability of La-doped BIMEVOX. J Alloys Compd 2008;451:676–8.
[47] Pasciak G, Chmielowiec J, Chan SH. Thermal and structural study of BIVOX undoped and doped with La in various atmosphere toward applications in IT-SOFC. Ceram Intern 2014;40(7):8969–74.
[48] Zajac W, Hanc E. Strontium-substituted $Ba(Ce,Zr)O_{3-\delta}$ oxides for proton conducting membranes. Fun Mater Lett 2014;7:1440014.
[49] Zajac W, Rusinek D, Zheng K, Molenda J. Applicability of Gd-doped $BaZrO_3$, $SrZrO_3$, $BaCeO_3$ and $SrCeO_3$ proton

conducting perovskites as electrolytes for solid oxide fuel cells. Cent Eur J Chem 2013;11:471–84.
[50] Zajac W, Hanc E, Gorzkowska-Sobas A, Swierczek K, Molenda J. Nd-doped Ba(Ce,Zr)$O_{3-\delta}$ proton conductors for application in conversion of $CO_2$ into liquid fuels. Solid State Ionics 2012;225:297–303.
[51] Holtappels P, Stimming U. Handb. Fuel Cells. John Wiley & Sons Ltd; 2010.
[52] Gdula-Kasica K, Mielewczyk-Gryn A, Molin S, Jasinski P, Krupa A, Kusz B, et al. Optimization of microstructure and properties of acceptor-doped barium cerate. Solid State Ionics 2012:245–9.
[53] Haugsrud R, Norby T. Proton conduction in rare-earth ortho-niobates and ortho-tantalates. Nat Mater 2006;5:193–6.
[54] Mather GC, Fisher CAJ, Islam MS. Defects, dopants, and protons in $LaNbO_4$. Chem Mater 2010;22:5912.
[55] Mokkelbost T, Andersen Ø, Strøm RA, Wiik K, Grande T, Einarsrud MA. High temperature proton conducting $LaNbO_4$-based materials. J Am Ceram Soc 2007;90:3395–400.
[56] Momma K, Izumi F. VESTA 3 for three-dimensional visualization of crystal, volumetric and morphology data. J Appl Crystallogr 2011;44:1272.
[57] Mielewczyk-Gryń A, Gdula K, Molin S, Jasinski P, Kusz B, Gazda M. Structure and electrical properties of ceramic proton conductors obtained with molten-salt and solid-state synthesis methods. J Non Cryst Solids 2010:1976–9.
[58] Gazda M, Mielewczyk-Gryn A, Gdula-Kasica K, Wachowski S, Nanosci J. Proton conducting ceramic powder synthesis by a low temperature method. Nanotechnol 2015;15:3626.
[59] Kolincio K, Gdula K, Mielewczyk A, Izdebski T, Gazda M. Molten salt synthesis of conducting and superconducting ceramics. Acta Phys Pol A 2010;118:326.
[60] Mielewczyk-Gryn A, Wachowski S, Zagorski K, Jasinski P, Gazda M. Characterization of magnesium doped lanthanum orthoniobate synthesized by molten salt route. Ceram Int 2015;41(6):7847–52.
[61] Mielewczyk-Gryn A, Gdula K, Lendze T, Kusz B, Gazda M. Document nano- and microcrystals of doped niobates. Cryst Res Tech 2010;45:1225–8.
[62] Mielewczyk-Gryn A, Gdula-Kasica K, Kusz B, Gazda M. Document High temperature monoclinic-to-tetragonal phase transition in magnesium doped lanthanum ortho-niobate. Ceram Int 2013;39:4239–44.
[63] Mielewczyk-Gryn A, Lendze T, Gdula-Kasica K, Jasinski P, Krupa A, Kusz B, et al. Characterization of $CaTi_{0.9}Fe_{0.1}O_3$/$La_{0.98}Mg_{0.02}NbO_4$ composite. Open Phys 2013;11:213–8.
[64] Wachowski S, Mielewczyk-Gryn A, Gazda M. Effect of isovalent substitution on microstructure and phase transition of $LaNb_{1-x}M_xO_4$ (M=Sb, v or Ta; X=0.05-0.3). J Solid State Chem 2014;219:201.
[65] Mielewczyk-Gryn A, Wachowski S, Lilova KI, Guo X, Gazda M, Navrotsky A. Document influence of antimony substitution on spontaneous strain and thermodynamic stability of lanthanum orthoniobate. Ceram Int 2015;41:2128–33.
[66] Swierczek K, Marzec J, Pałubiak D, Zając W, Molenda J. LFN and LSCFN perovskites – structure and transport properties. Solid State Ionics 2006;177(19–25):1811–7.
[67] Molenda J, Swierczek K, Zajac W. Functional materials for the IT-SOFC. J Power Sources 2007;173(2):657–70.
[68] Swierczek K, Gozu M. Structural and electrical properties of selected $La_{1-x}Sr_xCo_{0.2}Fe_{0.8}O_3$ and $La_{0.6}Sr_{0.4}Co_{0.2}Fe_{0.6}Ni_{0.2}O_3$ perovskite type oxides. J Power Sources 2007;173(2):695–9.
[69] Swierczek K. Thermoanalysis, nonstoichiometry and thermal expansion of $La_{0.4}Sr_{0.6}Co_{0.2}Fe_{0.8}O_{3-\delta}$, $La_{0.2}Sr_{0.8}Co_{0.2}Fe_{0.8}O_{3-\delta}$, $La_{0.9}Sr_{0.1}Co_{1/3}Fe_{1/3}Ni_{1/3}O_{3-\delta}$ and $La_{0.6}Sr_{0.4}Co_{0.2}Fe_{0.6}Ni_{0.2}O_{3-\delta}$ perovskites. Solid State Ionics 2008;179(1–6):126–30.
[70] Swierczek K. Electrolyte-supported IT-SOFC with LSCF - SCFN composite cathode. Solid State Ionics 2011;192(1):486–90.
[71] Swierczek K. Physico-chemical properties of $Ln_{0.5}A_{0.5}Co_{0.5}Fe_{0.5}O_{3-\delta}$ (Ln: La, Sm; A: Sr, Ba) cathode materials and their performance in electrolyte-supported intermediate temperature solid oxide fuel cell. J Power Sources 2011;196(17):7110–6.
[72] Gedziorowski B, Swierczek K, Molenda J. $La_{1-x}Ba_xCo_{0.2}Fe_{0.8}O_{3-\delta}$ perovskites for application in intermediate temperature SOFCs. Solid State Ionics 2012;225:437–42.
[73] Kulka A, Hu Y, Dezanneau G, Molenda J. Investigation of $GdBaCo_{2-x}Fe_xO_{5.5-\delta}$ as a cathode materials for intermediate temperature solid oxide fuel cells. Fun Mater Lett 2011;4:157–60.
[74] Tatko M, Mosiałek M, Kędra A, Bielańska E, Ruggiero-Mikołajczyk M, Nowak P. Thermal shock resistant composite cathode material $Sm_{0.5}Sr_{0.5}CoO_{3-\delta}$-$La_{0.6}Sr_{0.4}FeO_{3-\delta}$ for solid oxide fuel cells. J Solid State Electrochem 2016;20(1):143–51.
[75] Mosiałek M, Dudek M, Michna A, Tatko M, Kedra A, Zimowska M. Composite cathode materials Ag-$Ba_{0.5}Sr_{0.5}Co_{0.8}Fe_{0.2}O_3$ for solid oxide fuel cells. J Solid State Electrochem 2014;18:3011–21.
[76] Tatko M, Mosiałek M, Dudek M, Nowak P, Kedra A, Bielańska E. Composite cathode materials $Sm_{0.5}Sr_{0.5}CoO_3$-$La_{0.6}Sr_{0.4}FeO_3$ for solid oxide fuel cells. Solid State Ionics 2015;271:103–8.
[77] Zheng K, Swierczek K. Physicochemical properties of rock salt-type ordered $Sr_2MMoO_6$ (M = Mg, Mn, Fe, Co, Ni). J Eur Ceram Soc 2014;34:4273–84.
[78] Zheng K, Swierczek K, Bratek J, Klimkowicz A. Cation-ordered perovskite-type anode and cathode materials for solid oxide fuel cells. Solid State Ionics 2014;262:354–8.
[79] Zheng K, Swierczek K, Zajac W, Klimkowicz A. Rock salt ordered-type double perovskite anode materials for solid oxide fuel cells. Solid State Ionics 2014;257:9–16.
[80] Quadakkers WJ, Piron-Abellan A, Shemet V, Singheiser L. Document metallic interconnectors for solid oxide fuel cells – a review. Mater High Temp 2003;20:115–27.
[81] Yang Z, Weil KS, Paxton DM, Stevenson JW. Document selection and evaluation of heat-resistant alloys for SOFC interconnect applications. J Electrochem Soc 2003;150:A1188–201.
[82] Fergus JW. Metallic interconnects for solid oxide fuel cells. Mater Sci Eng A 2005;397:271–83.
[83] Brylewski T, Nanko M, Maruyama T, Przybylski K. Document Application of Fe-16Cr ferritic alloy to interconnector for a solid oxide fuel cell. Solid State Ionics 2001;143:131–50.
[84] Kadowaki T, Shiomitsu T, Matsuda E, Nakagawa H, Tsuneizumi H, Maruyama T. Applicability of heat resisting alloys to the separator of planar type solid oxide fuel cell. Solid State Ionics 1993;67:65–9.
[85] Montero X, Jordán N, Pirón-Abellán J, Tietz F, Stöver D, Cassir M, et al. Spinel and perovskite protection layers between crofer22APU and $La_{0.8}Sr_{0.2}FeO_3$ cathode materials for SOFC interconnects. J Electrochem Soc 2009;156:B188–96.
[86] Zhu WZ, Deevi SC. Development of interconnect materials for solid oxide fuel cells. Mater Sci Eng A 2003;348:227–43.
[87] Hilpert K, Das D, Miller M, Peck DH, Weib R. Select this article chromium vapor species over solid oxide fuel cell

interconnect materials and their potential for degradation processes. J Electrochem Soc 1996;143:3642–7.
[88] Kurokawa H, Jacobson CP, DeJonghe LC, Visco S. Chromium vaporization of bare and of coated iron–chromium alloys at 1073 K. Solid State Ionics 2007;178:287–96.
[89] Brylewski T, Przybylski K. Perovskite and spinel functional coatings for SOFC metallic interconnects. Ann Chimie Sci Materiaux 2008;33:75.
[90] Cabouro G, Caboche G, Chevalier S, Piccardo P. Opportunity of metallic interconnects for ITSOFC: reactivity and electrical property. J Power Sources 2006;156:39.
[91] Qu W, Li H, Ivey DG. Sol–gel coatings to reduce oxide growth in interconnects used for solid oxide fuel cells. J Power Sources 2004;138:162–73.
[92] Shaigan N, Qu W, Ivey DG, Chen W. A review of recent progress in coatings, surface modifications and alloy developments for solid oxide fuel cell ferritic stainless steel interconnects. J Power Sources 2010;195:1529–42.
[93] Yang ZG, Xia GG, Maupin GD, Stevenson JW. Evaluation of perovskite overlay coatings on ferritic stainless steels for SOFC interconnect applications. J Electrochem Soc 2006;153:A1852–8.
[94] Larring Y, Norby T. Spinel and perovskite functional layers between Plansee metallic interconnect (Cr-5 wt % Fe-1 wt % $Y_2O_3$) and ceramic $(La_{0.85}Sr_{0.15})_{0.91}MnO_3$ cathode materials for solid oxide fuel cells. J Electrochem Soc 2000;147:3251–6.
[95] Brylewski T, Dabek J, Przybylski K, Morgiel J, Rekas M. Screen-printed (La,Sr)$CrO_3$ coatings on ferritic stainless steel interconnects for solid oxide fuel cells using nanopowders prepared by means of ultrasonic spray pyrolysis. J Power Sources 2012;208:86–95.
[96] Yang Z, Xia G, Simner SP, Stevenson JW. Ferritic stainless steel SOFC interconnects with thermally grown (Mn,Co) 3O 4 spinel protection layers. J Electrochem Soc 2005;152:A1896–901.
[97] Yang ZG, Xia GG, Stevenson JW. $Mn_{1.5}Co_{1.5}O_4$ spinel protection layers on ferritic stainless steels for SOFC interconnect applications. Electrochem Solid-State Lett 2005;8:A168–70.
[98] Gannon P, Deibert M, White P, Smith R, Chen H, Priyantha W, et al. Advanced PVD protective coatings for SOFC interconnects. Int J Hydrog Energy 2008;33:3991–4000.
[99] Przybylski K, Brylewski T. Document interface reactions between conductive ceramic layers and Fe-Cr steel substrates in SOFC operating conditions. Mater Trans 2011;52:345–51.
[100] Brylewski T, Przybylski K, Morgiel J. Document microstructure of Fe-25Cr/(La, Ca)$CrO_3$ composite interconnector in solid oxide fuel cell operating conditions. Mater Chem Phys 2003;81:434–7.
[101] Przybylski K, Brylewski T, Morgiel J. Document interfacial interactions between some la-based perovskite thick films and ferritlc steel substrate with regard to the operating conditions of SOFC. Mater Sci Forum 2004;461–464:1099–106.
[102] Kruk A, Stygar M, Brylewski T. Mn-Co spinel protective-conductive coating on AL453 ferritic stainless steel for IT-SOFC interconnect applications. J Solid State Electrochem 2013;17:993–1003.
[103] Brylewski T, Gil A, Rakowska A, Chevalier S, Adamczyk A, Dąbek J, et al. Improving the physicochemical properties of Fe-25Cr ferritic steel for SOFC interconnects via Y-implantation and $Y_2O_3$-deposition. Oxid Met 2013;80:83–111.
[104] Meulenberg WA, Gil A, Wessel E, Buchkremer HP, Stöver D. Document corrosion and interdiffusion in a Ni/Fe-Cr-Al couple used for the anode side of multi-layered interconnector for SOFC applications. Oxid Met 2002;57:1–12.
[105] Petrovsky V, Gazda M, Anderson HU, Molin S, Jasinski P. Applications of spin coating of polymer precursor and slurry suspensions for solid oxide fuel cell fabrication. J Power Sources 2009;194:10–5.
[106] Szymczewska D, Karczewski J, Chrzan A, Jasiński P. Three electrode configuration measurements of electrolyte-diffusion barrier-cathode interface. J Ceram Soc Jpn 2015;123:268–73.
[107] Chrzan A, Karczewski J, Gazda M, Szymczewska D, Jasinski P. Investigation of thin perovskite layers between cathode and doped ceria used as buffer layer in solid oxide fuel cells. J Solid State Electrochem 2015;19(6):1807–15.
[108] Karczewski J, Bochentyn B, Molin S, Gazda M, Jasinski P, Kusz B. Solid oxide fuel cells with Ni-infiltrated perovskite anode. Solid State Ionics 2012;221:11–4.
[109] Molin S, Lewandowska-Iwaniak W, Kusz B, Gazda M, Jasinski P. Structural and electrical properties of Sr(Ti, Fe) $O_{3-\delta}$ materials for SOFC cathodes. J Electroceramics 2012;28:80–7.
[110] Szymczewska D, Karczewski J, Bochentyn B, Chrzan A, Gazda M, Jasiński P. Investigation of catalytic layers on anode for solid oxide fuel cells operating with synthetic biogas. Solid State Ionics 2015;271:109–15.
[111] Golec T, Antunes R, Jewulski J, Miller M, Kluczowski R, Krauz M, et al. The Institute of Power Engineering activity in the solid oxide fuel cell technology. J Fuel Cell Sci Technol 2010;7:011003-1–011003-5.
[112] Krauz M. Opracowanie technologii wytwarzania stałotlenkowych ogniw paliwowych. Bull Pol Assoc Hydr Fuel Cells 2010;5:95–6.
[113] Antunes R, Golec T, Miller M, Krauz M, Kluczowski R, Krzastek K. Geometrical and microstructure optimization of double-layer LSM/LSM-YSZ cathodes by electrochemical impedance spectroscopy. J Fuel Cell Sci Technol 2010;7:011011-1–011011-6.
[114] Kluczowski R, Krauz M, Kawalec M, Ouweltjes JP. Near net shape manufacturing of planar anode supported solid oxide fuel cells by using ceramic injection molding and screen printing. J Power Sources 2014;268:752–7.
[115] Molin S, Kusz B, Gazda M, Jasinski P. Protective coatings for stainless steel for SOFC applications. J Solid State Electrochem 2008;13:1695–700.
[116] Jasinski P, Lewandowska-Iwaniak W, Molin S. Metal supported solid oxide fuel cells – selected aspects. IOP Conf Ser Mater Sci Eng 2011;18:132004.
[117] Molin S, Tolczyk M, Gazda M, Jasinski P. Stainless steel/yttria stabilized zirconia composite supported solid oxide fuel cell. J Fuel Cell Sci Technol 2011;8:051019.
[118] Molin S, Gazda M, Kusz B, Jasinski P. Evaluation of 316L porous stainless steel for SOFC support. J Eur Ceram Soc 2009;29:757–62.
[119] Molin S, Gazda M, Jasinski P. High temperature oxidation of porous alloys for solid oxide fuel cell applications. Solid State Ionics 2010;181:1214–20.
[120] Karczewski J, Dunst KJ, Jasinski P, Molin S. High temperature corrosion and corrosion protection of porous Ni22Cr alloys. Surf Coat Technol 2015;261:385–90.
[121] Szymczewska D, Molin S, Chen M, Hendriksen PV, Jasinski P. Ceria based protective coatings for steel interconnects prepared by spray pyrolysis. Procedia Eng 2014;98:93–100.
[122] Giddey S, Badwal SPS, Kulkarni A, Munnings C. A comprehensive review of direct carbon fuel cell technology. Prog Energy Combust Sci 2012;38:360–99.
[123] Dudek M, Tomczyk P. Composite fuels for direct carbon fuel cell. Catal Today 2011;176:388–92.

[124] Dudek M, Tomczyk P, Socha R, Hamaguchi M. Use of ash-free "hyper-coal" as a fuel for a direct carbon fuel cell with solid oxide electrolyte. Int J Hydrog Energy 2014;39:12386–94.
[125] Dudek M, Tomczyk P, Socha R, Skrzypkiewicz M, Jewulski J. Biomass fuels for direct carbon fuel cell with solid oxide electrolyte. Int J Electrochem Sci 2013;8:3229–53.
[126] Dudek M. On the utilization of coal samples in direct carbon solid oxide fuel cell technology. Solid State Ionics 2015;271:121–7.
[127] Dudek M, Tomczyk P, Lis B, Mordarski G. Direct carbon fuel cells – selected domestic activities. Energy Policy J 2014;17:81–92.
[128] Skrzypkiewicz M, Jewulski J, Lubarska-Radziejewska I. The effect of $Fe_2O_3$ catalyst on direct carbon fuel cell performance. Int J Hydrog Energy 2015;40:13090–8.
[129] Jewulski J, Skrzypkiewicz M, Struzik M, Lubarska-Radziejewska I. Lignite as a fuel for direct carbon fuel cell system. Int J Hydrog Energy 2014;39:21778–85.
[130] Antunes R, Skrzypkiewicz M. Chronoamperometric investigations of electro-oxidation of lignite in direct carbon bed solid oxide fuel cell. Int J Hydrog Energy 2015;40:4357–69.
[131] Jewulski J, Błesznowski M, Stępień M. Flow distribution analysis of the solid oxide fuel cell stack under electric load conditions. In: Proceeding of Lucerne Fuel Cell Forum; 2009. Switzerland; B0705.
[132] (A1): SOFC stack with corrugated separator plate. European Patent EP2338195.
[133] Golec T, Kupecki J, Wierzbicki M, Skrzypkiewicz M, Stepien M, Rychlik M, et al. Zagadnienia modelowania, konstrukcji i badań eksploatacyjnych układu mikro-kogeneracyjnego z ceramicznymi ogniwami paliwowymi (SOFC). 2015. ISBN: 978-83-7789-394-4.
[134] Kupecki J, Jewulski J, Badyda K. Comparative study of biogas and DME fed micro-CHP system with solid oxide fuel cell. Appl Mech Mater 2013;267:53–6.
[135] Kupecki J. Off-design analysis of a micro-CHP unit with solid oxide fuel cells fed by DME. Int J Hydrog Energy 2015;40(35):12009–22.
[136] Kupecki J, Skrzypkiewicz M, Wierzbicki M, Stepien M. Analysis of a micro-CHP unit with in-series SOFC stacks fed by biogas. Energy Procedia 2015;75:2021–6.
[137] Fu CJ, Chan SH, Ge XM, Liu QL, Pasciak G. A promising NiFe bimetallic anode for intermediate-temperature SOFC based on Gd-doped ceria electrolyte. Int J Hydrog Energy 2011;36:13727–34.
[138] Liu QL, Chan SH, Pasciak G. Fabrication and characterization of large-size electrolyte/anode bilayer structures for low-temperature solid oxide fuel cell stack based on gadolina-doped ceria electrolyte. Electrochem Comm 2009;11:871–4.
[139] Głowacki P, Kawalec M. Aircraft emission during various flight phases. Combust Engines 2015;162(3):229–40.
[140] Advisory Council for Aeronautical Research in Europe (ACARE). European Aeronautics: a vision for 2020. 2001.
[141] Advisory Council for Aviation Research and Innovation in Europe (ACARE), Strategic Research & Innovation Agenda (SRIA); 2012;1.
[142] Krawczyk JM, Mazur AM, Sasin T, Stokłosa AW. Fuel cells as alternative power for unmanned aircraft systems – current situation and development trends. Trans Inst Aviat 2014;4(237):49–62.
[143] Spencer KM. Investigation of potential fuel cell use in aircraft, Institute for Defense Analyses. IDA Document D-5043; Log: H 13-001404. 2013.
[144] Dokiya M. SOFC system and technology. Solid State Ionics 2002;152–153:383–92.
[145] Palsson J, Selimovic A, Sjunnesson L. Combined solid oxide fuel cell and gas turbine systems for efficient power and heat generation. J Power Sources 2000;86:442–8.
[146] Waters D, Vannoy S, Cadou Ch. Hybrid turbine-solid oxide fuel cells for aircraft propulsion and power. In: University of Maryland, Department of Aerospace Engineering; Electric & Hybrid Aerospace Technology Symposium; 2015.
[147] Lisbona P, Corradetti A, Bove R, Lunghi P. Analysis of a solid oxide fuel cell system for combined heat and power applications under non-nominal conditions. Electrochim Acta 2007;53:1920–30.
[148] Bove R, Ubertini S. Modeling solid oxide fuel cell operation: approaches, techniques and results. J Power Sources 2006;159:543–59.
[149] Baharanchi AA. Multidisciplinary modeling, control, and optimization of a solid oxide fuel cell/gas turbine hybrid power system [Thesis]. University of Miami; 2009.
[150] Larminie J, Dicks A. Fuel cell systems explained. New York: John Wiley & Sons Ltd; 2000.
[151] Perullo CA, Trawick D, Clifton W, Tai JCM, Mavris DN. Development of a suite of hybrid electric propulsion modeling elements using NPSS. In: Turbo Expo 2014, Turbine Technical Conference and Exposition; 2014. Dusseldorf.
[152] Brus G. Experimental and numerical studies on chemically reacting gas flow in the porous structure of a solid oxide fuel cells internal fuel reformer. Int J Hydrog Energy 2012;37:17225–34.
[153] Brus G, Komatsu Y, Kimijima S, Szmyd JS. An analysis of biogas reforming process on Ni/YSZ and Ni/SDC catalysts. Int J Therm 2012;15.
[154] Brus G, Nowak R, Szmyd JS, Komatsu Y. An experimental and theoretical approach for the carbon deposition problem during steam reforming of model biogas. J Theor Appl Mech 2015;53(2):273–84.
[155] Sciazko A, Komatsu Y, Brus G, Kimijima S, Szmyd JS. A novel approach to the experimental study on methane/steam reforming kinetics using the Orthogonal Least Squares method. J Power Sources 2014;262:245–54.
[156] Sciazko A, Komatsu Y, Brus G, Kimijima S. A novel approach to improve the mathematical modelling of the internal reforming process for solid oxide fuel cells using the orthogonal least squares method. Int J Hydrog Energy 2014;39:16372–89.
[157] Brus G, Szmyd JS. Numerical modelling of radiative heat transfer in an internal indirect reforming-type SOFC. J Power Sources 2008;181:8–16.
[158] Mozdzierz M, Brus G, Sciazko A, Komatsu Y, Kimijima S, Szmyd JS. Towards a thermal optimization of a methane/steam reforming reactor. Flow Turbul Combust 2016:1–19.
[159] Nishino T, Szmyd JS. Numerical analysis of a cell-based indirect internal reforming tubular SOFC operating with biogas. J Fuel Cell Sci Technol 2010;7:051004-1–051004-8.
[160] Szmyd JS, Komatsu Y, Brus G, Ghigliazza F, Kimijima S, Sciazko A. The effect of applied control strategy on the current-voltage correlation of a solid oxide fuel cell stack during dynamic operation. Arch Therm 2014;35:129–43.
[161] Komatsu Y, Brus G, Kimijima S, Szmyd JS. The effect of overpotentials on the transient response of the 300W SOFC cell stack voltage. Appl Energy 2014;115:352–9.
[162] Komatsu Y, Kimijima S, Szmyd JS. Performance analysis for the part-load operation of a solid oxide fuel cell-micro gas turbine hybrid system. Energy 2010;35:982–8.
[163] Komatsu Y, Kimijima S, Szmyd JS. Numerical analysis on dynamic behavior of solid oxide fuel cell with power output control scheme. J Power Sources 2013;223:232–45.
[164] Brus G, Miyawaki K, Iwai H, Saito M, Yoshida H. Solid State Ionics 2014;265:13–21.

[165] Brus G, Miyoshi K, Iwai H, Saito M, Yoshida H. Change of an anode's microstructure morphology during the fuel starvation of an anode-supported solid oxide fuel cell. Int J Hydrog Energy 2015;40:6927–34.
[166] Brus G, Iwai H, Sciazko A, Saito M, Yoshida H, Szmyd JS. Local evolution of anode microstructure morphology in a solid oxide fuel cell after long-term stack operation. J Power Sources 2015;288:199–205.
[167] Brus G, Iwai H, Otani Y, Saito M, Yoshida H. Local evolution of triple phase boundary in solid oxide fuel cell stack after long-term operation. Fuel Cells 2015;288:199–205.
[168] Pianko-Oprych P, Kasilova E, Jaworski Z. CFD analysis of heat transfer in a microtubular solid oxide fuel cell stack. Chem Proc Eng 2014;35(3):293–304.
[169] Pianko-Oprych P, Zinko T, Jaworski Z. Modeling of thermal stresses in a microtubular solid oxide fuel cell stack. J Power Sources 2015;300:10–23.
[170] Pianko-Oprych P, Zinko T, Jaworski Z. Numerical analysis of thermal stresses in a new design of microtubular stack. Cent Eur J Chem 2015;13(1):1045–62.
[171] Pianko-Oprych P, Zinko T, Jaworski Z. Simulation of thermal stresses for new designs of microtubular solid oxide fuel cell stack. Int J Hydrog Energy 2015;40(42):14584–95.
[172] Zakrzewska B, Pianko-Oprych P, Jaworski Z. Multiscale modeling of solid oxide fuel cell systems. Chem Ing Tech 2015;86(7):1029–43.
[173] Kupecki J, Jewulski J, Milewski J. Multi-level mathematical modeling of solid oxide fuel cells [in] clean energy for better environment. Rijeka: Intech; 2012. p. 53–85. ISBN: 978-953-51-0822-1.
[174] Kupecki J. Modelling of physical, chemical and material properties of solid oxide fuel cells. J Chem 2015;1:414950.
[175] Kupecki J, Jewulski J, Motylinski K. Parametric evaluation of a micro-CHP unit with solid oxide fuel cells integrated with oxygen transport membranes. Int J Hydrog Energy 2015;40(35):11633–40.
[176] Kupecki J, Milewski J, Szczesniak A, Bernat R, Motylinski K. Dynamic numerical analysis of cross-, co-, and counter-current flow configurations of a 1 kW-class solid oxide fuel cell stack. Int J Hydrog Energy 2015;40(45):15834–44.
[177] Motylinski K, Kupecki J. Modeling the dynamic operation of a small fin plate heat exchanger – parametric analysis. Arch Therm 2015;36:85–103.
[178] Wolowicz M, Kupecki J, Wawryniuk K, Milewski J, Motylinski K. Analysis of nodalization effects on the prediction error of generalized finite element method used for dynamic modeling of hot water storage tank. Arch Therm 2015;36:123–38.
[179] Kupecki J, Milewski J, Jewulski J. Investigation of SOFC material properties for plant-level modelling. Cent Eur J Chem 2013;11(5):664–71.
[180] Kupecki J, Milewski J, Badyda K, Jewulski J. Evaluation of sensitivity of a micro-CHP unit performance to SOFC parameters. ECS Trans 2013;51(1):107–16.
[181] Kupecki J, Motylinski K, Ferraro M, Sergi F, Zanon N. Use of NaNiCl battery for mitigation of SOFC stack cycling in base-load telecommunication power system – a preliminary evaluation. J Power Technol 2016;96(1):63–71.
[182] Milewski J, Discepoli G, Desideri U. Modeling the performance of MCFC for various fuel and oxidant compositions. Int J Hydrog Energy 2014;39(22):11713–21.
[183] Milewski J, Biczel P, Kłos M. Triple-layer control system for molten carbonate fuel cell-gas turbine hybrid system. J Fuel Cell Sci Technol 2015;12(4), 041005.
[184] Milewski J, Wołowicz M, Miller A, Bernat R. A reduced order model of molten carbonate fuel cell: a proposal. Int J Hydrog Energy 2013;38(26):11565–75.
[185] Milewski J, Swiercz T, Badyda K, Miller A, Dmowski A, Biczel P. The control strategy for a molten carbonate fuel cell hybrid system. Int J Hydrog Energy 2010;35(7):2997–3000.
[186] Skibinski J, Cwieka K, Kowalkowski T, Wysocki B, Wejrzanowski T, Kurzydlowski KJ. The influence of pore size variation on the pressure drop in open-cell foams. Mater Des 2015;87:650–5.
[187] Wejrzanowski T, Skibinski J, Szumbarski J, Kurzydlowski KJ. Structure of foams modeled by Laguerre-Voronoi tessellations. Comp Mat Sci 2013;67:216–21.
[188] FCH-JU MAWP 2014–2020. http://www.fch.europa.eu/sites/default/files/documents/FCH2%20JU%20-%20Multi%20Annual%20Work%20Plan%20-%20MAWP_en_0.pdf [Accessed 12 November 2016].
[189] Energy audits. http://www.audytoenerg.pl/index.php/74-uncategorised/159-wskaznik-emisji-co2-dla-energii-elektrycznej [Accessed 15 November 2016].
[190] International Energy Agency: electricity and heat for 2014. http://www.iea.org/statistics/statisticssearch/report/?year=2014&country=POLAND&product=ElectricityandHeat [Accessed 15 November 2016].
[191] FuelCellToday: the fuel cell industry review 2013. http://fuelcelltoday.com/media/1889744/fct_review_2013.pdf [Accessed 15 November 2016].